
VOLUME 1

Grace Essential Articles



GRACE



A long history of looking

AHEAD

For nearly a century, Grace catalysts have kept fuel and petrochemical feedstocks flowing from the industry's largest refineries to the trucks, trains, planes, and ships that keep our world running.

We are leveraging our long history of innovation in fluid catalytic cracking to develop products that enable lower carbon fuels and help meet the challenges of the energy transition.

GRACE

[grace.com](https://www.grace.com)

Editing and Design

Matt Kirchner, Executive Editor

Shelly DeButts, Managing Editor

Michael Hawkins, Managing Editor

Lisa Schemm, Design

Regan Weldy, Design

Contributors

Victor Batarseh

Stefan Brandt

Ken Bryden

Gary Cheng

Clint Cooper

Rafael Gonzalez

Michael Hawkins

David Hunt

Claudia Janse van Rensburg

TABLE OF CONTENTS

EDITORIAL

- 3** A Long History of Looking Ahead

FEATURED ARTICLE

- 4** A Pioneer in FCC Ecat Analysis

MAIN ARTICLES

- 6** ZSM-5 Additive in Fluid Catalytic Cracking
- 18** New Opportunities for Co-Processing Renewable Feeds in Refinery Processes
- 34** Effect of Hydrocarbon Partial Pressure on Propylene Production in the FCC
- 46** Strategies for Maximizing FCC Light Cycle Oil
- 60** The Effects of Fe Poisoning on FCC Catalysts
- 72** Coke Selectivity Fundamentals
- 80** Trouble-Shooting FCC Standpipe Flow Problems
- 92** Understanding and Minimizing FCC Slurry Exchanger Fouling
- 100** Nitrogen Chemistry and NO_x Control in a Fluid Catalytic Cracking Regenerator
- 110** Highlights from Early Issues of *Catalagram* Magazine

A Long History of Looking Ahead



Matt Kirchner
Vice President, Marketing, Fluid Catalytic Cracking (FCC)
W. R. Grace & Co.

Dear Colleagues and Partners,

We are thrilled to share a collection of some of the most requested and referenced articles produced by Grace's subject matter experts in Refining Technologies over the past four decades. Each article is paired with an introduction from current Grace experts commenting on the impact of the article when published and its relevance to today's industry.

The articles appear as they were originally published, without significant editing, to demonstrate their continued relevance. We deeply appreciate the contributions of the original authors to the body of knowledge that Grace has helped advance over 80 years of developing FCC catalysts. Regardless of the year of initial publication, this incredible collection of articles covers many of the drivers of catalyst value today – traditional fuel production, on purpose propylene, and the decarbonization value chain.

This incredible collection of articles covers many of the drivers of catalyst value today.

Grace has a long history of looking ahead to the future of FCC demonstrated by the many innovations that have come from our R&D teams. Part of our ability to anticipate what the industry will need next comes from the long-term perspective we take. And, throughout our history many things have remained consistent – our world-class technical service and support, cutting-edge analytical assistance, and our commitment to customer-driven innovation. Together, we will continue to advance the industry.

We hope you find this anthology of articles as valuable as we do and look forward to strengthening our partnership in the years to come.

A handwritten signature in black ink, appearing to read 'MKirchner', written in a cursive style.

A Pioneer in FCC Ecat Analysis

Innovation and Improvement Require Deep Technical Support



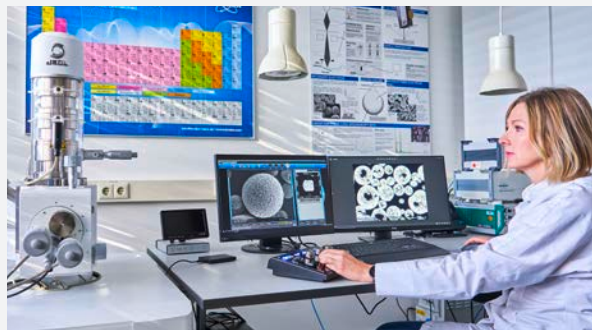
Ken Bryden
Director, Catalyst Evaluation
Research & Services
W. R. Grace & Co.

Routine testing of refinery equilibrium catalyst (Ecat) properties is important in tracking unit health and catalyst performance. In 1947, Grace was the first vendor to start this analysis. In Issue #1 of the *Catalagram* magazine (1959), Grace published the first survey of industry Ecat results, helping refiners understand industry trends and how their Ecat properties compared to other units.

Grace's Ecat testing results are used by our technical service and GCT teams to proactively address, troubleshoot, and solve customer issues. Ecat analysis can identify issues with mechanical status of equipment, feedstock changes, and unit upsets. It also provides a baseline of unit performance. A 1961 article on the service stated "When and if serious difficulty does arise, it helps to have the historical background in terms of consistent data which then becomes a means for diagnosing exactly what did happen and when. Much of the value of the program lies in its scope; the experience gained from studying catalyst from some 79 units can all be brought to bear on the study of the 80th unit."*

As the FCC industry has grown, Grace's Ecat analysis program has grown also. From one lab in Curtis Bay, Maryland USA, in 1947, we have expanded to four Ecat analysis labs, located in Germany, Kazakhstan, Oman and the United States. Each year, more than 10,000 Ecat samples are tested, representing Ecat from more than 200 FCC units worldwide.

At the start of the program, results were provided via telegram and postal mail – Grace now provides results via email and online through the e-catalysts.com customer portal. Testing methods and equipment have also evolved with new tests added and the accuracy and speed of other tests improved.



Each year, more than 10,000 Ecat samples are tested, representing Ecat from more than 200 FCC units worldwide.

What has not changed in the last 75+ years is Grace's commitment to our customers and to the refining industry. We view Ecat analysis as a critical part of our technical service offering that allows refiners to maximize the performance and profitability of their FCC units.

* How Catalyst Test Service Aids Fluid Unit Operations - World Petroleum, February 1961, p. 45.

MAIN ARTICLES

Over 25 years ago, two Grace researchers wrote a compelling paper for the American Chemical Society demonstrating that the use of a ZSM-5 additive in Fluid Catalytic Cracking (FCC) was more effective than increasing temperature for maximizing propylene in the FCC process. Grace first described the commercialization of ZSM-5 in *Catalagram* No. 72 in 1985, together with Mobil Corporation as an avenue to achieve higher gasoline octane. In this paper from 1999, Xinjin Zhao and Terry G. Roberie examined the effect of varying levels of ZSM-5 additives versus reactor temperature for maximizing light olefins in FCC products and the implications for gasoline olefins. Most of the tests were conducted in the Grace DCR™ Pilot Plant. While the effect of ZSM-5 on gasoline olefins varies with different systems, the work by Zhao and Roberie proved that ZSM-5 additives reduced C6+ olefins under all the conditions studied.


Employing a catalyst additive approach allows FCC units to accommodate a variety of operational needs without hardware changes or capital investment. Today, ZSM-5 additive technology has become instrumental in producing propylene from the FCC. Grace has continued to innovate in this space and recently launched game-changing catalytic technology with the highest propylene activity and best activity retention in the industry. Grace's ZAVANTI™ ZSM-5 additive is specifically designed for max propylene FCC units and incorporates best-in-class ZSM-5 zeolite, manufacturing techniques, and binding chemistry.



Michael Hawkins
Regional Marketing Manager
W. R. Grace & Co.

ZSM-5 Additive in Fluid Catalytic Cracking

Effect of Additive Level and Temperature in Light Olefins and Gasoline Olefins

 Xinjin Zhao, Terry Roberie

 Originally published in *Industrial and Engineering Chemistry Research* in 1999 (38 3847-3853)

The effects of ZSM-5 additive and riser reactor temperature on the product selectivity in fluid catalytic cracking of gas oil were systematically investigated in an adiabatic circulating riser reactor. In addition to the fact that ZSM-5 can substantially increase propylene and butene, it is found that ethylene yield linearly increases with the amount of ZSM-5 in the system. The ethylene is likely from the overcracking of C5 and C6 olefins. The effect of ZSM-5 on gasoline range olefins was clarified. In the temperature range of 794-839 K (970-1050°F) studied in the current work, ZSM-5 additive always reduces C6 + olefins. The effect of ZSM-5 on C5= is

different. C5 olefin increases at 794 K, but decreases at 839 K. Since C5 olefins account for about one-third to one-half of the gasoline olefins, the overall gasoline olefin contents were dominated by the behavior of C5 olefins. Compared with the effect of ZSM-5, the effects of temperature on light olefins are relatively small. Most of the olefin increases with increasing temperature were due to the increased conversion at higher temperature, rather than a selectivity shift. The yields of diolefins increase with temperature. The effect of ZSM-5 on gasoline diolefins was found to be minimal.

Introduction

The use of a variety of additives has significantly improved the flexibility and operation of fluid catalytic cracking (FCC) units over the years.^{1,2} Without hardware change, the catalyst additive approach allows FCC units to accommodate a variety of operational needs. In fact, there are probably few commercial FCC units that do not use some kinds of additives for various applications. Although various zeolites have been studied, ZSM-5 remains the only known commercially used zeolite in FCC units other than faujasite. ZSM-5 was first introduced into the fluid catalytic cracking process as an additive for improving gasoline octane in the 1980s.³ As the current primary role of fluid catalytic cracking as a gasoline fuel producer is shifting toward being a producer for light olefins and other petrochemical feedstocks in many refiners, ZSM-5 is now used primarily to increase the yields of C3 and C4 olefins for alkylations, oligomerization, and other petrochemical processes. With the ever-increasing demands for high proportions of propylene and butene, greater propylene production in refineries will be required. Propylene demand was approximately 39 million tons in 1995 and this is forecast to increase to almost 90 million tons by 2015.⁴ The other incentive for propylene production in FCC is to balance the increasing gap between C3=/C2= demand and the C3=/C2= yield ratio from steam naphtha cracking.

There have been numerous studies on the effect of ZSM-5 additive on FCC product selectivity.⁵⁻⁷ Most of the earlier studies were focusing on octane enhancement and gasoline composition change. For example, Young et al.⁸ reported the effects of ZSM-5 additive on gasoline composition and octane levels for various different base catalysts. It was shown that ZSM-5 reduced heavy gasoline olefins (C6+) while increased light olefins (C5-). Much of the earlier work on ZSM-5 application in FCC has been summarized in the book by Chen et al.⁹ The most comprehensive studies on the effects of high levels of ZSM-5 additive on light olefins and gasoline compositions were reported by Mobil researchers.^{10,11} In those studies, a commercial ZSM-5 additive was used to study the effect of various additive levels at various temperatures. It was found that addition of ZSM-5 additive was much more effective than simply increasing riser temperature for maximizing LPG olefins in fluid catalytic cracking operations. The study also provided detailed analyses of the effect of ZSM-5 on gasoline compositions.

In this paper, we will examine the effect of high levels of ZSM-5 additives vs high temperature for (i) maximizing light olefins in FCC products and (ii) the implications for gasoline olefins. The current study uses a ZSM-5 additive with high crystal content and covers a wide range of ZSM-5 vs faujasite cracking and more systematic data on the additive level. Other than propylene, we will also compare the two different strategies:

ZSM-5 additive vs temperature on butene and ethylene levels. The effect of ZSM-5 on FCC gasoline range olefins, the major source of gasoline pool olefins, will also be examined in detail. The effect of temperature and ZSM-5 on gasoline diolefins will also be discussed.

The effects of ZSM-5 on branching, isomerization, etc. have been studied extensively in the literature.^{6,8,12} We will focus on the issues that have not been fully explored.

Experiments

Most of the tests were conducted in the Davison circulating riser (DCR). A schematic of the unit is shown in Figure 1. A more detailed description of the unit features and capabilities can be found in the literature.¹³ The DCR is a simulated laboratory scale fluid catalytic cracking unit equipped with an adiabatic circulating riser reactor (as in commercial FCC units) and a continuous regenerator. The riser feed rate is controlled at 1000 g/h. The catalyst circulation rate is adjusted by changing the feed preheater temperature to achieve the set reactor outlet temperature. The catalyst circulation rate varies between about 5000 to 9000 g/h for a typical catalyst. For each catalyst and feed combination, we typically obtain four different conversion levels with four different catalyst-to-oil ratios, achieved by adjusting the different feed preheating temperatures from 422 to 644 K (from 300 to 700°F). The experiments were conducted at riser outlet temperatures of 794 K (970°F), 816 K (1010°F), and 839 K (1050°F). Since the riser is adiabatic, the reactor bottom mixing temperature is significantly higher than the reactor top control temperature. A typical temperature gradient from the reactor top to the reactor bottom mixing temperature is about 50 K. The total unit pressure is controlled at 273.7 kPa. As in typical commercial FCC operations, about 3 wt% of steam is used for feed atomization. The vapor phase residence time in the riser is about 1.5-2 s. The liquid and gaseous products were analyzed by gas chromatographs. The liquid effluent products were also analyzed by using GC-simulated distillations for conversion and yield calculations. The conversion was defined as 100% less the weight percent amount of light cycle oil (494-644 K) and heavy cycle oil (>644 K) obtained by GC-simulated distillation. Carbonaceous deposits on the catalyst were analyzed by carbon analyzer (Leco, Corp., St. Joseph, MI). The gasoline composition was analyzed by a Grace-Davison's proprietary octane calculation software based on detailed GC analyses of the gasoline portion of the liquid products. The GC (HP6890) was equipped with a 100 m capillary column. The GC identified typically about 350 components of the gasoline and condensed them into structural groups for data analyses. Some description of the software can be found in the literature.^{14,15}

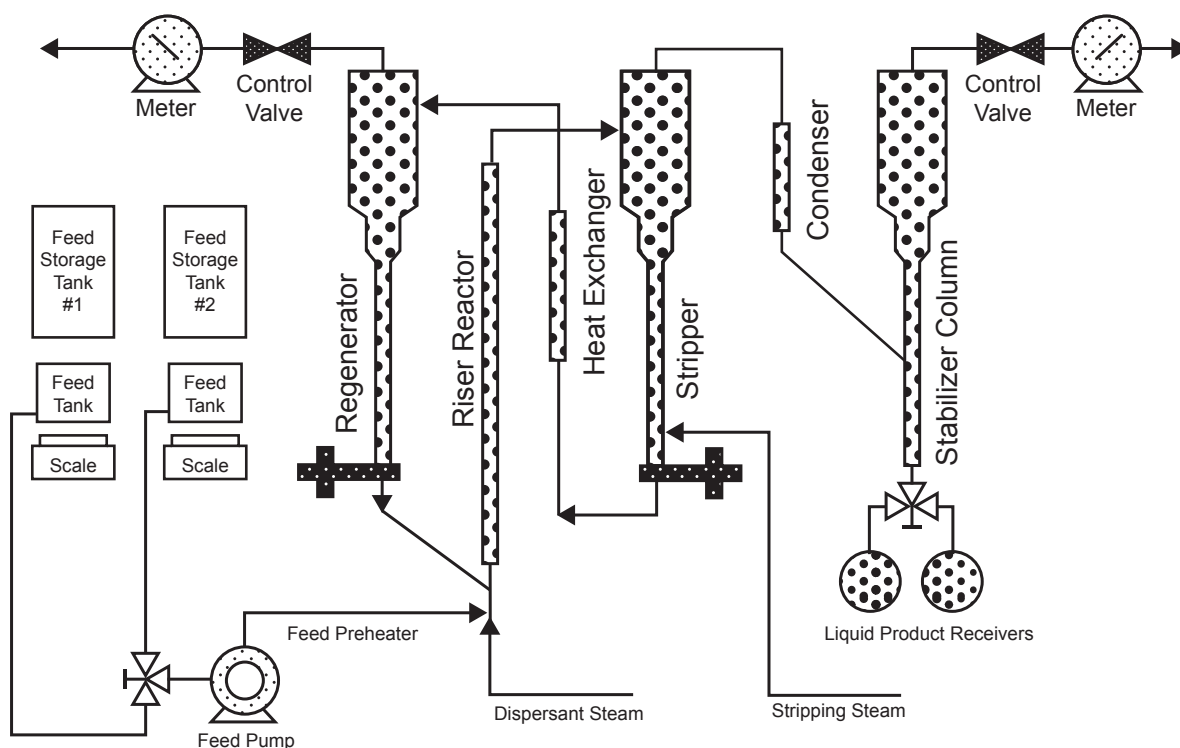


Figure 1. DCR pilot plant schematic.

Description	GCVGO F96-579
API gravity at 60°F	23.9
aniline point, °F	198
sulfur, wt%	0.73
total nitrogen, wt%	0.1
basic nitrogen, wt%	0.042
Conradson carbon, wt%	0.33
average mol wt	388
simulated distillation for vol %, °F	
IBP	464
10	637
50	806
90	977
FBP	1152
K factor	11.81
Cp	59.8
Cn	20.6
Ca	19.6

Table 1. Feed Properties

A commercial FCC gas oil feedstock from a U.S. Gulf Coast refinery was used for the DCR testing. The properties of the feed are shown in Table 1. The feed contains 0.33 wt% of Conradson carbon and has an average molecular weight of about 388. It has a UOP K factor of 11.81. The n-d-M analysis (ASTM D3238) results on the carbon types are also shown in Table 1. It has a feed naphthenic carbon content of 20 wt%.

The base cracking catalyst used in the study was a commercially deactivated equilibrium catalyst originally supplied by Grace Davison. The catalyst properties are shown in Table 2. The catalyst consists of ultrastable Y-zeolites and modified hydrosol matrixes for matrix activity,¹⁶ and balanced with Kaolin clay. The amount of rare earth oxide on catalyst was about 0.75 wt%. The deactivated unit cell size was 2.425 nm. The levels of contaminant nickel and vanadium on the equilibrium catalyst were about 1164 and 1560 ppm. Overall, both the feed and the catalyst used in the current study are representative of a typical commercial FCC system in a current refinery. As a follow up to this work, the effect of base cracking catalyst and feedstocks on the catalytic performance of ZSM-5 in FCC will be systematically investigated and the results will be reported separately.¹⁷

Continued on Page 9

Continued from Page 8

	Base Catalyst EQ97-17	ZSM-5 Additive C96-285
Chemical Analysis		
Al ₂ O ₃ , wt%	32.0	32.4
SiO ₂ , wt%	63.4	45.2
RE ₂ O ₃ , wt%	0.75	0.02
P ₂ O ₅ , wt%	0.73	16.81
Physical Properties (Thermal, 3h/811K)		
surface area, m ² /g	171	
ZSA, m ² /g	139	
MSA, m ² /g	32	
unit cell size, Å	24.26	
Properties After Deactivation (4h/1089K, 100% stm)		
surface area, m ² /g		94
ZSA, m ² /g		77
MSA, m ² /g		17

Table 2. Catalyst Properties

The ZSM-5 additive was a commercially available ZSM-5 additive manufactured by Grace Davison. The additive contains 25% of ZSM-5 zeolite. It contains phosphorus for ZSM-5 stabilization. The additive was hydrothermally deactivated at 4 h/1500°F to simulate a commercial deactivation process. The chemical analyses and physical properties of the ZSM-5 additive are shown in Table 2. The effect of the deactivation procedure on the performance of the ZSM-5 additive will be reported separately.¹⁸ The ZSM-5 additive was steam deactivated separately and then blended with the base catalyst to the desired level. Additive levels were adjusted to achieve ZSM-5 crystal levels of 0.5, 1, 2, 4, 8 wt% in the overall catalyst inventory. As a reference, a typical commercial FCC unit today operates at about 1 wt% of ZSM-5 crystal or less.

Experimental Results

Table 3 shows the conditions we studied. For each condition, we obtained full mass balance yields at four different conversion levels to allow data interpretations under constant conditions or conversion levels. Most of the data reported are interpreted at a constant conversion level to allow a more meaningful comparison. The detailed yield distribution will not be the main focus of the paper. The current paper will mostly discuss the results on olefin products ranging from ethylene to gasoline range olefins.

temp, K	0 wt%	0.5 wt%	1 wt%	2 wt%	4 wt%	8 wt%
794	X	X	X	X	X	X
816	X		X		X	
839	X		X		X	X

Table 3. ZSM-5 (wt%) Riser Testing Study Conditions

Propylene Yields

The effects of varying ZSM-5 level and temperature on propylene yield are shown in Figure 2. Propylene increases with conversion. As shown by Wojciechowski et al., it is considered a primary, stable product.¹⁹ For the yield data at 794 K, propylene yield at an interpolated constant conversion of 72.5 wt% [second-order kinetic conversion $x/(1-x)$ of 2.64] is shown in Figure 3. The first 2 wt% of additive provided a 30% increase in propylene yield from the base case without ZSM-5. With up to 32 wt% of additive, propylene yield increased from 4.6 to 11.1 wt%, an increase of 150%. The propylene yield continuously increases with the additive level. However, it is clear that the incremental propylene yield from ZSM-5 decreases rapidly with increasing level. The incremental propylene yield from 10 to 32 wt% of additive is equivalent to the incremental propylene yield from the first 4 wt% of additive.

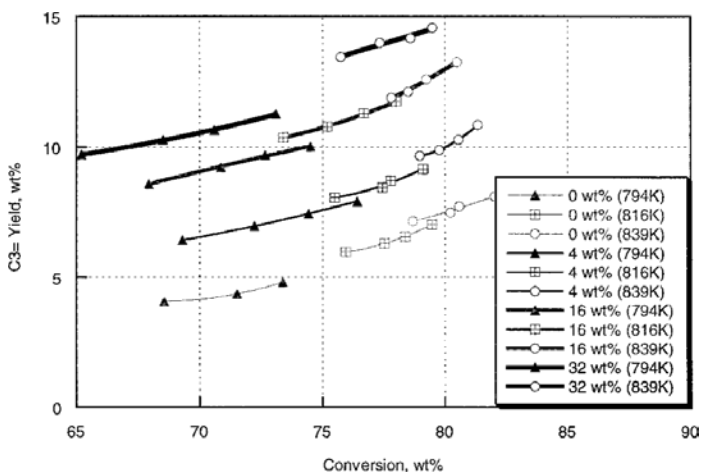


Figure 2. Effect of ZSM-5 additive/temperature on C3= yield.

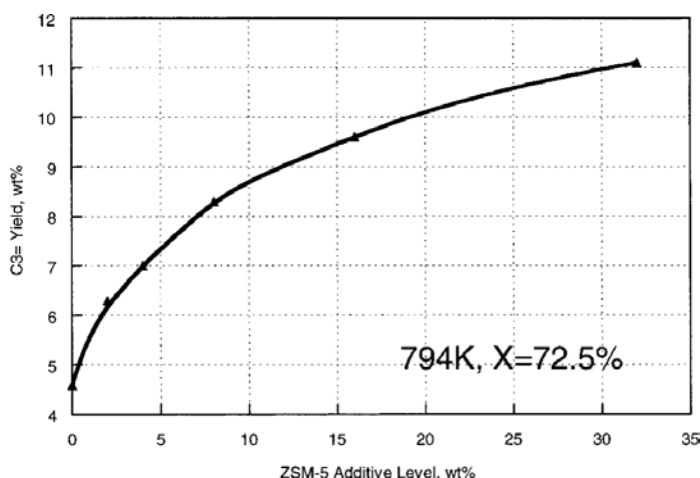


Figure 3. Effect of ZSM-5 additive on C3= yield.

At constant conversion, the effect of temperature increase on propylene yield is very small. Although higher temperature does provide higher propylene, the increase is mostly due to the increased conversion level. At high conversion, the overcracking of gasoline starts to significantly contribute to the yields of propylene and butene products. Comparison of the two different approaches for maximizing propylene clearly favors the use of ZSM-5 over increasing temperature. In fact, a temperature increase from 794 to 839 K only gave a propylene increase equivalent to about 4 wt% of the ZSM-5 additive from the current study. In a commercial FCC unit, 4 wt% of additive is certainly much easier to cope with than a reactor temperature increase of 45 K (80°F).

The trend of C3 olefinicity is worth noting. ZSM-5 naturally increases C3 olefinicity due to the high C3= yield. However, C3 olefinicity actually decreases with increasing temperature. Since propane is a thermal cracking product, the low olefinicity with increasing temperature indicates the increasing contribution of thermal cracking at higher temperature.

Butene Yield

Both hydrogen transfer and isomerization reactions can significantly affect the distribution of C4 olefin products. Figure 4 shows the butene yield change with varying levels of ZSM-5 additive at three different temperatures. Unlike the propylene yield, butene yield typically goes through a maximum with varying conversion. At high conversion, butene tends to get saturated to butane. As in the case of propylene, butene also increases monotonically with increasing additive level. The first 4% of additive gave a 25% increase in butene yield. Within the range of additive levels studied, there is no indication that butene reached a maximum, though the incremental yield after 10 wt% of additive is relatively small. Due to the high isomerization activity of ZSM-5, a large fraction of the butene increase comes from an increase in isobutene in Figure 5.

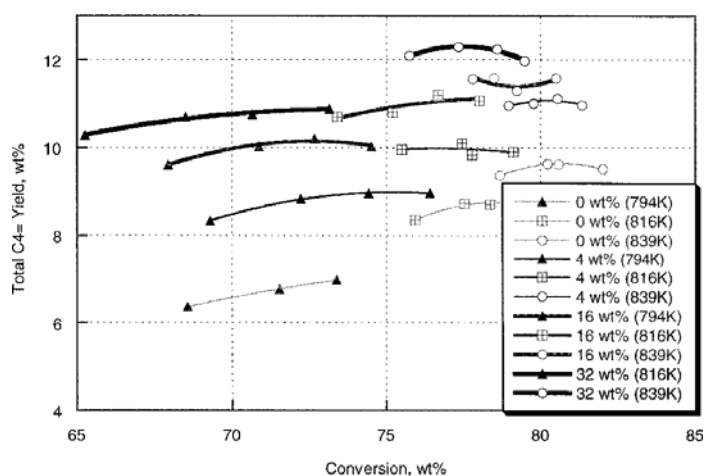


Figure 4. Effect of ZSM-5 additive/temperature on C4= yield.

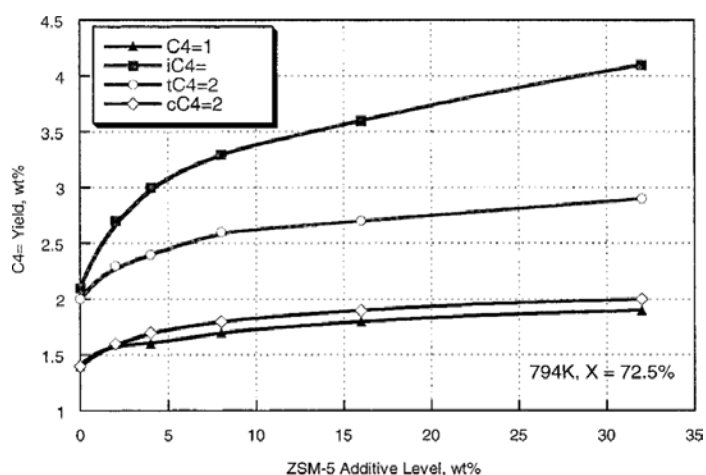


Figure 5. Effect of ZSM-5 additive on butylene yields.

Isobutene selectivity increases drastically with the increasing of ZSM-5 level. It indicates that a major portion of the C4= made by ZSM-5 is isobutene, which is the most desired product. ZSM-5 has very little effect on either nC4 or iC4 (Figure 6). As a result, the C4 olefinicity improves drastically with increasing ZSM-5 additive level. Literature work has also shown that ZSM-5 increases the branching of gasoline range olefins.⁸ Temperature increases affect the relative rate of cracking vs hydrogen transfer reaction. At higher temperature, the rate of cracking increases faster than the rate of hydrogen transfer due to its higher activation energy.^{10,20} As a result, the fraction of iC4= which is converted to isobutane is substantially less at higher temperature. The sums of isobutane and butene are relatively temperature independent (Figure 7).

Continued on Page 11

Continued from Page 10

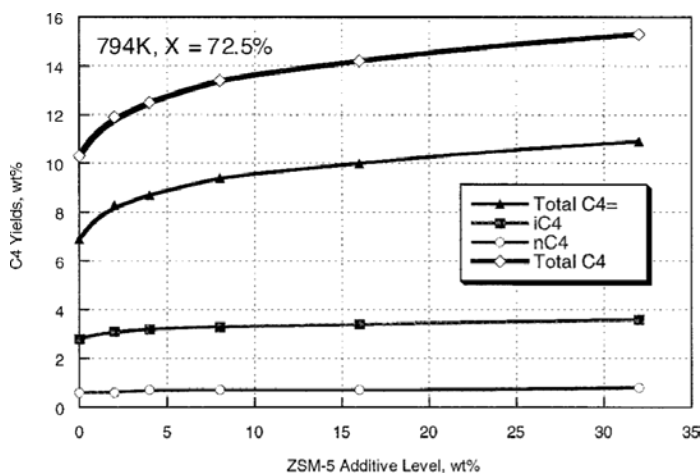


Figure 6. Effect of ZSM-5 additive on C4 yields.

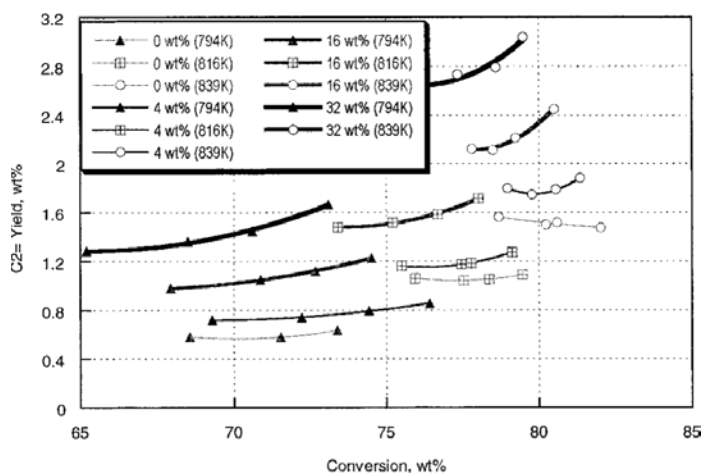


Figure 8. Effect of ZSM-5 additive/temperature on C2= yield.

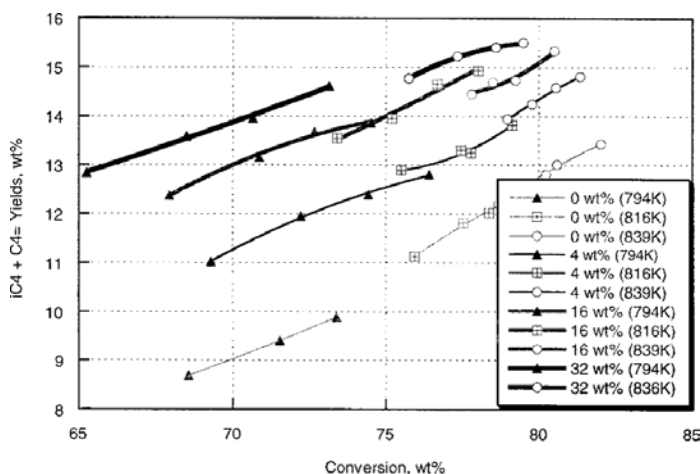


Figure 7. Effect of ZSM-5 additive/temperature on iC4 + C4= yields.

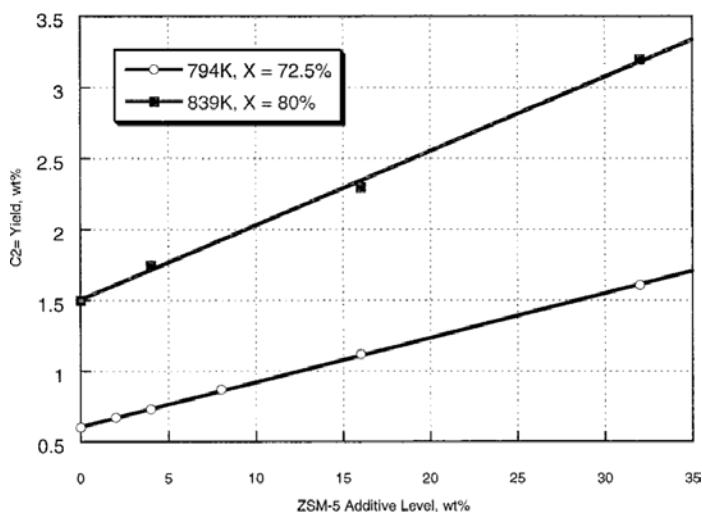


Figure 9. Effect of ZSM-5 additive on ethylene yield.

Ethylene Yield

It is generally not economical to separate ethylene from FCC products due to its low concentration. Therefore, ethylene yield from FCC is typically not a major concern. However, it has been noted that ethylene yield increases with use of ZSM-5.¹⁰ The effects of ZSM-5 additive level and temperature on ethylene yields from the current study are shown in Figure 8. Both ZSM-5 addition and temperature increases can substantially increase ethylene yield. The highest level of ethylene we obtained was about 3 wt%. More significantly, the increase of ethylene at constant conversion is linearly proportional to the amount of ZSM-5 in the system (Figure 9). Therefore, a high level of ZSM-5 significantly increases ethylene yield from FCC. Extrapolation of the yield to 100% of ZSM-5 catalyst indicates about 7 wt% of

ethylene at a riser temperature of 839 K. Recovery of ethylene at the high concentration is expected to be more economical. It certainly becomes more economical to recover this high level of ethylene. The fact that ethylene levels linearly correlated with ZSM-5 levels indicates that faujasite contributes very little to the ethylene yield. It is probably an overcracking product of C5+ gasoline range olefins or disproportionation of C6=. It has been reported that olefins smaller than C6 are stable with respect to direct cracking and must dimerize before a species is formed which is unstable enough to crack.²¹ At the temperature range we used in the current study, especially at 839 K, the production of ethylene is probably associated with the cracking of pentenes or even butenes. It should be pointed out that dimerization and re cracking reactions play a significant role in the product olefin distribution.^{22,23}

Figure 10 shows the effect of ZSM-5 and temperature on ethane production. Higher temperature yielded more ethane due to the incremental thermal cracking. However, ZSM-5 additive did not contribute to ethane production. It is indicative of the mechanism for ethylene production from olefins cracking rather than free radical mechanism.

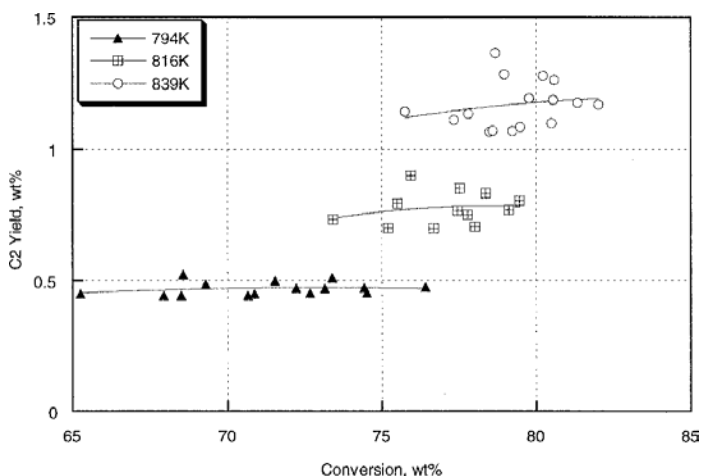


Figure 10. Effect of temperature on C2 yield.

Gasoline Olefins

Due to the environmental concerns, gasoline olefin content is increasingly regulated in the United States. It has been shown that ZSM-5 reduces the heavier olefins while increasing C5 olefins in gasoline.⁸ However, the effect of ZSM-5 catalyst on total FCC gasoline olefins has been somewhat mixed. In the current study, Figure 11 shows the gasoline olefin variations with increasing ZSM-5 additive at two different temperatures. At 794 K, ZSM-5 increases gasoline olefins by about 2-3 wt%. At the higher riser temperature of 839 K, gasoline olefins had an initial increase with ZSM-5 but then decreased significantly with further increase of ZSM-5 level.

To rationalize the different trends for gasoline olefins, we summarized all the olefin yields ranging from gas to gasoline products (Figures 12 and 13). It is clear that ZSM-5 converts the gasoline range olefins (from C6= to C9=+) to light olefins (from C2= to C4=). With increasing ZSM-5 level, more heavy olefins (C6=+) are converted to light olefins (C4=-). C5 olefin is at the crossover point of this process. Depending on the specific system, C5 olefin can either increase or decrease with increasing ZSM-5. In the two examples, we have C5 olefin levels increasing with ZSM-5 at 794K (Figure 12), while they decrease with ZSM-5 at 839K (Figure 13). A possible explanation is that C5= cracking has a higher activation energy than heavier olefins. Since C5 olefins consist of 30-50 wt% of the total gasoline olefins (Figure 14), the trend of C5 olefins can dominate the direction of total gasoline olefins one way

or another. Although the two current examples are based on a change in riser temperature, it is expected that different feeds or catalysts or other change could also affect where exactly the crossover is. As a result, the effect of ZSM-5 on gasoline olefins can be different for different systems. The effect of operating temperature, C/O, and feed effect on gasoline olefin can be found in the literature.²⁴

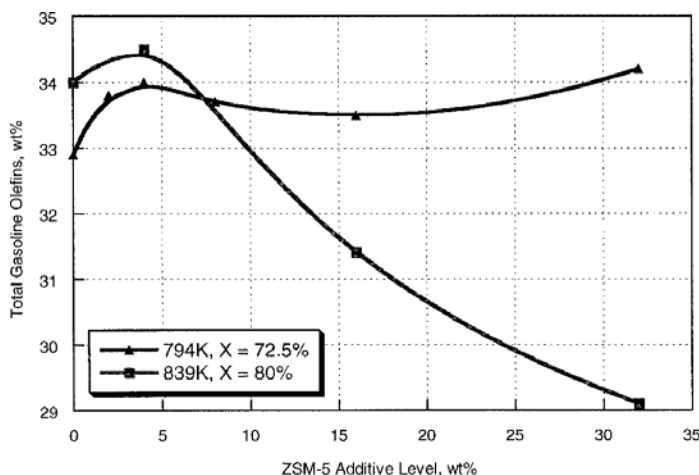


Figure 11. Effect of ZSM-5 additive on gasoline olefins.

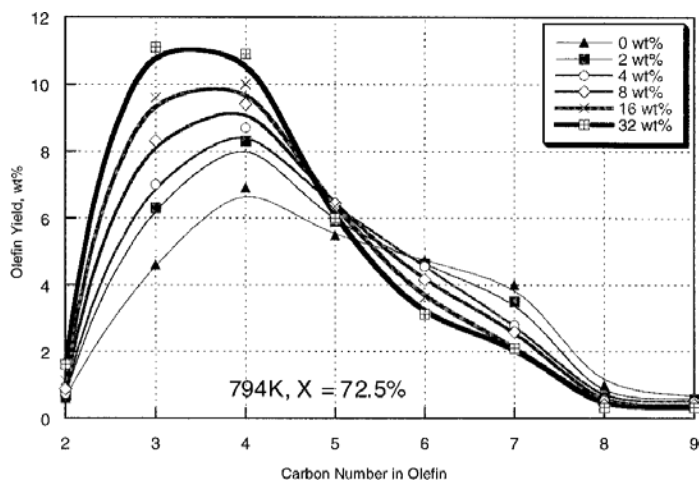


Figure 12. Effect of ZSM-5 additive on olefin distribution.

Continued from Page 12

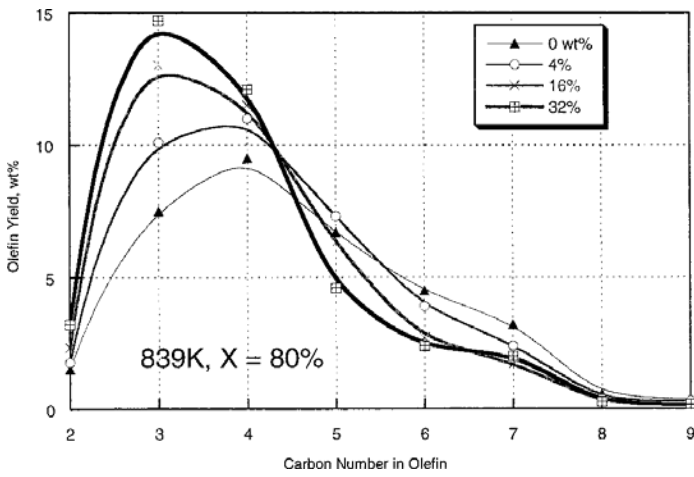


Figure 13. Effect of ZSM-5 on olefin distribution.

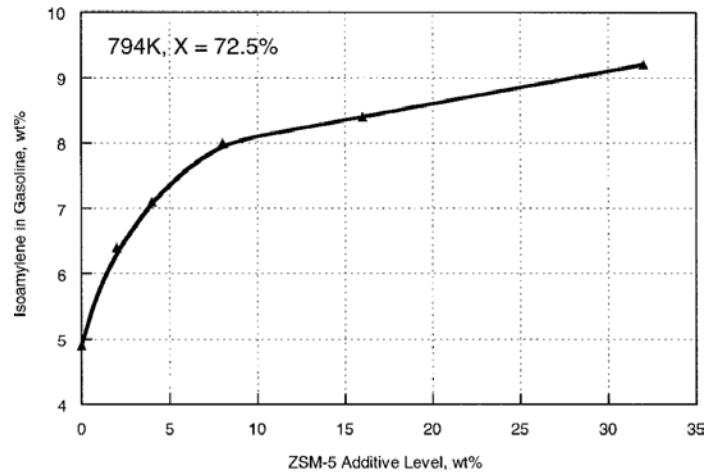


Figure 15. Effect of ZSM-5 additive on isoamylenes yield.

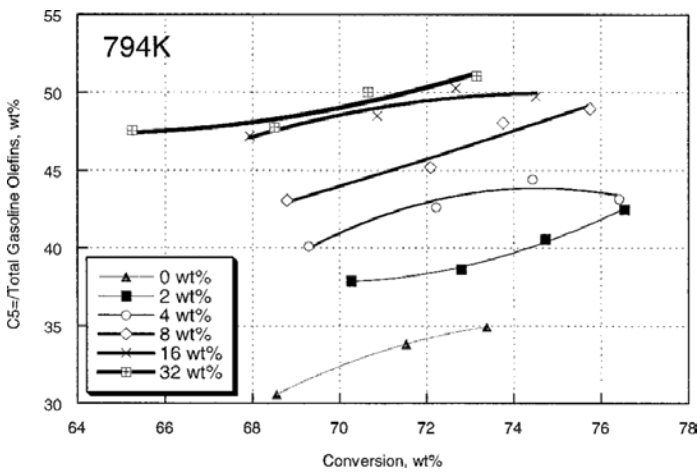


Figure 14. Total C5= olefins in gasoline olefin.

Figure 15 shows the effect of ZSM-5 on isoamylenes at 794K. Since C5 olefins increase with ZSM-5 addition, one can expect that isoamylenes also increase with ZSM-5 additive level. Certain commercial FCC units are expected to separate C5 olefins from the gasoline stream in order to obtain feedstocks for TAME production. In those cases, ZSM-5 can have a double benefit: increasing isoamylenes yield and reducing gasoline olefins.

Gasoline Diolefins

The existence of diolefins in gasoline can significantly affect the stability of the gasoline due to the highly reactive nature of diolefins. Light diolefins in the LPG stream can also significantly impact the down stream alkylation economics by increasing the acid consumption. Figures 16 and 17 show the effect of ZSM-5 vs temperature on the gasoline diolefin concentrations. Increasing the temperature from 794 to 839 K almost tripled the amount of diolefins in the gasoline from about 0.6 to about 1.7 wt%. Although there were some scattering in the data, the addition of ZSM-5 additive seems to have very little effect on the diolefins concentration, another advantage of using ZSM-5 over temperature for maximizing propylene yield. In the current study, we did not detect a significant amount of butadiene under the conditions we used.

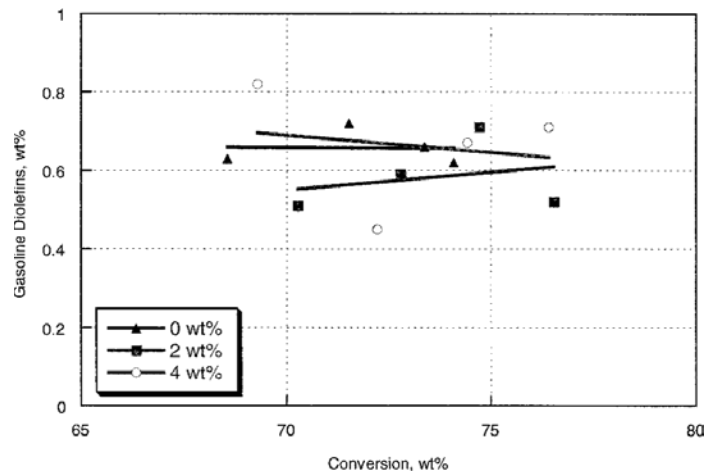


Figure 16. Effect of ZSM-5 additive on gasoline diolefins yields.

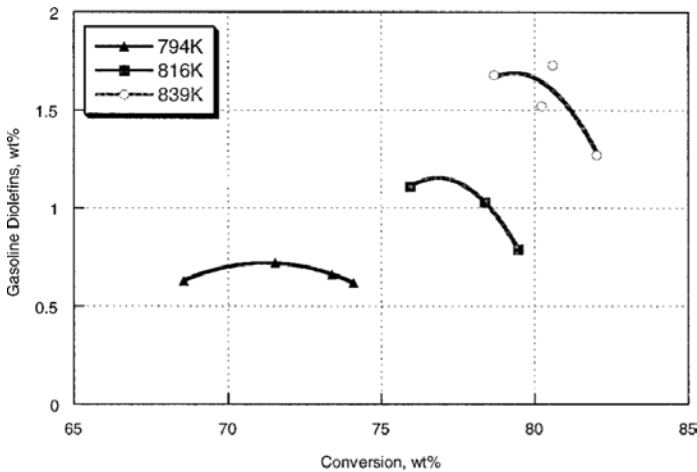


Figure 17. Effect of temperature on gasoline diolefins yields.

Discussion

The current work provided similar results to that of Buchanan et al.^{10,11} for the light olefins. For example, both studies showed that very high propylene yield can be obtained with ZSM-5, while increasing the riser temperature is not nearly as effective for maximizing propylene. However, there are some minor differences in some of the observations. Within the additive levels we studied (32 wt%), we did not observe a maximum yield for the light olefins (e.g., propylene or butene). Judging from the zeolite surface areas, the additive used in the current study contains more than twice as much ZSM-5 crystal in the additive. Therefore, the current study in effect covers a wider range of ZSM-5 levels than the previously reported study. It is not clear to us why the production of olefins should go down with higher additive level. Since the reported work was not compared at a constant conversion level, the observed effect could be due to the lower activity of ZSM-5 for overall conversion. At a very high ZSM-5 level, the overall conversion goes down, which could result in lower olefins yields.

Another minor difference between the two studies is the effect of temperature. The effect of temperature was reported to be different for the base case and the case with ZSM-5.¹⁰ The authors observed that increasing temperature did not result in an olefin increase when high levels of ZSM-5 additive were present. In the current work, the effect of temperature on propylene yield is relatively small, but the effect is the same with or without additives (Figure 2). On the other hand, temperature does have a significant effect on butene yield. The effect of temperature is mostly due to the different activation energy of cracking vs hydrogen transfer.

Another point worth mentioning is the effectiveness of ZSM-5 at different temperatures. Figures 18 and 19 compare the percentage increase of all the olefins due to ZSM-5 at two

different temperatures: 794K vs 839K. At 794K, 8 wt% of ZSM-5 crystal provided a 145% increase of propylene and 58% of butene increase. At 839K, the same level of ZSM-5 only increases the yield of propylene by 95% and of butene by about 25% at 839K. Higher temperature typically means more gasoline olefins. The greater gasoline olefins did not result in more LPG olefins. Careful examination of the gasoline composition shows that higher temperature increases the production of light gasoline olefins (e.g. C5=) versus the heavier gasoline olefins. The lighter gasoline olefins are more difficult to crack than the heavier olefins. The cracking of the lighter gasoline olefins does make a substantial amount of ethylene, which was observed in the current study.

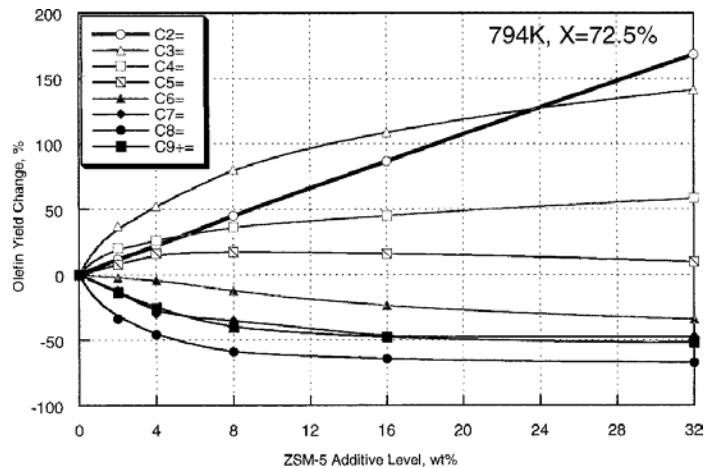


Figure 18. Olefin yield change with ZSM-5 additive level.

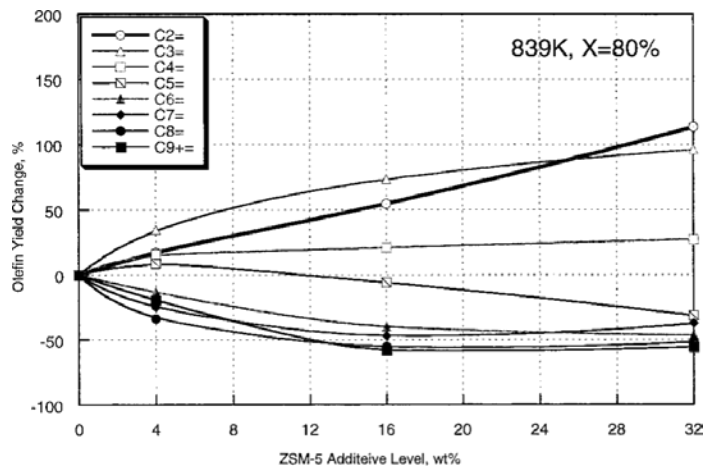


Figure 19. Olefin yield change with ZSM-5 additive level.

Continued on Page 15

Continued from Page 14

Conclusions

Using ZSM-5 additive is more effective than increasing temperature for maximizing propylene in the FCC process. Ethylene yield increases linearly with the level of ZSM-5 additive, indicating that faujasite contributes little to the formation of ethylene. The effect of ZSM-5 on gasoline olefins varies with different systems. ZSM-5 reduces C6+ olefins under all the conditions we studied. However, the effect of ZSM-5 on C5 olefins is dependent on the temperature. ZSM-5 increases C5= under typical FCC operating conditions, while it reduces pentenes at higher temperatures. The increase of ethylene yield is correlated with the reduction in pentene yield at high temperature. Increasing riser temperature increases diolefins in both the C4 and gasoline range. No appreciable effect of ZSM-5 on diolefins was observed.

Acknowledgment

The authors thank N. Dale McCrary for his assistance in the experimental work, and Dr. W.-C. Cheng for many helpful discussions. The authors also thank Grace Davison for permission to publish this work.

Literature Cited

1. Cheng, W.-C.; Kim, G.; Peters, A. W.; Zhao, X.; Rajagopalan, K.; Ziebarth, M.; Pereira, C. *Catal. Rev. Sci. Eng.* **1998**, *40* (1-2), 39-79.
2. Krishna, A. S.; Hsieh, C. R.; English, A. R.; Pecoraro, T. A.; Kuehler, C. W. *Additives Improve FCC Process, in Hydrocarbon Processing*. **1991**, 59-66.
3. Schipper, P. H.; Dwyer, F. G.; Sparrell, P. T.; Mizrahi, S.; Herbst, J. A. *Zeolite ZSM-5 in Fluid Catalytic Cracking: Performance, Benefits, and Applications, in Fluid Catalytic Cracking: Role in Modern Refining*, M. L. Occelli, Editor. 1988, American Chemical Society: Washington, D. C. p 64-86.
4. Manning, T. J. *Hydrocarbon Process.* **1997**, *76* (5), 85-88.
5. Biswas, J.; Maxwell, I. E. *Appl. Catal.*, **1990**, *58*, 1-18.
6. Hsing, L. H. In *International Symposium on Advances in Fluid Catalytic Cracking*; ACS Meeting, 1993, Chicago, IL, August 22-27, 1993.
7. Madon, R. J. *J. Catal.* **1991**, *129*, 275-287.
8. Young, G. W.; Suarez, W.; Roberie, T. G.; Cheng, W.-C. In *1991 NPRA Annual Meeting*; San Antonio, TX, 1991.
9. Chen, N. Y.; Degnan, J. T. F.; Smith, C. M. *Molecular Transport and Reaction in Zeolites*; VCH Publishers: New York, 1994.
10. Buchanan, J. S.; Adewuyi, Y. G. *Appl. Catal. A: Gen.* **1996**, *134*, 247-262.
11. Adewuyi, Y. G.; Klocke, D. J.; Buchanan, J. S. *Appl. Catal. A: Gen.* **1995**, *131*, 121-133.
12. Adewuyi, Y. G. *Appl. Catal. A: Gen.* **1997**, *163*, 15-29.
13. Zhao, X.; Weatherbee, G. D.; Rajagopalan, K. R. In *The Fifth World Congress of Chemical Engineering*; San Diego, CA, 1996.
14. Haas, A.; McElhiney, G.; Ginzel, W.; Nuchsbaum, A. *Petrochem./Hydrocarbon Technol.* **1990**, *43*, 21-26.
15. Cotterman, R. L.; Plumlee, K. W. *ACS Meeting*; Miami Beach, FL, 1989.
16. Rajagopalan, K.; Habib, E. T. Understanding FCC Matrix Technology. *Hydrocarbon Process.* **1992**, 43-46.
17. Zhao, X.; Harding, R. H. *Ind. Eng. Chem. Res.* 1999, *38*, 3854-3859 paper in this issue).
18. Zhao, X.; Roberie, T. G., in preparation.
19. Wojciechowski, B. W.; Corma, A. *Catalytic Cracking*; Marcel Dekker: New York, 1986.
20. Venuto, P. B.; Habib, E. T. *Fluid Catalytic Cracking with Zeolite Catalysts*; Marcel Dekker: New York, 1979.
21. Abbot, J.; Wojciechowski, B. W. *Can. J. Chem. Eng.* **1985**, *63* (June): 462-469.
22. Smirniotis, P.; Ruckenstein, E.; *Ind. Eng. Chem. Res.*, **1994**, *33*, 800-813.
23. Buchanan, J. S.; Santiesteban, J. G.; Haag, W. O. *J. Catal.* 1995, *158* 279-287.
24. Mott, R. W.; Roberie, T.; Zhao, X. 1998 NPRA Annual Conference, 1998.

e-Catalysts.com



Leverage the power of data

Log in to your customer portal today at **e-Catalysts.com** and discover what you can do with easy access to sample analysis, order status, Certificates of Analysis, and valuable technical resources.

Not a member yet?

Reach out to your Grace partner to sign up!

GRACE

What's available:

- Easy access to samples including Ecat, fines, feedstock, slurry and more. Quickly find information on various properties, analyze the results and connect with your support team.
- Sample analysis with interactive dashboards for one or multiple units
- Order management system to easily track status of shipped orders or view complete history
- Certificates of Analysis for detailed product quality information
- Easy ordering of free Ecat containers!
- The latest editions of *Catalagram* and Grace's Comprehensive Guide to Fluid Catalytic Cracking



Rapid decarbonization of the way we live requires the use of existing assets and processes. Co-processing of biomass-derived feedstocks in refining processes reduces the carbon intensity of transportation fuels and gained significant momentum in the 2020's. Co-processing is forecasted to increase with the progression of government mandates and incentives and as renewable feedstock becomes more available. Co-processing of bioderived feedstocks is being trialed and implemented around the world with some regional differences.

The article here, published in the Spring 2008 *Catalagram*, discusses biofeed composition, contaminants, and reaction chemistry in hydroprocessing and FCC units. Though the focus was on first generation biofeeds (edible oils) at the time of publication, the discussed effects are valid for the co-processing of second generation biofeedstocks like waste cooking oils, animal fats and other fats, oils and greases (FOGs).


ART Hydroprocessing and Grace FCC catalyst technologies are used in numerous co-processing applications around the world and have proven to support optimum refinery profitability by meeting activity, stability and selectivity requirements in biofeed co-processing. This iconic paper has been the basis for the multiple successful applications in the last 15 years and guides the industry on its endeavor to explore new unconventional feedstock applications.



Stefan Brandt
FCC Market Development Director, Energy Transition
W. R. Grace & Co.



New Opportunities for Co-Processing Renewable Feeds in Refinery Processes

 Brian Watkins, Charles Olsen, Kevin Sutovich, Natalie Petti

 Originally published in *Catalagram* #103 in 2008 (1)

The use of renewable or biobased sources of feed to produce fuels is becoming more widely employed as a means of decreasing dependence on nonrenewable fossil fuel sources. There are typically three common production routes for biodiesel. Fuel which is produced by the FAME (Fatty Acid Methyl Ester) process to meet a fuel specification of ASTM

D6751 is considered biodiesel. Fuels produced from biological material using thermal depolymerization to meet ASTM D975 or ASTM D396 are considered renewable diesel. Fuels that are produced when vegetable oils or animal fats are processed in traditional refining processes are considered co-processed renewable diesel.

Continued from Page 18

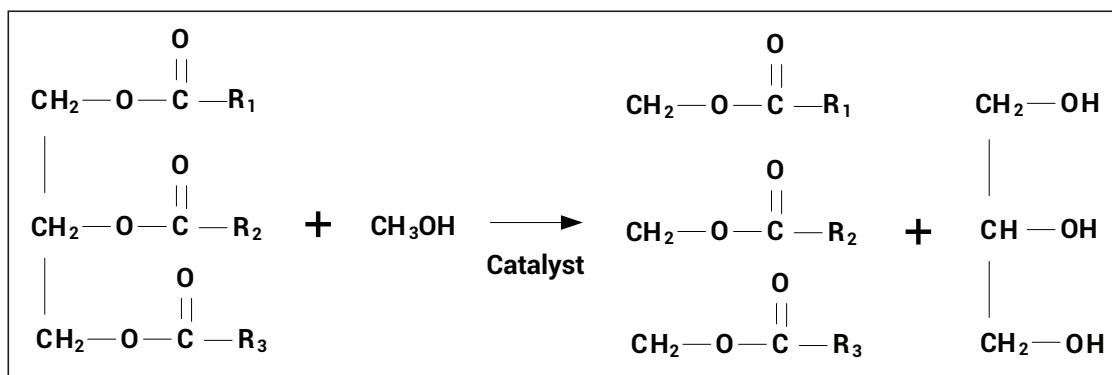


Figure 1. Transesterification reaction

Some common sources of renewable feeds are those produced for food grade oils such as soybean, rapeseed and other vegetable oils. The traditional process for introducing these sources into the diesel pool is to use the transesterification reaction for breaking the glycerol from the fatty acid chains. This reaction requires the use of an alcohol (such as methanol) and a catalyst (such as sodium or potassium hydroxide, NaOH or KOH) in order to break the long chained fatty acids apart from the glycerin molecule. (Figure 1)

These long chained fatty acids (Fatty Acid Methyl Esters or FAME) are most commonly between 16-20 carbons in length with a few exceptions. The long carbon chains are similar in structure to the 16-20 carbon chains found in typical diesel except that FAME compounds contain almost no sulfur or nitrogen and no aromatics, which make them excellent blending components in the diesel pool. FAME products, however, do have a high percentage of oxygen that enables them to be tracked directly at the pump. FAME production occurs in separate facilities and requires a distribution infrastructure to transport the biofuels to a location where they can be blended with conventional diesel. Discrete storage and supporting inventory of the biofuels would be required to guarantee continuous supply. Using one of Advanced Refining Technologies LLC (ART)'s high performance catalysts, we

have been able to capitalize on renewable sources of fuel by bypassing the purchase of FAME products and instead processing the raw materials through conventional hydrotreating equipment to produce a higher quality ULSD product. Refiners who use the co-processing method would have exact knowledge of the bio-based fuels that are incorporated into the diesel pool which helps to ensure the finished blend quality.

Background

Taking a detailed look at the compounds found in typical renewable oils shows that these oils can be treated as classic petroleum based compounds. ART analyzed several different renewable sources of fuels in order to better understand the possible chemistry that would occur if they were processed in a conventional hydrotreater. Soybean, palm and rapeseed oils were studied, as these materials are readily available. A listing of various oils and their structural makeup is shown in Table 1. Bio-based sources of oils can be of significant value when incorporated into the ULS diesel pool due to the low contaminant concentrations and high cetane number of the resulting products.

Components and Description

The major saturated and unsaturated fatty acids found in these oils consist

of palmitic acid (C16:0), linolenic acid (C18:3), linoleic acid (C18:2), oleic acid (C18:1), eicosenoic (C20:1) and erucic acids (C22:1) in varying percentages. If each of these fatty acid chains were to be separated from the glycerol molecule they can be included easily into the diesel pool as normal paraffin components in the 500-650°F boiling range. These n-paraffins can be of significant value for ULSD as they have typical cetane numbers ranging from 95 to 110, which can provide a significant boost for those refiners processing feeds with lower cetane (i.e. FCC LCO's). The typical diesel hydrotreater has only a small effect on cetane with cetane upgrade of about 2-4 numbers.

In the unbroken, unprocessed form, the triglyceride molecules are significantly outside the diesel pool range as they have molecular weights of 700 or greater, while the typical diesel pool has a molecular weight of less than 400. The simulated GC analysis of soybean oil is shown in Figure 2 and indicates that these materials have a fairly narrow distillation showing up in the C₅₀-C₆₀ range. Note that simulated distillation of these compounds is based on the carbon content and molecular weight of the materials and this can sometimes skew the estimated boiling points. Biofeed sources typically have a true boiling point that is much lower than that reported by simulated distillation equipment due to molecular weight

New Opportunities for Co-Processing Renewable Feeds in Refinery Processes

Fats and Oils	C4:0 Butyric	C6:0 Caproic	C8:0 Caprylic	C10:0 Capric	C12:0 Lauric	C14:0 Myristic	C16:0 Palmitic	C16:1 Palmitoleic	C18:0 Stearic	C18:1 Oleic	C18:2 Linoleic	C18:3 Linolenic	C20:0 C22:0 Arachydic- Behenic &	Monoun- saturated acids <C16:1	C20:1 C22:1 Arachidonic- Erucic & others
Molecular wt.	88	116	144	172	200	228	256	254	284	282	280	278	326	226	324
Tallow, wt%						3	27	2	24.1	40.7	2		0.7		0.3
Lard, wt%						1	26	2	13	45.2	10.3				2.5
Butter, wt%	3.5	1.5		25	3	11	30	3.5	12	26	3		1.65	1.5	0.85
Coconut, wt%			8	8	48	16	8.5		2.5	6.5	2				0.5
Palmkernel, wt%			3	5	48.5	17	7.5	0.5	2	14	1		1.5		
Palm, wt%						3.5	395		3.5	46	7.5				
Safflower, wt%							52		2.2	76.4	16.2				
Peanut, wt%						0.5	7	1.5	4.5	52	27		7.5		
Cottonseed, wt%						1.5	19		2	31	44				2.5
Maize, wt%						1	9	1.5	2.5	40	45				1
Olive, wt%						1	13	2	2	68	12		0.5		1
Sunflower, wt%							6		4.2	18.7	69.4	0.3	1.4		
Soy, wt%						0.3	7.8	0.4	2.5	26	51	5	7		
Rapeseed, wt%							3.5	0.2	2	13.5	17	7.5	0.9		56.3
Mustard, wt%						4	3		1.5	39.5	12	8			36
Codliver Oil, wt%						0.2	10	14.5	0.5	28				1	42
Linseed, wt%							6		5	17.3	16	55	0.5		
Tung, wt%										8	12	80			

Table 1. Composition of Various Oils and Fats^{1,2}

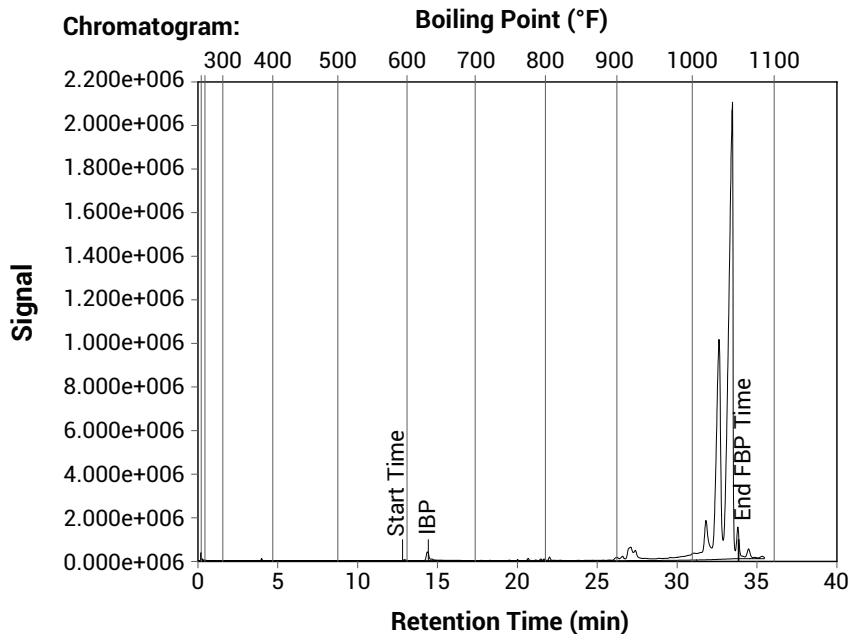


Figure 2. Simulated Distillation (D2887) of Soybean oil

interference. In the unconverted state these triglyceride molecules cannot be blended into the diesel pool at the levels required to meet renewable fuel standards.

Another concern is that these renewable feed sources can include various contaminants. An analysis of several different biofeed sources has indicated the presence of contaminants such as sodium, calcium and phosphorus. Table 2 shows the measured contaminant levels of the soybean, rapeseed oil and palm oils used in this work. The palm oil shows no trace impurities, which indicates that it has been previously processed while the soybean and rapeseed oils have not. In the foreseeable future it is unlikely that the use of these renewable sources would exceed 20% in conventional hydrotreating applications, which would bring the level of all of these contaminants down to 2.5 ppm or less.

Continued on Page 21

Continued from Page 20

	Soybean Oil	Rapeseed Oil	*Palm Oil
API (°)	21.58	21.98	22.98
Specific Gravity (g/cc)	21.6	22.0	23.0
Sulfur, ppm	0	3	1
Oxygen, wt%	10.5	10.62	11.33
Nitrogen, ppm	3.9	16	1.6
D2887 Distillation, °F			
IBP	702	710	625
5%	1059	1065	941
10%	1069	1077	1026
30%	1090	1095	1062
50%	1102	1106	1079
70%	1111	1115	1090
90%	1183	1188	1146
95%	1232	1238	1197
FBR	1301	1311	1302
Metals Contamination, ppm			
Na	2.0	4.7	0.0
Ca	3.0	13.8	0.0
Mg	0.9	0.3	0.0
P	6.5	4.0	0.0
Zn	0.1	0.6	0.0
Al	0.1	0.2	0.0
Mn	0.0	0.1	0.0

* Oil was pre-processed to remove impurities

Table 2. Analysis of Different Biofeed Sources

At these levels ART's high capacity guard materials and Grace Davison specialty catalysts are capable of protecting the downstream high activity catalysts from these damaging poisons.

Since these renewable feeds are derived from a biological source, they also contain a high concentration of oxygen. For the materials listed in Table 1 the oxygen content ranges from 10 to 15%, and is entirely dependent on the length and degree of saturation of the fatty acid chains.

This quantity of oxygen is important, as under normal hydrotreating conditions the oxygen will react with the hydrogen to form water. This water, if generated in a significant enough quantity, may cause problems such as weakening the catalyst support or redistribution of the active metals and

loss of surface area. At the expected blending ratios of 10%, the oxygen content is around 1 to 1.5 wt%, and even if all the oxygen is converted, this is unlikely to generate enough water to be a significant problem.

General Co-Processing Ideas

Looking at these compounds from a hydrotreating perspective, the biofeeds can be classified as mono and di-olefins, since a majority of these compounds have one or two double bonds per fatty acid chain with a few having three. Using the numbers listed in Table 1, palm oil has an average of 1.1 double bonds per chain, rapeseed oil has 1.3 and soybean oil has 1.7. It has been widely established that the olefin saturation reactions occur quite rapidly and tend to happen near the top of the catalyst bed in a hydrotreater. The reactions go to near completion at typical hydrotreating conditions, and will generate between 130-150 BTU's per standard cubic foot of hydrogen consumed. The reaction pathways to hydrotreat the bio-oils is shown in Figure 3. In the first step of the reaction, the unsaturated fatty acid chains are quickly converted into fully saturated n-paraffins. The second reaction that must occur in order to ensure that the compounds will be of the appropriate size for the diesel pool is the breaking of the fatty acid chains away from the glycerin molecule which requires cleavage of a carbon – oxygen bond.

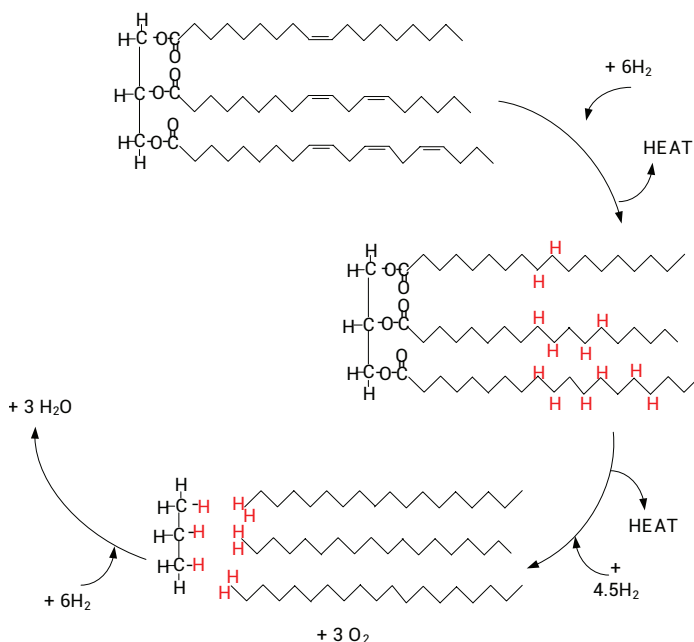


Figure 3. Pathways to Hydrotreating of Renewable Oils

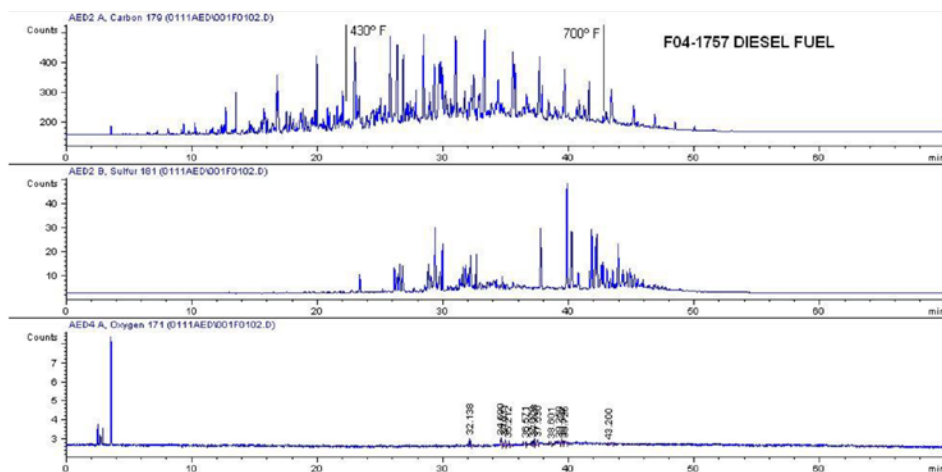


Figure 4. Chromatogram of Sulfur, Carbon & Oxygen in a Diesel Feedstock

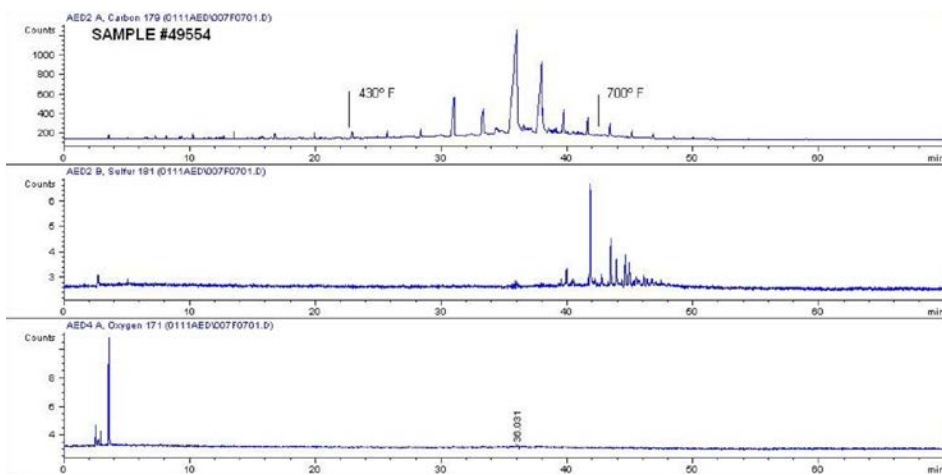


Figure 5. Chromatogram of Sulfur, Carbon and Oxygen in a Co-Processed Product

This reaction is expected to take place at a rate similar to that of sulfur compounds such as sulfides and disulfides. In order to verify that this is indeed the reaction that is taking place, several different feed sources were analyzed for oxygen in order better understand where they are likely to be distributed in the feeds. This analysis has a detection limit of approximately 2.6 ppm oxygen. Figure 4 is a Carbon-Sulfur-Oxygen chromatogram for a diesel feedstock that contains 263 ppm oxygen.

Analytical techniques using GCAED have shown that in normal ULSD operation, no oxygen is detected in the products

at levels below 500 ppm sulfur. This can be seen in Figure 5 which shows the analysis of one of the co-processed products which has a total sulfur of 31 ppm and less than 1 ppm nitrogen.

Pilot Plant Testing of Renewable Oils

In order to understand the process for co-treating renewable fuel components in a hydrotreater, ART completed a number of pilot plant studies. A wide range of ULSD operating conditions were investigated to determine if there is an optimal operating window for

processing these types of feeds. The conditions included hydrogen pressures from 450 to 1100 psia and hydrogen to oil ratios of 1000 to 3000 SCFB.

The three different renewable sources of oil were blended in separately with a typical straight run (SR) diesel feedstock. The renewable component level was varied from 10% to 80% and hydrotreated over the range of processing conditions listed here. The SR component properties are listed in Table 3, along with 5 different blends of the bio components. As can be seen in the table, the effects of blending in the renewable source are to dilute the sulfur, nitrogen and aromatic contents and decrease the API gravity.

ART then conducted testing on blends containing the various renewable sources of feedstock at the targeted 10% level. Figure 6 summarizes some of the results of the testing. The testing showed that soybean and rapeseed oils behave similarly when co-processed in a SR diesel. The feed blends required essentially the same temperature for 10 ppm product sulfur, and the apparent activation energy (temperature response) for the two feed blends is similar to that of the SR feedstock alone. The palm based oil, which had been previously processed, was apparently easier to treat to low sulfur diesel levels, but for 10 ppm product sulfur the temperature was only slightly lower than that for the SR feed. The apparent activation energy for this feed blend was lower than the SR component indicating the temperature response in the unit was lower. Comparing the feeds at ultra low sulfur levels suggests the co-processing of the renewable oils has only a small effect on the performance of the hydrotreater. The data indicates that the least reactive blend contains rapeseed oil, followed by the soybean oil blend and finally the palm oil blend. The difference, however, is only about 10°F for <10 ppm product sulfur.

Continued on Page 23

Continued from Page 22

	SR Oil	10% Soybean	10% Palm	10% Rapeseed	40% Soybean	80% Soybean
API	34.44	33.03	33.50	33.29	29.24	24.38
Specific Gravity, g/cc	0.852	0.859	0.857	0.858	0.879	0.907
Sulfur, wt%	1.123	1.083	1.092	1.042	0.670	0.210
Nitrogen, ppm	130	82	75	67	47	16
Oxygen, wt%	0.0	1.2	1.2	1.1	4.7	8.9
Aromatics, wt%						
Mono	17.76	15.85	15.87	15.86	10.32	3.34
Di	7.39	6.60	6.60	6.60	4.29	1.39
Poly	2.1	1.87	1.88	1.87	1.22	0.39
Total	27.25	24.32	24.34	24.33	15.84	5.12
D2887 Distillation, °F						
IBP	222	209	209	210	239	329
10%	477	465	459	465	498	571
30%	579	559	557	559	579	1009
50%	613	595	592	594	631	1119
70%	643	632	628	630	1108	1130
90%	681	720	688	715	1130	1135
FBP	740	1127	1121	1127	1134	1139
Cloud Point, °F	19.9	21.7	24.1	22.8	22.0	19.1
Cetane Index	53.8	50.6	51.2	50.9	46.4	NA

Table 3. Straight-Run (SR) and Bio-Blend Analyses

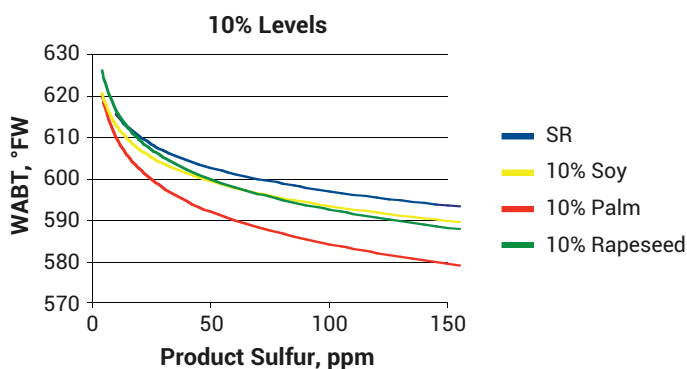


Figure 6. Results of Various Renewable Components

Looking at other diesel product properties that are important to refiners reveals that there is a boost in the product cetane index by almost 2 numbers. This increase in cetane was seen over the wide range of conditions tested and is a reflection of the normal paraffins from the renewable oil discussed above.

Figure 7 summarizes some of the cetane index results achieved at higher pressure for each of the bio-feed blends.

The impact of low pressure operation on cetane improvement is shown in Figure 8 for a 10% renewable feed blend. Not surprisingly, lower pressure operation results in a lower cetane index for the SR feed, but the addition of the renewable oil again provides a consistent two number increase in cetane index.

This is a good indicator that the large fatty acid molecules are being broken down into the three individual fatty acid chains via the breaking of the C-O bonds. Figure 9 compares the D-2887 distillation chromatograms of the SR products at 10 ppm sulfur to that of the coprocessed products, and it is evident that there is an increase in the concentration of the n-paraffins between 500°F and 600°F boiling points. It is this increase that yields the significant boost in cetane.

New Opportunities for Co-Processing Renewable Feeds in Refinery Processes

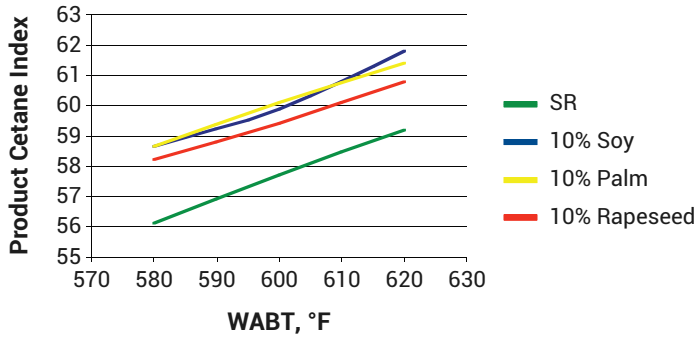


Figure 7. Cetane Boost when Co-Processing Bio-Feeds at High Pressure

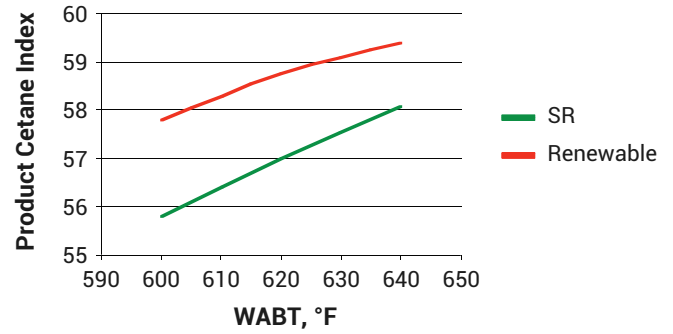
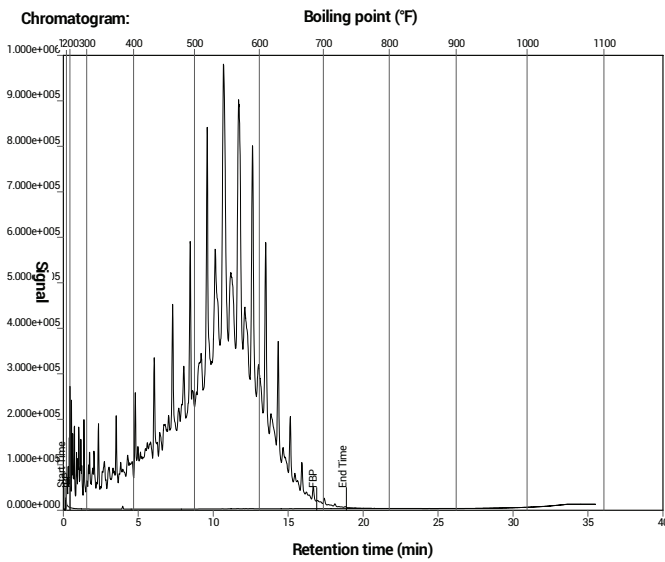
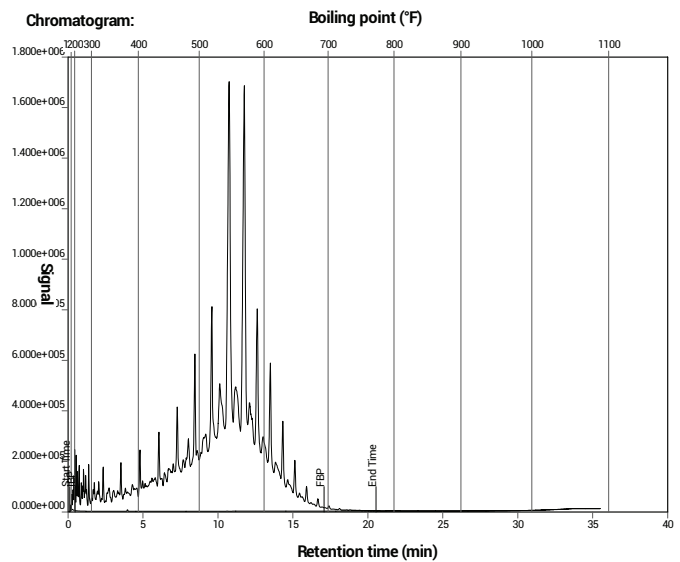


Figure 8. Cetane Boost when Co-Processing Bio-Feeds at Low Pressure



**Straight-run product
@ 10 ppm sulfur**



**Co-processed product
@ 10 ppm sulfur**

Figure 9. Results of Various Renewable Components

The hydrotreating of the bio-blended oil results in a product that no longer contains material in the C₅₀ to C₆₀ range. This is consistent with the theory that the individual fatty acid chains are being broken apart to hydrocarbons of similar size to those in the SR diesel.

Due to the addition of unsaturated chains from the bio component, there is expected to be an increase in hydrogen consumption to saturate these C=C bonds. With this additional hydrogen usage, it is important to also be aware of any changes in product aromatics, as reactions to saturate aromatics are high consumers of hydrogen and would compete with the saturation reactions under hydrogen limited conditions. Figure 10 summarizes the product aromatics for one of the bio-blended feeds. The total aromatics are consistently two

numbers lower than the SR feed, which is the same as the actual difference in the total aromatic content of the two feeds. The lower aromatic content of bio-blended feeds allows the refiner to achieve lower product aromatic content, which may be valuable as future regulations may require a lower total aromatic limit on diesel fuel.

At lower pressure and H₂/oil ratios, the total aromatic content shows a similar response, with two numbers lower total aromatics when co-processing bio-based feedstock. With reduced operating pressure, there is a decrease in the aromatic saturation ability of the catalyst, and the possible use of renewable oils may help to offset this.

Continued on Page 25

Continued from Page 24

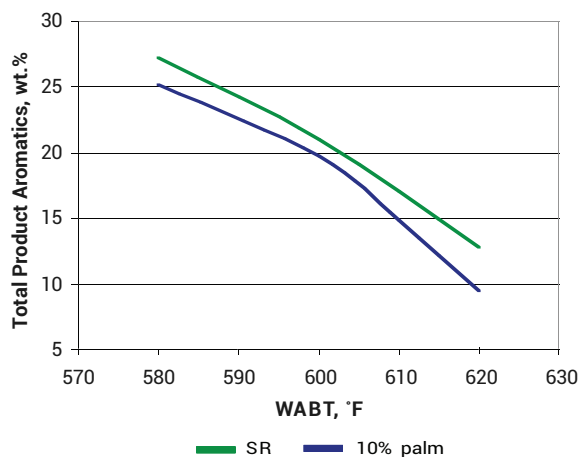


Figure 10. Comparison of Total Aromatics of SR Oil with 10% Renewable Oil at High Pressure

Cloud point specifications vary based on the location of the refinery and the end user of the fuel. Although the blending of the bio components yields improvements in the diesel cetane, there is the concern about the biofeed based diesel cloud point. It is widely known that n-paraffins have a significantly higher cloud point than other same carbon number hydrocarbons. Since hydrotreating converts the fatty acid chains into long chained n-paraffins, the cloud point of the mixture will increase. Figure 11 summarizes the product cloud points after hydrotreating the three blended feeds. The SR feed is included for comparison.

Processing the SR feed has essentially no impact on the product cloud point and the products are all within a few degrees of the feed cloud point shown in Table 3. The renewable containing feeds all have slightly higher cloud points compared to the SR feed (see Table 3), and after hydrotreating the cloud point increases by 6 to 10°F. This increase in cloud point can be significant especially in cold weather climates. By using other technology provided by ART, the problem of increased cloud point can be reduced or eliminated.

Co-Processing in FCC Units

Another option for refiners could be to co-process bio components in fluid catalytic cracking units (FCCUs). Unlike hydrotreater units where catalyst cannot be changed without taking the unit out of service to reload the reactor, continuous replacement of catalyst in the FCC unit enables the refiner to adjust the catalyst formulation to optimize yields. Characterization of the biofeedstock and an understanding of the refiner's objectives can allow the catalyst supplier to develop a formulation to maximize profits.

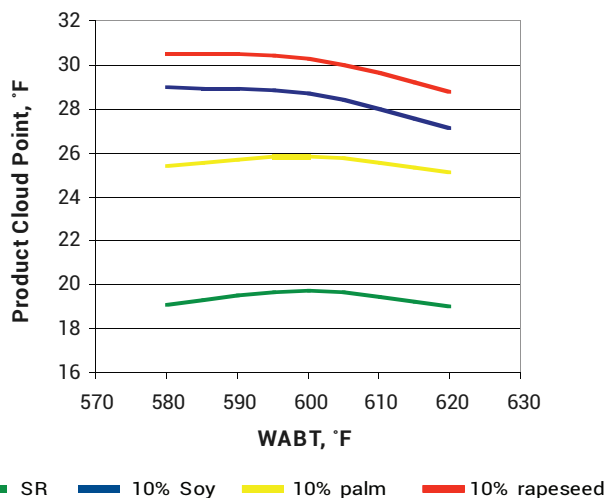


Figure 11. Cloud Points of Bio-Blended Feeds Compared to SR Feed

Pilot Plant Testing of Renewable Oils

To illustrate the impact on FCC yields with the incorporation of vegetable oil feedstocks into FCC feed, a pilot plant study was conducted by starting with a composite feed of VGO and resid with properties shown in Table 4, then the soybean, palm and rapeseed oils used in the hydrotreating testing were blended to 0%, 7.5% and 15% concentrations. The hydrotreated VGO in this table is used in a later study to compare the effects of different base feedstocks.

The blended FCC feeds were cracked over an FCC catalyst, which was deactivated using a CPS-3 type protocol^{3,4} to 1000 ppm nickel and 2000 ppm vanadium. The catalyst was formulated to provide maximum bottoms upgrading. Properties of the deactivated catalyst are shown in Table 5.

The pilot unit was run at a constant reactor temperature of 1000°F, and the deactivated catalyst was tested at three catalyst-to-oil ratios (4,6,8) for each of the blended feeds in the pilot unit.

Figure 12 shows that all three of the blended bio-feeds are easier to crack than the base feed. The addition of the bio component increases the cracking activity (lower cat to oil for a given conversion), and increasing the concentration of a given bio component yields an increase in conversion at constant cat to oil ratio.

	Composite Resid	Hydrotreated VGO
API	24.4	27.3
Sulfur, wt%	0.53	0.20
Nitrogen Total/Basic, ppm	813/287	800/280
Concarbon, wt%	1.12	0.2
K-Factor	11.96	12.23
Aromatic Ring, wt%	22.7	18.9
Naphthenic Ring, wt%	13.6	11.5
Paraffinic Carbons, wt%	63.8	69.5
Vanadium, ppm	2.5	1.8
Nickel, ppm	1.1	0.7
D6352 Distillation, °F		
IBP	494	460
10	689	703
30	775	786
50	834	849
70	899	923
90	1018	1034
95	1110	1088
FBP	1279	1226

Table 4. Feedstock Analysis for FCC Study

MAT, wt%	
Total Surface, m ² /g	175
Zeolite Surface, m ² /g	99
Matrix Surface, m ² /g	76
Unit Cell Size, Å	24.29
Rare Earth, wt%	2.04
Alumina, wt%	50.23

Table 5. Deactivated Catalyst Properties

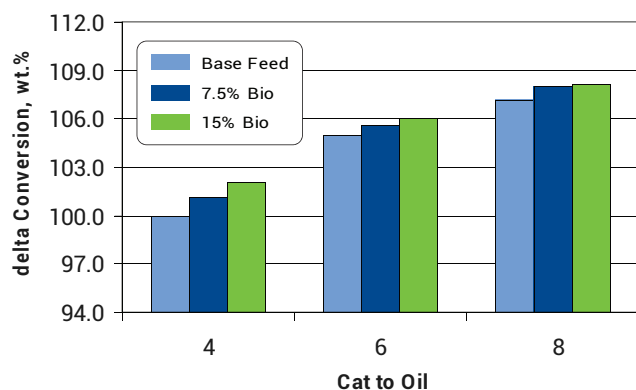


Figure 12. Conversion vs. Cat to Oil

Figure 13 shows that the bio-feeds produce significantly less coke per unit conversion than the base feed. Increasing the concentration of any of the three bio components further reduces the amount of coke produced for a given conversion. The rapeseed oil is the easiest to crack, followed by the soybean oil with the palm oil being the most difficult of the components to crack.

The trends observed in Figures 12 and 13 can be explained by the individual fatty acid compositions for each of the bio components reported previously in Table 1. The reaction pathways for triglycerides have been studied extensively by Dupain et. al.⁵, and under FCC conditions, were found to occur in two distinct steps. First, thermal cracking of the triglyceride occurs, releasing the fatty acid chains from the glycerin backbone. Conversion of free fatty acids via thermal cracking is very low, requiring catalytic cracking in the subsequent step to break the high molecular weight fatty acid molecules into smaller, more valuable products. Free fatty acids with more saturation will be more difficult to crack than those that contain greater amounts of double bonds⁶. With the lowest average of 1.1 double bonds per fatty acid chain, this explains the performance of the palm oil versus the soy or rapeseed oils.

The bio-feeds also have significantly less contaminants (sulfur, nitrogen, and potentially metals) than the base feed, but additional characterization of these materials is very difficult. Traditional analysis methods developed for fossil based hydrocarbons will not apply to the bio-based materials. Measurements such as concarbon, n-d-M (which is an estimate of the chemical composition of the feedstock using refractive index (n), the density (d) and the molecular weight (M) of the feed to calculate the amount of paraffinic (Cp), naphthenic (Cn), and aromatic (Ca) carbon species in the feed) and even GC based distillations can be flawed due to the thermal cracking

Continued on Page 27

Continued from Page 26

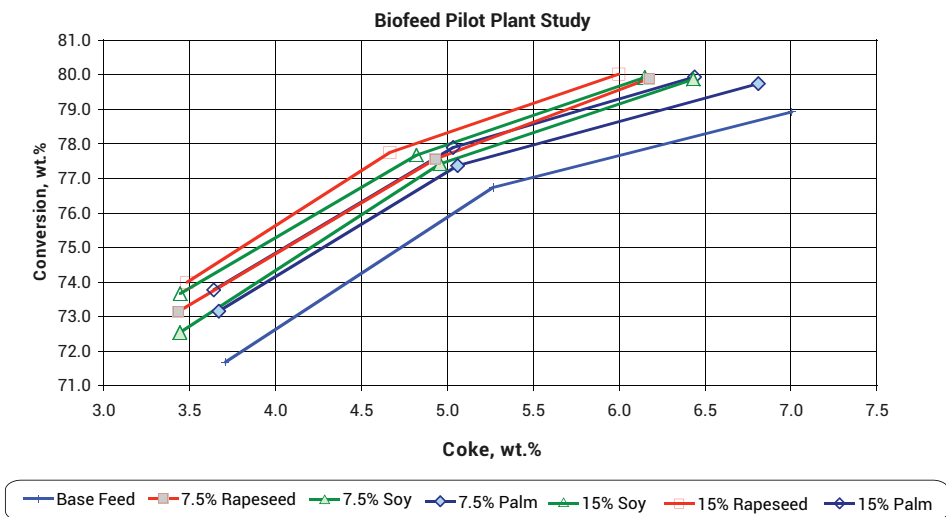


Figure 13. Conversion vs. Coke

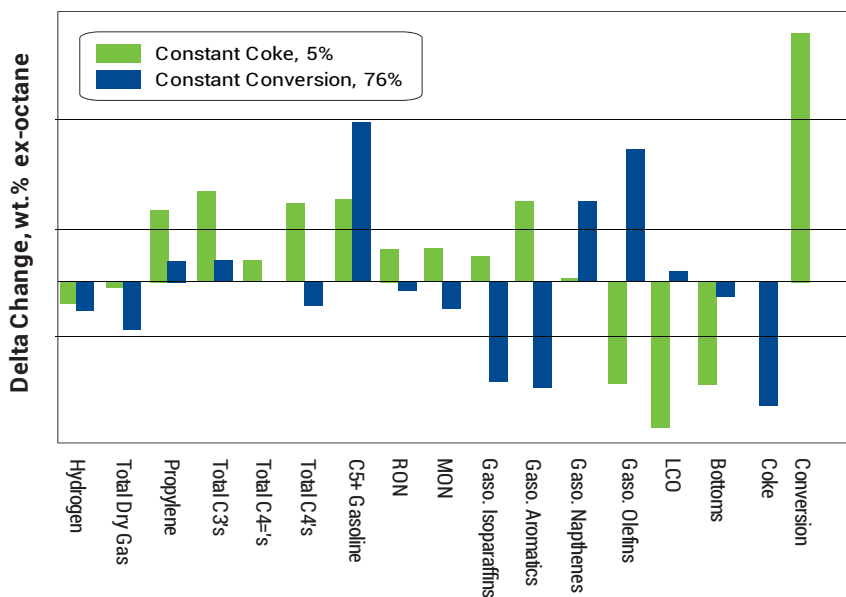


Figure 14. Comparison of 15% Blended Feeds

response of the bio-feeds. With virtually no sulfur in each of the bio-feeds, incorporating them into FCC feed would dilute key FCC product stream sulfur levels, potentially allowing for downstream hydrotreating benefits (less gasoline octane loss, extended catalyst run length) or for a lower cost base FCC feed at constant product sulfur.

Since the increase in the concentration of the biofeeds in the feed directionally increases the magnitude of the response in the FCC yields, to simplify the trends the remaining results will be presented for only 15% blends. Additionally, while commercial FCC units operate to constant coke, if there is a significant difference in coke yield when comparing individual product yields, the constant coke comparison will accentuate the

differences in yields. Comparing data on a constant conversion basis will smooth out the data and allow for a more representative comparison. Figure 14 shows the yields for the biofeeds at 15% concentration for constant coke and conversion compared to the base feed.

Beginning with hydrogen, Figure 15 confirms that the reduction in hydrogen yield with the biofeeds is significant. Hydrogen can come from three sources: a by-product of dehydrogenation with metals, a product of thermal cracking, or a product of catalytic cracking.

One potential method to determine the reason for the reduction in hydrogen with the bio-based materials involves a comparison of the C₅ olefins yields in gasoline for the feeds tested. During dehydrogenation reactions, gasoline range olefins react with the metals on the catalyst to produce hydrogen⁷. If the biofeed materials produce less gasoline range olefins than the base feed, this could be the cause for the reduction in hydrogen.

From our analysis, the addition of biofeeds to the base feed does not reduce the amount of gasoline olefins produced, and therefore the reduction in hydrogen observed with the biofeeds is not likely due to reduced dehydrogenation reactions.

Alternatively, the potential for the biofeeds to produce hydrogen during the catalytic cracking process can be evaluated by comparing the propane yield for the feeds tested. In cracking a biofeed, the fatty acid molecules that were liberated by the initial thermal cracking step will subsequently crack along the pathways defined for either paraffin or olefin molecules. If the fatty acid mixture is more olefinic, it will be very reactive and will easily crack to produce smaller gasoline range olefins⁶. A more paraffinic fatty acid mixture can react along multiple potential pathways to produce a variety of products (Figure 16).

The initiation step occurs on either Bronsted or Lewis acid sites on the catalyst, and on the Bronsted site there

are two additional potential pathways for the paraffin to react to produce a carbenium ion. Protolytic cracking can occur with the elimination of the paraffin,

or the carbenium ion can be formed with the elimination of a hydrogen molecule (Figure 17).

If protolytic cracking is prevalent, the chain terminating product is propane. Figure 18 shows that the propane yield for all three of the biofeeds is lower than the base feed. Thus there is an indication that the reduction in propane and hydrogen is potentially due to reduced protolytic cracking of the fatty acids compared to a typical FCC feed. This also indicates that the double bonds on each of the free fatty acid molecules, which are more reactive, are the initiation sites for the cracking reactions.

The fatty acid molecules are cracking into gasoline and propylene, as can be seen in Figures 19 and 20.

The gasoline trend indicates overcracking for all three of the biofeeds, and also for the base feed. Over cracking occurs when the gasoline molecules produced are subsequently cracked into lighter molecules. Catalyst activity, cat to oil ratio, and temperature can all drive a feed to over-cracking, and the easier the feed is to crack, the higher the tendency to over-crack. Table 4 shows that the base feed itself is fairly paraffinic, with a Watson K-Factor that indicates it will produce high conversions. The incorporation of the highly paraffinic fatty acids from the biofeeds makes the blended feeds even easier to crack. Catalyst activity will be determined based on specific unit constraints and objectives when commercial processing of the blended bio-containing feeds. The overcracking trends observed in the pilot plant testing can be corrected and is not expected in commercial operations.

The influence of the bio-based materials on the gasoline properties is important, as the oxygen species in the triglycerides could break down to water, or they could potentially be converted into aldehyde and furan species which are undesirable from an environmental, health and safety perspective. Gas Chromatography-Atomic Emission Detector (GC-AED) was performed on the liquid product, which was recovered after each test run through the pilot unit.

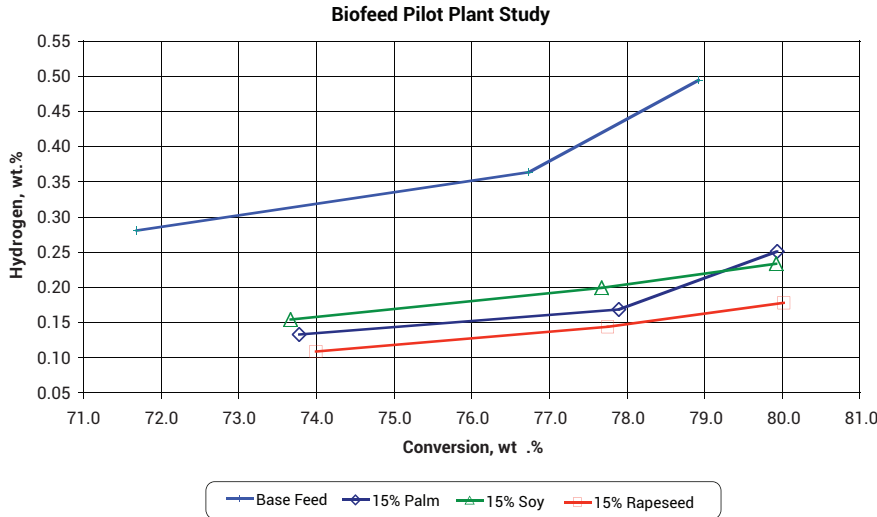


Figure 15. Hydrogen Yield vs. Conversion

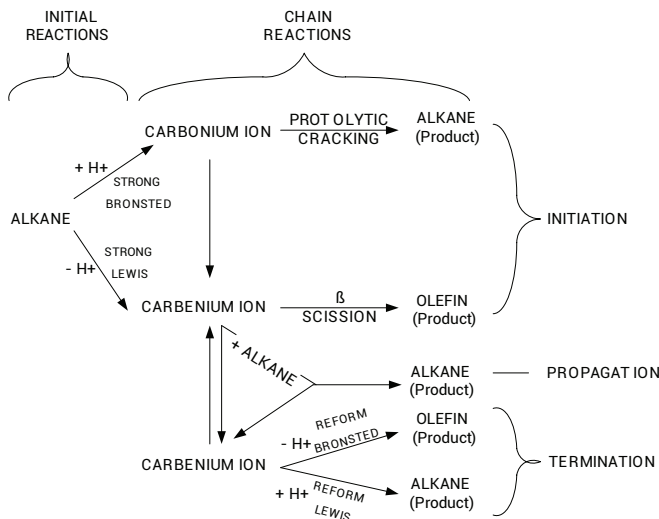


Figure 16. Reaction Pathway Network for Alkane Cracking

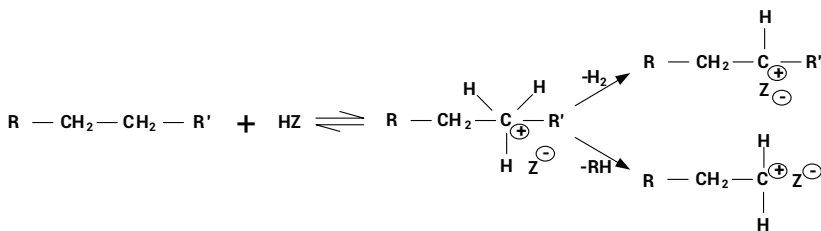


Figure 17. Paraffin Reaction Pathway

Continued on Page 29

Continued from Page 28

The GC-AED was run in oxygen mode in order to detect oxygen species using the same technique as in Figure 4 and 5. The only peaks that showed up were initial peaks between two and four minutes from the syringe wash solvents. No discernible oxygen peaks were present in the liquid product thus, no undesirable oxygen species were present.

The (R+M)/2 octane of the gasoline produced by the biofeeds is lower than the base feed, with contributions from both RON and MON contributing to the trend. The magnitude of the response in gasoline RON may depend on the source of the biofeed, but in general the loss of RON is fairly small. (Figure 21) MON is consistently lower with the biofeeds, and this is due to the lower aromatics content of the gasoline produced with the biobased materials in the feed.

The response in C₄ yields can be explained by again reviewing the individual fatty acid compositions for the three biofeeds as shown earlier. Palm oil contains significant percentages of both C₁₆ (palmitic) and C₁₈ (oleic) acids. The highest % fatty acid in soybean oil is C₁₈ (linoleic), and C₂₀ and C₂₂ (arachidonic and erucic) acids are present in the largest concentrations in rapeseed oil. Once these molecules are liberated from the glycerin backbone via thermal cracking, they follow a typical FCC rule of thumb, which is that the longer the chain (ie. the higher the carbon number in the molecule), the more broad the distribution of product olefins that will result from catalytic cracking of the molecule. Thus, the palm oil produces the largest amount of C₄ olefins, as seen in Figure 22.

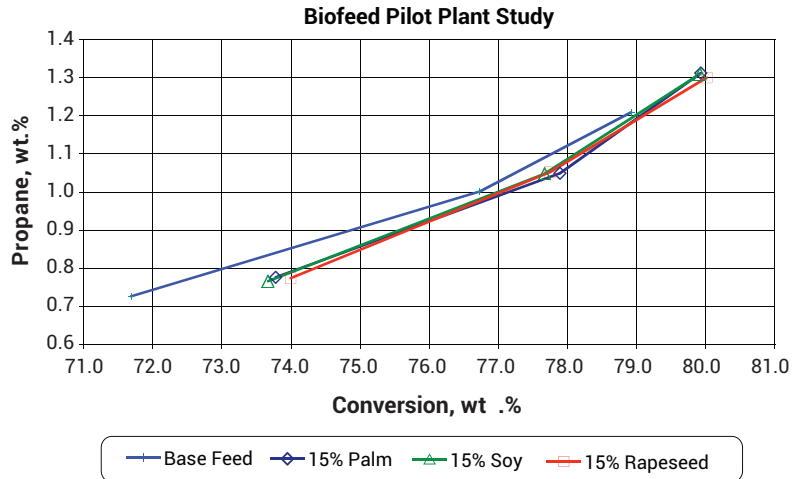


Figure 18. Propane Yield vs. Conversion

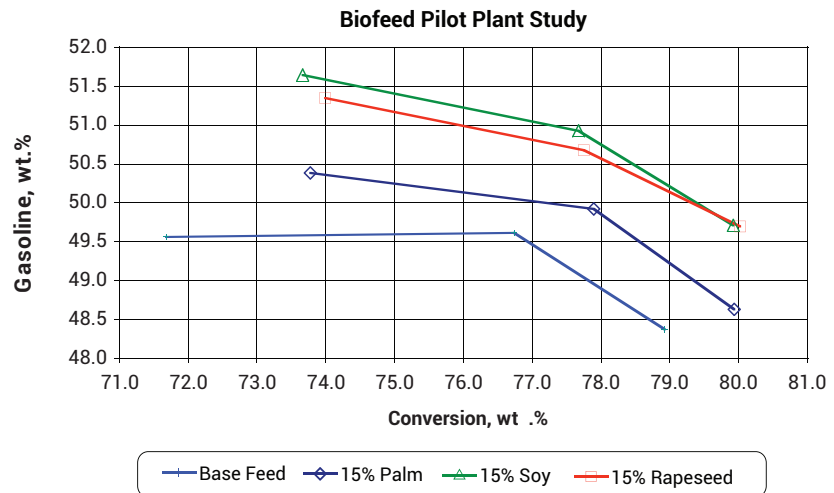


Figure 19. Gasoline Yield vs. Conversion

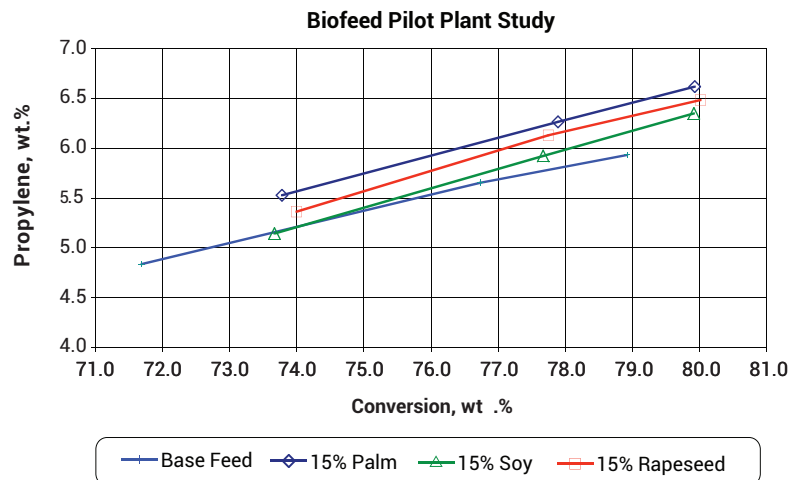


Figure 20. Propylene Yield vs. Conversion

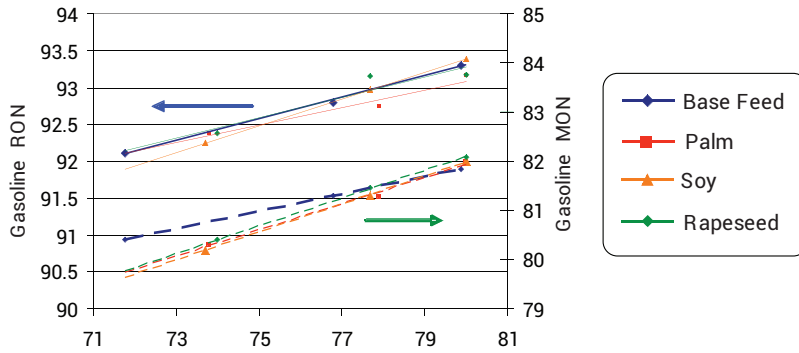


Figure 21. Gasoline RON & MON for Bio-blends

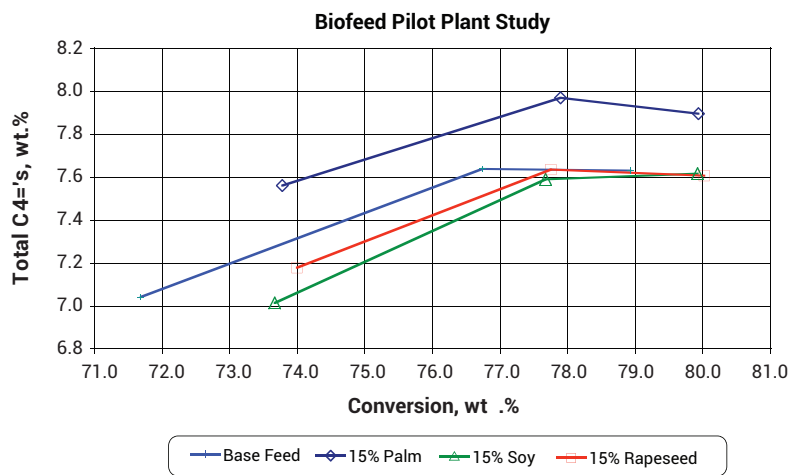


Figure 22. Butylene Yield vs. Conversion

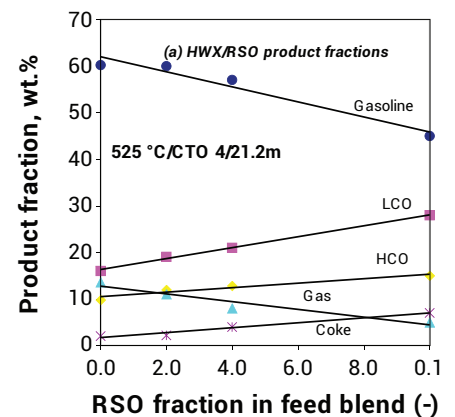
Influence of Base Properties

Ultimately the yield response for the addition of a bio-feed material into FCC feed will depend on the properties of the base FCC feed. Dupain et al.⁵ observed that the addition of rapeseed oil to a hydrowax feed would yield less gasoline and C4 minus products, and higher amounts of LCO, slurry and coke (Figure 23).

While the properties of the specific hydrowax feed are not known, in general these feeds are highly paraffinic and the addition of vegetable oils to that type of feed would in fact degrade the overall properties of the feed. This is confirmed by comparing the response in yields for the addition of rapeseed oil to the two base FCC feeds from Table 4. The general trends in yields for constant conversion

are shown in Figure 24. The addition of rapeseed oil to the hydrotreated VGO feed produced more coke and hydrogen, at constant conversion, but at constant coke the conversion was actually lower with the rapeseed oil in the feed. By comparison, the composite feed shows strong improvements in yields with the addition of rapeseed.

These trends suggest that if a base FCC feed is paraffinic, yields may in fact worsen with the addition of a bio based material into the feed, whereas for VGO or resid types of feed, yields may instead improve. Future work will include examining the role of the base feed on yields with the incorporation of biofeed materials into the FCC feed.



Applied Catalysis B, Environmental 72, reprinted by permission

Figure 23. Quantitative Yields for Different Hydrowax/Rapeseed Oil Blends

Continued on Page 31

Continued from Page 30

	Hydrotreated VGO	Composite Feed
Hydrogen	↑	↓
Wet Gas	↓	↑
Gasoline	↑	↑
LCO	↑	↓
Bottoms	↓	↓
Coke	↑	↓

Red: Undesirable

Green: Undesirable

Grey: Depends on the refiners objectives and constraints

Figure 24. Yield Trend Comparison for Feeds at Constant Conversion

Conclusion

Based on these results, the use of ART's high activity hydroprocessing catalysts or Grace's high performance FCC catalysts can enable refiners to co-process renewable oils through conventional refining equipment. Co-processing can be incorporated into a refiner's operating strategy with minimal detriment to catalyst stability or yields, but the effect on an individual operation will depend on the base feed and conditions. Grace Davison's Biofuel Technologies Group utilizes resources across Grace and its affiliates to evaluate options for refiners who wish to consider incorporating co-processing biofeeds into their operation, but want to understand the optimum configuration to maximize their profitability.

The authors of this paper would like to thank the following people for their contributions to this project:

Susan Ehrlich, Business Director Biofuel Technologies Group;
Rick Wormsbecher, Research and Development Fellow, Refining Technologies

References

1. Data derived from **Organic Chemistry**, W.W. Linstromberg, D.C. Health and Co., Lexington, MA, 1970
2. Data derived from **Organic Chemistry**, Morrison and Boyd, 6th Edition, 1992
3. Wallenstein, D., Roberie, T., and Bruhin, T., *Catalysis Today* 127, 2007, pp. 54-69.
4. Wallenstein, D., Harding, R.H., Nee, J.R.D., and Boock, L.T., **Applied Catalysis A: General** 204, 2000, pp. 89-106.
5. Dupain, X., Costa, D.J., Schaverien, C.J., Makkee, M., Moulijn, J.A., **Applied Catalysis B: Environmental** 72, 2007, pp. 44-61.
6. W.-C. Cheng, E.T. Habib, Jr., K. Rajagopalan, T.G. Roberie, R.F. Wormsbecher, M.S. Ziebarth, **Handbook of Heterogeneous Catalysis**, 2nd edition, G. Ertl, H. Knoezinger, F. Schueth, J. Weitkamp (Editors), Wiley-VCH, Weinheim, 2008, Chapter 13.5.
7. Zhao, X., J. A. Rudesill, W-C. Cheng, Preprints of Symposia - American Chemical Society, Division of Fuel Chemistry, 46(1), 2001, pp. 240-244.
8. B. W. Wojciechowski, and A. Corma, **Catalytic Cracking. Catalysts, Chemistry, and Kinetics**. Chemical Industries 25, 1986, New York: Marcel Dekker

A photograph of a vast agricultural field with rows of green crops stretching towards a horizon under a blue sky with light clouds. The word "AHEAD" is superimposed in large, thin, black-outlined letters across the middle of the image.

A long history of looking

AHEAD

For nearly a century, Grace catalysts have kept fuel and petrochemical feedstocks flowing from the industry's largest refineries to the trucks, trains, planes, and ships that keep our world running.

We are leveraging our long history of innovation in fluid catalytic cracking to develop products that enable lower carbon fuels and help meet the challenges of the energy transition.

GRACE

[grace.com](https://www.grace.com)




Effective management of hydrocarbon (HC) partial pressure is crucial for many FCC units operating at high feed rate while targeting high octane gasoline and petrochemical yields. In the article "Effect of Hydrocarbon Partial Pressure on Propylene Production in the FCC," published in *Catalagram* No. 103 in 2008, results of comprehensive laboratory work are discussed to better understand this relationship. There is a clear correlation between HC partial pressure and hydrogen transfer (HT), explained by the increase of bimolecular reaction rate relative to monomolecular reactions such as cracking. This higher HT has a detrimental impact on gasoline octane and LPG olefin yield, as well as the efficiency of ZSM-5 based additives. The results of this study help to build more realistic simulation models for optimizing both operating conditions and catalyst technologies. High-activity ZSM-5 additives like ZAVANTI™ enables refiners to overcome high HC partial pressure and maintain required propylene yields. Grace also has a wide portfolio of ultra-low HT catalysts that provide improved high unit HC partial pressure management. Ask your Grace representative how to extract the most value of your unit's operation.



Rafael Gonzalez
Regional Marketing Manager
W. R. Grace & Co.

Effect of Hydrocarbon Partial Pressure on Propylene Production in the FCC

 Ruizhong Hu, Gordon Weatherbee, Hongbo Ma, Terry Roberie, Wu-Cheng Cheng

 Originally published in *Catalagram* #103 in 2008 (22)

Many refiners have continually revamped and debottlenecked their FCC units to increase feed throughput and improve profitability. Most FCC units are running at a significantly higher feed rate than the original design. With higher throughput, in order to maintain catalyst and vapor velocity in the riser and cyclones, the unit pressure and consequently the hydrocarbon partial pressure need to be increased. Current laboratory methods for evaluating FCC catalysts and additives cannot match hydrocarbon partial pressures in commercial FCC units. One reason

is that available laboratory testing equipment, such as ACE and MAT typically operate at atmospheric pressure. The Davison Circulating Riser (DCR), a pilot plantscale testing unit, is regularly operated under total pressure similar to commercial FCC units¹. However, due to the small diameter of the DCR riser, a relatively large amount of nitrogen is needed to lift the catalyst, thus decreasing the hydrocarbon partial pressure. Studies documenting the effect of hydrocarbon partial pressure on FCC yields are scarce.

Continued from Page 34

It is generally expected that an increase in hydrocarbon partial pressure will increase the rate of all bimolecular reactions, including hydrogen transfer, relative to cracking, which is unimolecular. An increase in the rate of hydrogen transfer will result in a reduction of olefins in both gasoline and LPG and an increase in gasoline range aromatics and paraffins. The change in the rate of hydrogen transfer could also affect gasoline sulfur concentration and the effectiveness of gasoline sulfur reduction catalysts and additives. Moreover, the effectiveness of ZSM-5 additives, which are used to produce light olefins, especially propylene, could be affected by hydrocarbon partial pressure. Since ZSM-5 works by cracking gasoline range olefin molecules, changing the rate of hydrogen transfer could have a profound impact on propylene yield.

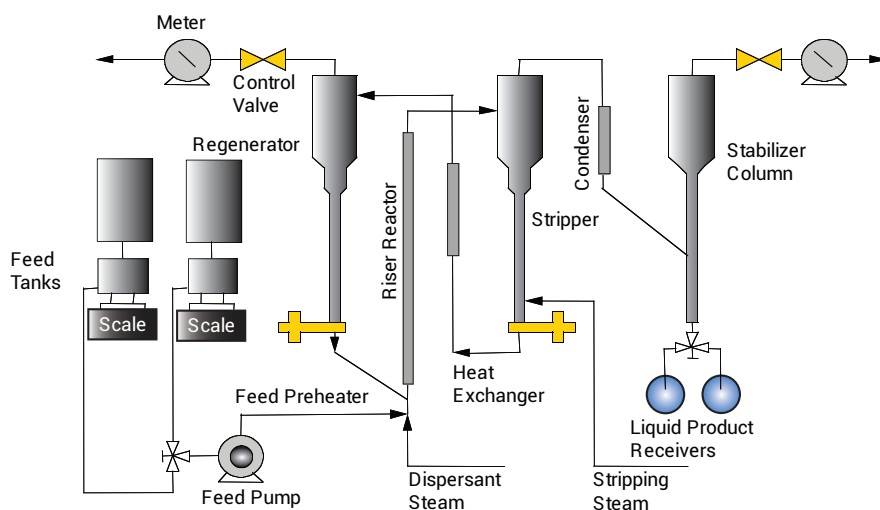
This paper will discuss the results of a series of cracking experiments in the DCR, where the hydrocarbon partial pressure was varied by varying the total reactor pressure, the feed rate and the amount of lift gas. The effect of changing hydrocarbon partial pressure on hydrocarbon yields, especially that of light olefin, and gasoline sulfur will be discussed.

Experimental

At the right is a schematic diagram of the standard DCR setup. The range of operating conditions in the DCR is shown in Table X. Operation of the DCR has been described previously¹. Similar to commercial FCC units, the DCR is operated in adiabatic mode. In typical DCR operation, the regenerator temperature, the riser outlet temperature and the feed rate are set. The catalyst circulation rate and thus, the catalyst to oil ratio, is changed by varying the feed pre-heat temperature. During operation of the DCR, a metering pump precisely controls the feed rate as feed is pumped from the load cell through a preheater. Nitrogen and steam, injected through

a separate preheater/vaporizer, are used as a feed dispersant. Catalyst and product pass from the riser to the stripper overhead disengager. Products exit the disengager through a refrigerated stabilizer column to a control valve which maintains unit pressure at the desired level. A section of the stripper-regenerator spent catalyst transfer line consists of a shell and tube heat exchanger. The rate of heat transfer across this exchanger provides a precise and

reliable method to calculate the catalyst circulation rate. The stabilizer column, also called the debutanizer column, is operated to separate C₄ minus from the liquid product, which is condensed and collected. The collected liquid is analyzed by GC (SIMDIS – simulated distillation) to provide gasoline (ibp - 430°F), LCO (430-700°F), and 700°F + bottoms fractions. The gaseous products are metered and batch collected for subsequent analysis by GC.



Schematic Diagram of Grace Davison DCR

Control Parameter	Range
System Pressure	< 45 psig
Catalyst Charge	1500-4000 g
Catalyst Circulation Rate	2500-15000 g/h
Feed Rate	350-2000 g/h
Feed Types	GO, VGO, Resid
Feed Preheater Temperature	120-400°C (250-750°F)
Riser Temperature	<590°C (<1100°F)
Disengager Temperature	<746°C (800-1100°F)
Stripper Temperature	427-593°C (800-1100°F)
Stabilizer Column Temperature	-34°C (-30°F)

Table X. DCR Operating Ranges

Effect of Hydrocarbon Partial Pressure on Propylene Production in the FCC

	DCR			ACE	Commercial FCCU
	Condition 1	Condition 2	Condition 3		
Reactor Top Temp (°F)	970	970	970		
Regenerator Temp (°F)	1300	1300	1300		
Unit Pressure (psig)	40	25	25		
Reactor Delta P (in H ₂ O)	5.24	4.11	3.45		
Feed Temp (°F)	575	575	300		
Feed Rate (g/h)	1500	1000	1000	180	
Reactor Water Rate (g/h)	30	30	30		
Reactor N ₂ (L/h)	25	31	131	7.8	
Catalyst Cir. Rate (g/H)	8820	6160	6790		
C/O RATIO	5.9	6.1	6.9	6.0	6 to 9
Conversion wt%	72.0	72.2	72.7		
Molar Expansion	4.3	4.3	4.2		
Gas Residence time (s)	2.4	2.3	1.7	2.0	2 to 4
Slip Factor	2.0	2.0	1.7	Infinite	1 to 1.3
Catalyst Contact Time (s)	4.9	4.6	2.9	30 to 150	2 to 5
Catalyst Hold Up (g)	11.9	7.9	5.4	9	
WHSV (h-1)	125	126	183	20	100 to 250
HC Partial Pressure 1/3					
inlet + 2/3 outlet (psia)	44	28	20	12	20 to 50

Table XI. Operating Conditions in the DCR

We investigated two methods of changing hydrocarbon partial pressure. The first method involved keeping the total pressure, feed rate, and steam injection rate constant while reducing the nitrogen lift gas. The second method involved keeping the nitrogen lift gas and steam injection rate constant while increasing the total pressure and feed rate. The latter case is similar to some commercial FCC unit revamps where the total pressure of a FCC unit is increased to accommodate higher feed and catalyst circulation rate.

Table XI shows the three DCR operation conditions. Condition 3 is a commonly used DCR operating condition, while Conditions 1 and 2 are modifications to raise the hydrocarbon partial pressure closer to the value in commercial

FCC operations. Since cracking is a molecular weight reduction process, the hydrocarbon mole fraction and, therefore, partial pressure increase along the riser. The molar expansion (moles of product/moles of feed) in a typical FCC unit is between four and five. For the purpose of engineering calculations, it is common to approximate the hydrocarbon mole fraction as equal to 1/3 of the mole fraction at the inlet and 2/3 of the mole fraction at the outlet of the riser. The total moles of the hydrocarbon products are calculated by using GC analyses of the light gases and gasoline PIONA and assuming average molecular weight values of 220 and 350 for LCO and bottoms, respectively.

In varying hydrocarbon partial pressure, we chose operating conditions so

as not to greatly change the weight hourly space velocity (WHSV), as that in itself could change the selectivity and complicate the interpretation of the results. The slip factor in the riser (ratio of the gas velocity to catalyst velocity), estimated by the correlation of Pugsley and Berruti², varied from 1.7 to 2. These values were consistent with those reported by Bollas et al.³ Once the slip factor was determined, the catalyst holdup (the amount of catalyst in the riser), catalyst contact time and WHSV were readily calculated (Table XI). The catalyst holdup values followed the trend of pressure drop measurements across the riser. Conditions 1 and 2 varied in hydrocarbon partial pressure by a factor of 1.55. However, the values of the WHSV, catalyst-to-oil ratio and

Continued on Page 37

Continued from Page 36

Analysis	Catalyst A	Catalyst B
Al ₂ O ₃ , wt%	40.8	46.9
RE ₂ O ₃ , wt%	1.16	3.05
Na ₂ O, wt%	0.39	0.28
Ni, ppm	537	523
V, ppm	520	510
Surface Area, m ² /g	219	146
ZSA, m ² /g	179	113
MSA, m ² /g	40	33
Unit Cell Size, Å	24.24	24.32

Table XII. Properties of Catalysts Deactivated at 500ppm Ni/500ppm V CPS-3/1480°F

conversion were essentially identical. Therefore, the changes in selectivity could be attributed principally to the change in hydrocarbon partial pressure. Compared to Conditions 1 and 2, the hydrocarbon partial pressure of Condition 3 was 2.3 times lower. However, its WHSV was also somewhat greater, due to the higher level of lift nitrogen used. In this case, we would need to rationalize the contribution of hydrocarbon partial pressure to the selectivity shifts.

Table XI also compares the current DCR operating conditions with that of commercial FCC units and ACE. Compared to the earlier operating conditions (Condition 3), Conditions 1 and 2 are closer to the commercial units, especially in hydrocarbon partial pressure. Furthermore, compared to the operating conditions of ACE, the operating conditions of the DCR are much closer to those of the commercial unit.

API Gravity	25.5
Specific Gravity, g/cm ³	0.9012
K Factor	11.94
Refractive Index	1.5026
Sulfur, wt%	0.369
Basic Nitrogen, wt%	0.05
Total Nitrogen, wt%	0.12
Conradson Carbon, wt%	0.68
ndm Analysis	
Arom Ring Carbons Ca, wt%	18.9
Naphthenic Ring Carbons Cn, wt%	17.4
Paraffinic Carbons Cp, wt%	63.6

Two Davison commercial FCC catalysts, labeled Catalyst A and Catalyst B, containing 1.2 and 3.1% RE₂O₃, respectively, were used in this study. Both catalysts were steam deactivated according to CPS-3 protocol⁴ at 1480°F with 500 ppm nickel and 500 ppm vanadium. The chemical and physical properties of the two catalysts are listed on Table XII. The deactivated unit cell size measurements of the low and high RE₂O₃ catalysts are 24.24Å and 24.32Å, respectively. Catalyst A was also blended with 20% OlefinsUltra[®] additive, a commercially available ZSM-5 additive and deactivated according to CPS-3 protocol at 1480°F with 500 ppm nickel and 500 ppm vanadium. A Gulf Coast vacuum gas oil feed was used in this study. The properties of the feedstock are shown on Table XIII.

Results and Discussion

Case I

In this example, Catalyst A was tested in the DCR under both Conditions 1 and 2. Under Condition 1, the unit pressure was 40 psig, the feed rate was 1500 g/h, the dispersing steam was 30 g/h, and 25 l/h nitrogen was injected to help disperse the feed as well as to lift the catalyst. Based on the above discussion, the time-averaged (1/3 inlet + 2/3 outlet) hydrocarbon partial pressure under this condition was 44 psia. Under Condition 2, the unit pressure was 25 psig, the feed rate was 1000 g/h, whereas the steam and nitrogen flow rates were the same as that of Condition 1. The hydrocarbon partial pressure under this condition is 28 psia. The above comparison is very similar to a common revamp of a commercial FCC unit where in order to increase feed rate and catalyst circulation the total pressure of the unit has to be increased to maintain velocity.

Average MW	406
Ni, ppm	0.4
V, ppm	0.2
Simulated Distillation	
IBP	307
10%	607
30%	740
50%	818
70%	904
90%	1034
End Point	1257

Table XIII. Properties of VGO Feedstock

Effect of Hydrocarbon Partial Pressure on Propylene Production in the FCC

The plots of catalyst to oil ratio, total C₃, total C₄, gasoline, LCO, and coke yields against conversion are shown in Figure 32. Increasing HC partial pressure increases dry gas and coke at the expense of gasoline. The yields of total C₃, C₄ and LCO remain about the same. The higher coke yield may be attributed to a higher rate of oligomerization, which is a bimolecular reaction and favored at high pressure. The higher dry gas could be the result of oligomerization/recracking.

Figure 33 shows that increasing the HC partial pressure decreases the yields of propylene, butenes, and gasoline olefins, while increasing the yield of gasoline isoparaffins. Increasing HC partial pressure substantially lowers the C₃ and C₄ olefinicities. These yield shifts suggest that the rate of hydrogen transfer increases with HC partial pressure, as would be expected for a bimolecular reaction.

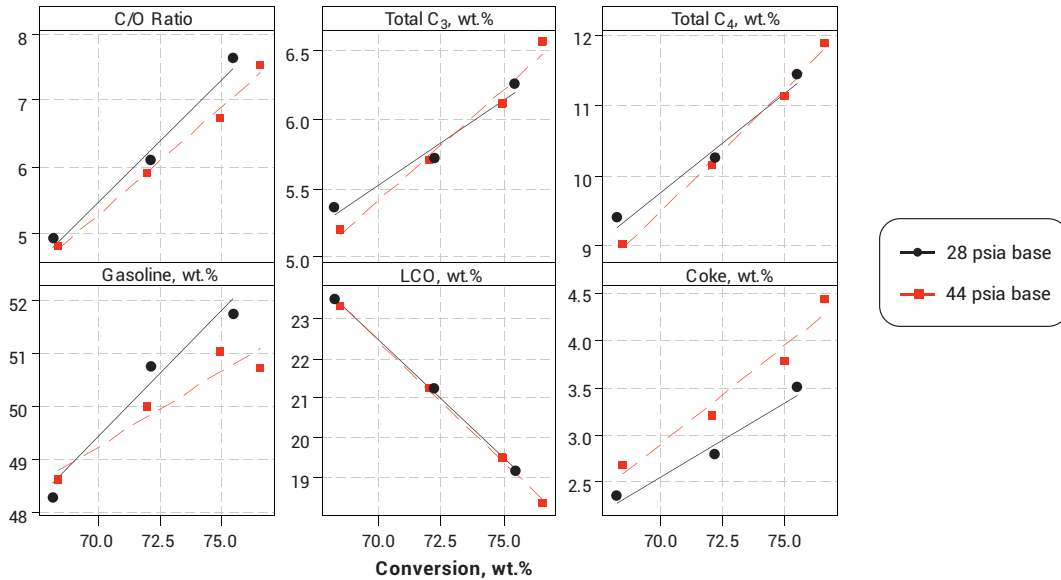


Figure 32. Effect of DCR Operating Conditions on the Yields of Catalyst A

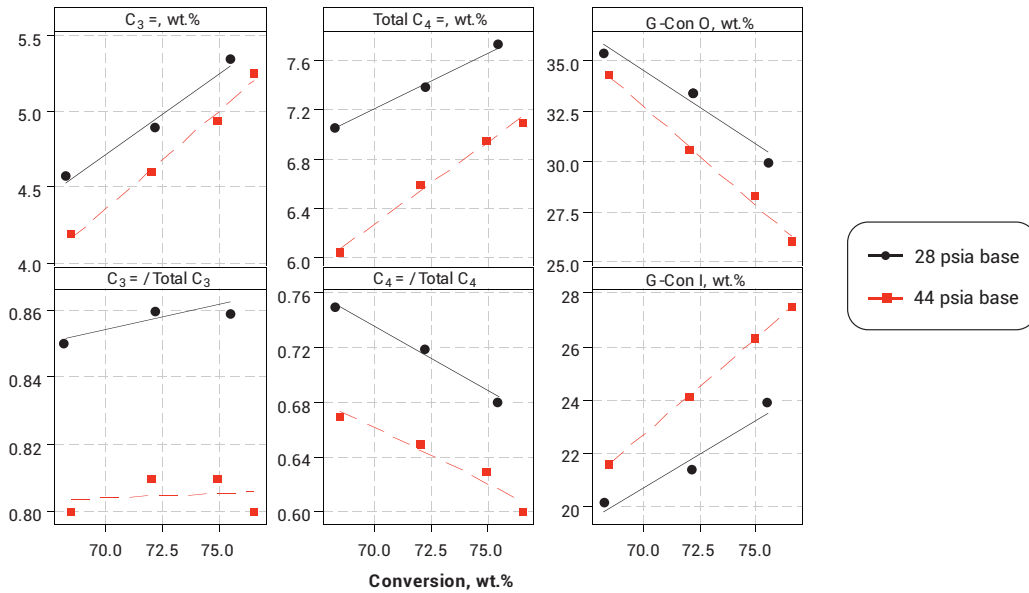


Figure 33. Effect of DCR Operating Conditions on the Olefins Yield and Olefinicity of Catalyst A

Continued from Page 38

The interpolated yields at 73 wt% conversion are listed on Table XIV. A convenient way to gauge the hydrogen transfer rate is to look at the paraffins to olefins ratio of C₃, as well as linear and branched C₄ compounds⁵. The hydrogen transfer indices are defined as the ratios of propane/propylene, n-butane/(1-butylene + trans-2-butylene + cis-2-butylene) and isobutane/isobutylene. These ratios are shown in Table XIV. In this analysis we are assuming that the C₃ and C₄ alkanes are the product of hydrogen transfer from their parent alkenes and ignoring the alkanes formed by thermal or protolytic cracking.

The hydrogen transfer reaction of isobutene proceeds via a tertiary carbenium ion intermediate and thus occurs at a much faster rate than the hydrogen transfer reactions of propylene and linear butenes, which proceed through a less stable secondary carbenium ion intermediate. All of the hydrogen transfer indices increase by a factor of 1.5, as the HC partial pressure increases almost proportionally by a factor of 1.6 from 28 to 44 psia. Thus, all the yield shifts are consistent with an increase in the rate of hydrogen transfer with the increase in HC partial pressure.

	Condition 1	Condition 2	
HC Partial Pressure, psia	44	28	Ratio of HC Pressure 1.6
Cat to Oil	6.1	6.5	
H ₂ Yield, wt%	0.05	0.05	
C ₁ + C ₂ 's, wt%	2.8	2.4	
C ₂ =, wt%	0.8	0.8	
Total C ₃ , wt%	5.9	5.9	
C ₃ =, wt%	4.7	5.0	
Total C ₄ , wt%	10.5	10.6	
iC ₄ , wt%	3.0	2.5	
nC ₄ , wt%	0.8	0.6	
Total C ₄ =, wt%	6.7	7.5	
iC ₄ =, wt%	1.9	2.4	
Gasoline, wt%	50.1	50.8	
G-Con P, wt%	4.0	3.7	
G-Con I, wt%	24.8	22.2	
G-Con A, wt%	30.5	30.2	
G-Con N, wt%	10.9	11.5	
G-Con O, wt%	29.6	32.2	
G-Con RON EST	92.2	92.0	
G-Con MON EST	79.8	79.2	
LCO, wt%	20.5	20.7	
Bottoms, wt%	6.3	6.2	
Coke, wt%	3.5	3.0	
Hydrogen Transfer Index			Ratio of HT Index
C ₃ /C ₃ =	0.24	0.17	1.4
nC ₄ / (1C ₄ = + t2 C ₄ = +c2 C ₄ =)	0.18	0.12	1.5
iC ₄ /iC ₄ =	1.56	1.05	1.5

Table XIV. Interpolated Yields at 73 wt% Conversion Over Catalyst A

Case II

Catalyst A was blended with 20% OlefinsUltra® additive and tested in the DCR under Conditions 1 and 2. The catalyst to oil ratio, total C₃, total C₄, gasoline, LCO, and coke yields against conversion plots are shown in Figure 34. The yields of C₃=, C₄=, gasoline olefins and gasoline isoparaffins, as well as the olefinicities of C₃, C₄, and gasoline are shown in Figure 35. As in the case without OlefinsUltra® additive (Case I), increasing HC partial pressure increases coke and dry gas and dramatically decreases gasoline and LPG olefinicity. The C₃ olefinicity of ca. 0.84 at the higher HC partial pressure is much more realistic and close to the commercially observed values.

The interpolated yields at constant conversion of 73 wt% are shown on Table XV. Remarkably, increasing the HC partial pressure from 28 to 44 psia decreases the propylene yield by 1 wt% absolute and decreases the butylenes yield by 0.6 wt% absolute. It is known that the addition of ZSM-5 increases LPG olefins by cracking gasoline range olefins⁶⁻⁸. Increasing the rate of hydrogen transfer, by increasing the HC partial pressure, depletes the gasoline range olefins and decreases the effectiveness of ZSM-5. The rate of hydrogen transfer, as estimated by the hydrogen transfer indices, described above, increases approximately proportionally to HC partial pressure.

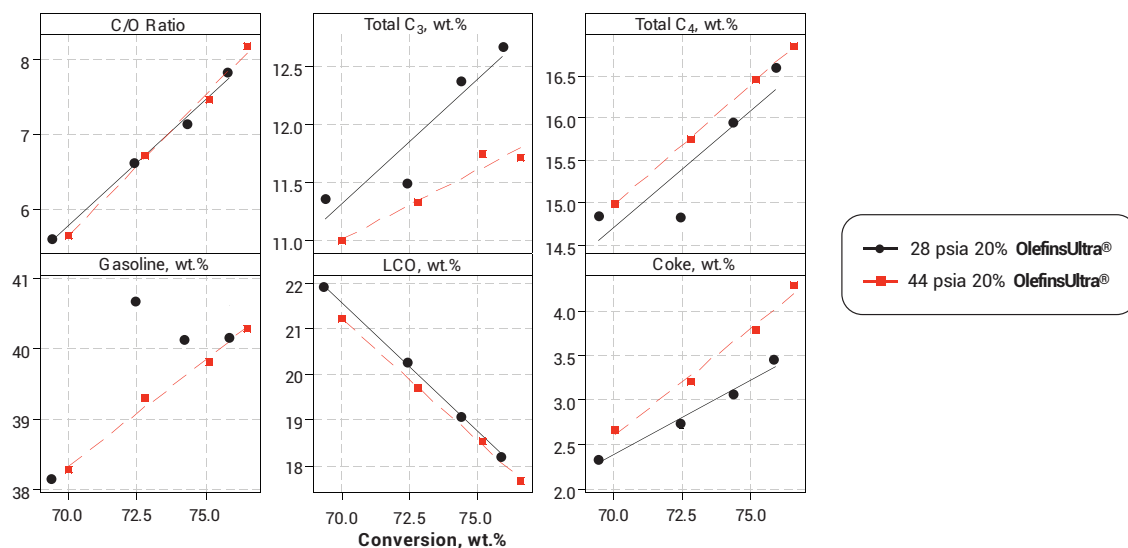


Figure 34. Effect of DCR Operating Conditions on the Yields of Catalyst A with 20% OlefinsUltra® Additive

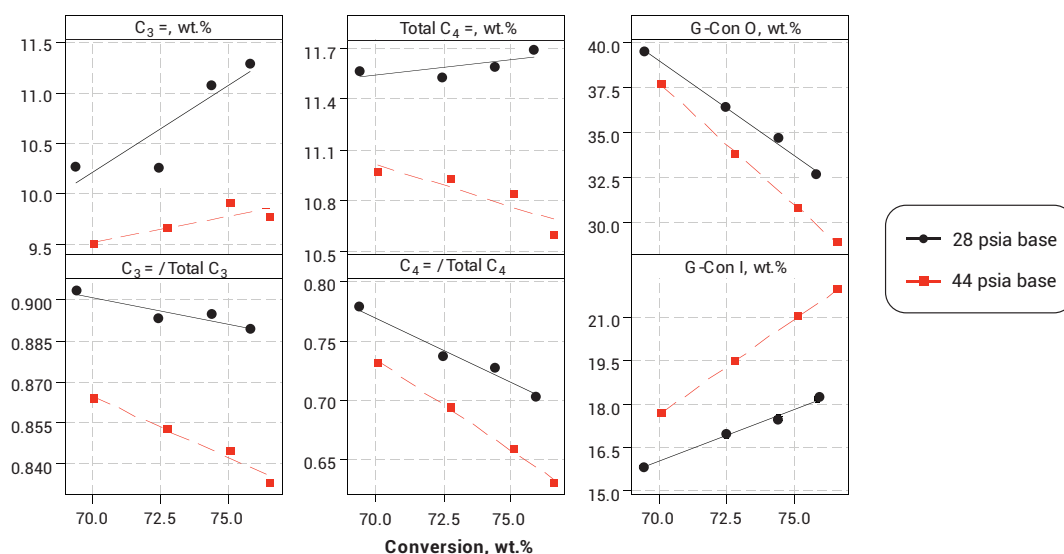


Figure 35. Effect of DCR Operating Conditions on the Olefins Yield and Olefinicity of Catalyst A with 20% OlefinsUltra® Additive

Continued on Page 41

Continued from Page 40

	Condition 1	Condition 2	
HC Partial Pressure, psia	44	28	Ratio of HC Pressure 1.6
Cat to Oil	6.7	6.7	
H ₂ Yield, wt%	0.04	0.05	
C ₁ + C ₂ 's, wt%	3.0	2.6	
C ₂ =, wt%	1.4	1.3	
Total C ₃ , wt%	11.4	12.0	
C ₃ =, wt%	9.7	10.7	
Total C ₄ , wt%	15.8	15.5	
iC ₄ , wt%	3.9	3.3	
nC ₄ , wt%	1.0	0.8	
Total C ₄ =, wt%	10.9	11.4	
iC ₄ =, wt%	4.1	4.3	
Gasoline, wt%	39.2	39.8	
G-Con P, wt%	4.0	3.8	
G-Con I, wt%	19.6	17.1	
G-Con A, wt%	33.7	33.9	
G-Con N, wt%	8.9	9.2	
G-Con O, wt%	33.5	35.8	
G-Con RON EST	95.2	94.9	
G-Con MON EST	81.5	80.9	
LCO, wt%	19.6	19.8	
Bottoms, wt%	7.3	7.1	
Coke, wt%	3.3	2.9	
Hydrogen Transfer Index			Ratio of HT Index
C ₃ /C ₃ =	0.17	0.12	1.5
nC ₄ / (1C ₄ = + t ₂ C ₄ = +C ₂ C ₄ =)	0.15	0.11	1.4
iC ₄ /iC ₄ =	0.95	0.76	1.2

Table XV. Interpolated Yields at 73 wt% Conversion Over Catalyst A with 20% OlefinsUltra® Additive

Case III

In this example, Catalysts A and B, having unit cells size values of 24.24Å and 24.31Å, respectively, were tested under DCR Conditions 1 and 3. Condition 3 featured a unit pressure of 25 psig, 1000 g/h feed rate, 30 g/hour steam, and 128 l/h nitrogen. The main difference between Condition 1 and Condition 3 was the greater amount of nitrogen lift gas used in Condition 3, which not only decreased the HC partial pressure by a factor of 2.3, from 44 to 19 psia, but also increased the WHSV by a factor of 1.4. The effect of the change in WHSV will be discussed.

The main yields are shown in Figure 36, while the LPG and gasoline composition are shown in Figure 37. For both the high and low unit cell size catalysts, the response of the LPG and gasoline olefin yields to the changes in DCR conditions are very similar to that observed in Case 1, namely increasing HC partial pressure decreases LPG and gasoline olefins and olefinicity. The hydrogen transfer indices increased by a factor of two as HC partial pressure increased by a factor of 2.3 (Table XVI). Thus, as in Case I, the change in the hydrogen transfer indices are nearly proportional to the change in HC partial pressure. This suggests that the change in HC partial pressure is mainly responsible for the yield changes while the shifts in WHSV may be responsible for the shifts in conversion at a given catalyst to oil ratio.

Effect of Hydrocarbon Partial Pressure on Propylene Production in the FCC

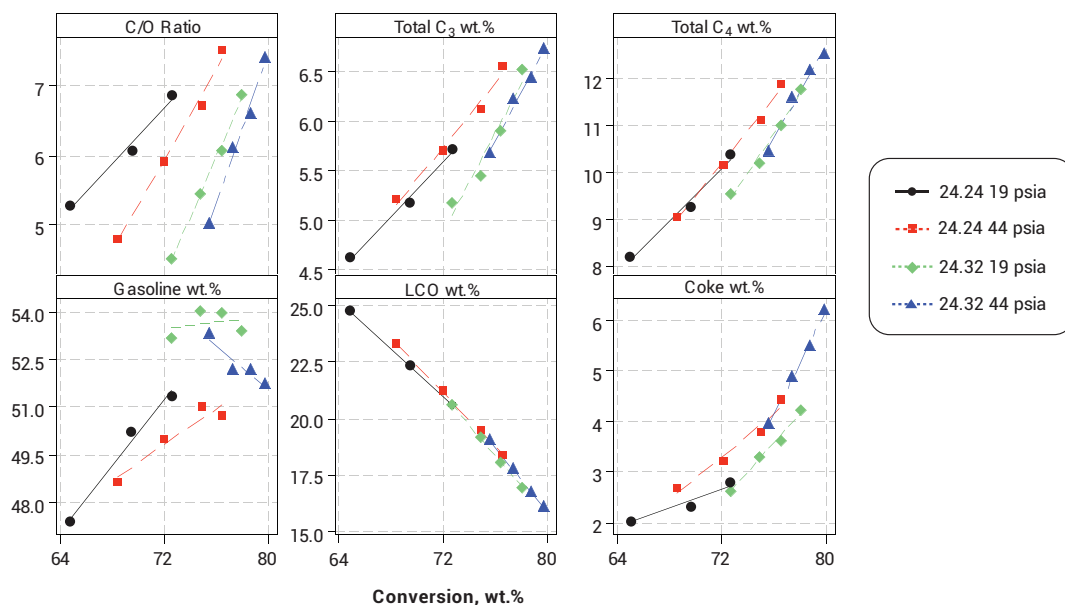


Figure 36. Variation of Yields with Unit Cell Size and DCR Operating Conditions

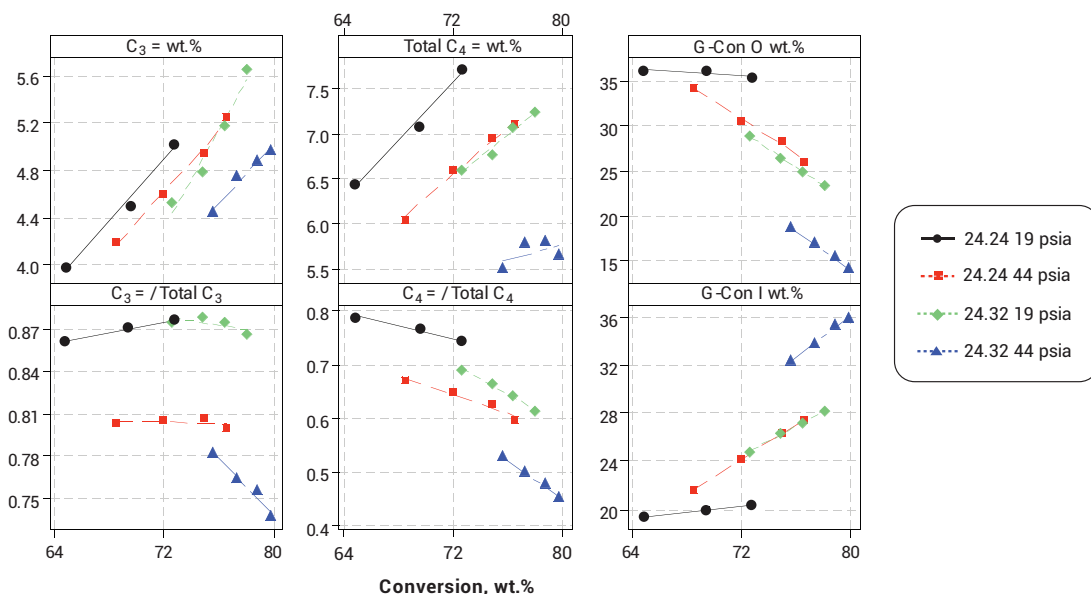


Figure 37. Variation of Olefins Yield and Olefinicity with Unit Cell Size and DCR Operating Conditions

The yields shifts due to changing unit cell size are consistent with what has been reported in the literature^{9,10}, namely that the higher UCS catalyst makes higher gasoline, lower LPG and gasoline olefins. These trends are observed at both DCR conditions. The effect of unit cell size and HC partial pressure on the rate of hydrogen transfer appears to be simply additive.

The rate of bimolecular reactions can be increased by increasing acid site density as well as increasing HC partial pressure. The ratios of the hydrogen transfer indices of Catalyst B to Catalyst A are about the same at both low and high HC partial pressure (Table XVI).

Continued from Page 42

	Catalyst A		Catalyst B	
	Condition 3	Condition 1	Condition 3	Condition 1
HC Partial Pressure, psia	19	44	19	44
Cat to Oil	7	7	5	5
H ₂ Yield, wt%	0.04	0.05	0.03	0.03
C ₁ + C ₂ 's, wt%	2.2	2.7	1.9	2.2
C ₂ =, wt%	0.7	0.8	0.6	0.7
Total C ₃ , wt%	5.9	6.2	5.6	5.6
C ₃ =, wt%	5.2	5.0	4.9	4.4
Total C ₄ , wt%	10.8	11.2	10.4	10.3
iC ₄ , wt%	2.4	3.4	2.9	3.7
nC ₄ , wt%	0.5	0.9	0.6	1.0
Total C ₄ =, wt%	8.0	6.9	6.8	5.5
iC ₄ =, wt%	2.7	1.9	1.8	1.4
Gasoline, wt%	53.6	50.7	53.6	53.4
G-Con P, wt%	3.4	4.0	4.0	4.6
G-Con I, wt%	20.8	26.3	26.3	31.8
G-Con A, wt%	29.1	31.3	30.8	32.3
G-Con N, wt%	11.4	10.6	12.5	12.1
G-Con O, wt%	35.4	27.7	26.3	19.5
G-Con RON EST	92.4	92.1	89.9	88.8
G-Con MON EST	79.2	80.0	78.4	78.6
LCO, wt%	20.0	19.3	19.0	19.5
Bottoms, wt%	6.0	5.6	5.9	5.6
Coke, wt%	2.9	3.9	3.2	3.7
Hydrogen Transfer Index				
C ₃ /C ₃ =	0.13	0.24	0.14	0.27
nC ₄ /(1C ₄ = + t ₂ C ₄ = +c ₂ C ₄ =)	0.09	0.18	0.12	0.24
iC ₄ /iC ₄ =	0.88	1.79	1.57	2.69

Table XVI. Interpolated Yields at 75 wt% Conversion Over Catalyst A and B

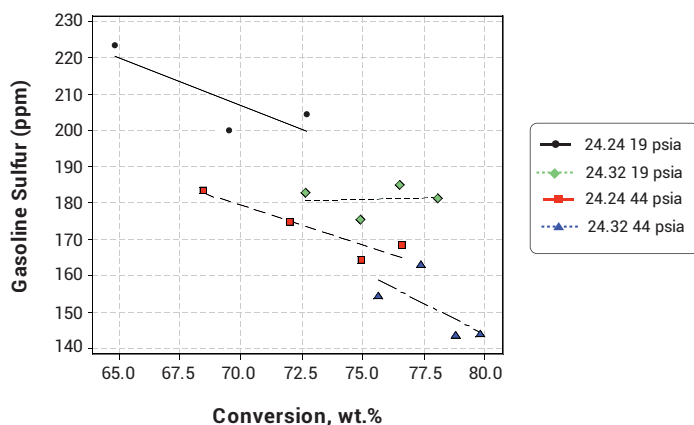
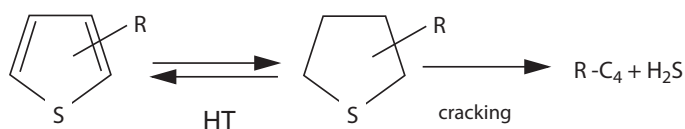


Figure 38. Effect of UCS and DCR Operating Conditions on Gasoline Sulfur Concentration

Figure 38 shows the concentration of gasoline sulfur (including all thiophene species with a boiling point below 430°F, tetrahydrothiophene, and benzothiophene) for both Catalysts A and B under the two DCR operation conditions. Gasoline sulfur concentration decreases with increasing unit cell size and with increasing HC partial pressure. These results suggest that the reduction of gasoline sulfur follows the trend of increase hydrogen transfer activity and are consistent with the previously proposed mechanism, shown below^{11,12}.

Scheme 1

High rate of hydrogen transfer speeds up this reaction by promoting the formation of the reaction intermediate, tetrahydrothiophene.



Scheme 1

Conclusions

By varying the operating conditions of the DCR, we have been able to conduct cracking experiments over a wide range of hydrocarbon partial pressure. The results indicate that increasing the hydrocarbon partial pressure decreases the olefinicity and olefins yield of LPG and gasoline. This observation is consistent with the notion that hydrogen transfer reactions, being bimolecular in nature, increase with increasing HC partial pressure. The hydrogen transfer index, defined as the paraffin/olefin ratio of C₃, linear C₄ and branched C₄ species increase almost linearly with HC partial pressure. It has been demonstrated that the effectiveness of ZSM-5 additives is lessened at high HC partial pressure due to the depletion of gasoline range olefins via hydrogen transfer reactions. The concentration of gasoline sulfur species decreases at higher HC pressure, again due to higher rate of hydrogen transfer. Recent advancements in DCR operation enable more realistic simulation of commercial FCCU operation.

References

- G.W. Young, G.D. Weatherbee, "FCCU Studies with an Adiabatic Circulating Pilot Unit," AIChE Annual Meeting, November, 1989.
- S. T. Pugley, F. A. Berruti, "A Predictive Hydrodynamic Model for Circulating Fluidized Bed Risers," Powder Technol., 89 (1996) 57.
- G. M. Bollas, I. A. Vasalos, A. A. Lappas, D. Iatridis, "Modeling Small-Diameter FCC Riser Reactors, A Hydrodynamic and Kinetic Approach," Ind. Eng. Chem. Res., 41 (2002) 5410.
- D. Wallenstein, R.H. Harding, J.R.D. Nee, L.T. Boock, "Recent Advances in the Deactivation of FCC Catalysts by Cyclic Propylene Steaming (CPS) in the Presence and Absence of Metals," Appl. Catal. A: General 204 (2000) 89.
- Cheng, W.-C., Suarez, W., and Young, G. W; "The effect of catalyst properties on the selectivities of isobutene and isoamylene in FCC," AIChE Symposium Series, 291 (1992) 38.
- K. Rajagopalan, G.W. Young, in Fluid Catalytic Cracking – Role in Modern Refining, M.L. Occelli (Ed.), ACS Symposium Series 375 (1988) 34.
- X. Zhao, T.G. Roberie, "ZSM-5 Additive in Fluid Catalytic Cracking. 1. Effect of Additive Level and Temperature on Light Olefins and Gasoline Olefins," Ind. Eng. Chem. Res. 38 (1999) 3847.
- R.J. Madon, "Role of ZSM-5 and Ultrastable Y Zeolites for Increasing Gasoline Octane Number," J. Catal. 129 (1991) 275.
- L.A. Pine, P.J. Maher, W.A. Wachter, "Prediction of Cracking Catalyst Behavior by a Zeolite Unit Cell Size Model," J. Catal. 85 (1984) 466.
- G.W. Young, W. Suarez, T.G. Roberie, W.C. Cheng, "Reformulated Gasoline: The Role of Current and Future Catalysts," NPRA Annual Meeting, AM-91-34, 1991.
- R.H. Harding, R. Gatte, J.A. Whitecavage, R.F. Wormsbecher, "Reaction Kinetics of Gasoline Sulfur Compounds," in Environmental Catalysis, J.N. Armor (Ed.), American Chemical Society, Symposium Series 552 (1994) 286.
- F. Can, A. Travert, V. Ruaux, J.-P. Gilson, F. Maugé, R. Hu, R.F. Wormsbecher, "FCC Gasoline Sulfur Reduction Additives: Mechanism and Active Sites," J. Catal. 249 (2007) 79.



In recent years, major geopolitical events, extreme weather, shifting consumer priorities, and global health emergencies have emphasized the need for operational flexibility if refiners are to remain profitable and competitive. We have observed shifts in the profitability of FCC units geared towards maximum petrochemicals feedstocks, gasoline, and distillates. In addition, the ongoing energy transition is expected to reduce transportation fuel demand over the long-term, although diesel and gasoil markets will be less impacted than gasoline.

The dynamic nature of liquid product margins provides an opportunity for refiners to capitalize on flexible operation of their FCC units. This was demonstrated in the first publication of this article, when favorable diesel economics drove the investigation into finding optimized combinations of product cut points, operating conditions, and FCC catalyst technology to derive maximum value out of FCC operation. A host of advanced analytical techniques and Grace DCR™ Pilot Plant studies determined optimum recycle stream compositions and rates, techniques which we continue to advance and deploy to this day. In addition, we showed how MIDAS®-300, with its higher activity matrix surface area balanced with optimized zeolite content, could ensure high LCO yield while minimizing bottoms and coke yield.


Today we are proud to have continued progressing our MIDAS® platform towards industry leading contaminant tolerance. The recent introduction of MIDAS® Pro demonstrates improved iron tolerance and porosity, and PARAGON™ integrates a coke selective V trap into the matrix while maintaining bottoms upgrading capabilities at low coke yield.

Despite uncertainties and market flux, Grace continues to look ahead and partner with the industry to support them in meeting the challenges of remaining flexible and profitable in their operations.



Claudia Janse van Rensburg
Sr. Regional Marketing Manager
W. R. Grace & Co.

Strategies for Maximizing FCC Light Cycle Oil

 David Hunt, Ruizhong Hu, Hongbo Ma,
Larry Langan, Wu-Cheng Cheng

 Originally published in *Catalagram* #105 in 2009 (9)

Maximizing FCC light cycle oil (LCO) yield to take advantage of high diesel prices relative to gasoline requires re-optimization of product cut point, operating conditions and catalyst technology. It is well known that the LCO-to-gasoline ratio can be increased through lowering conversion by adjusting FCCU operating conditions and decreasing catalyst activity.^[1,11] The drawback of this approach is the increase in bottoms yield. Recycle is often required to fully maximize LCO while maintaining bottoms yield consistent with a traditional maximum gasoline operation.

This article is a general discussion of strategies to maximize LCO in the FCCU. We will present laboratory results which quantify the effects of various recycle streams. A resid feedstock was cracked over a low Z/M MIDAS[®] catalyst in Grace Davison's circulating riser pilot plant (DCR). The product bottoms was distilled to five recycle fractions (650-750°F, 650-800°F, 650-850°F, 650°F+ and 750°F+), blended back at various levels with the original feedstock and cracked over a MIDAS[®] catalyst in the ACE unit. Laboratory testing results were used to model a commercial operation to demonstrate the yield advantage of selecting the appropriate recycle stream, recycle ratio and catalyst technology.

Continued from Page 46

Introduction

The Energy Information Administration (EIA) expects higher diesel prices relative to gasoline to continue through 2010. An average diesel price of 2.27 \$/gallon is expected in 2009, increasing to an average 2.54 \$/gallon in 2010. Gasoline is expected to be an average 1.87 \$/gallon in 2009, reaching an average 2.18 \$/gallon in 2010.^[2]

New Corporate Average Fuel Economy (CAFE) standards are also expected to increase diesel demand relative to gasoline in upcoming years. This new standard requires auto manufacturers to boost fuel mileage to 35 mpg by 2020 and applies to all passenger automobiles, including light trucks. To meet this challenging new standard, more efficient vehicles powered by hybrid and diesel engines are expected.

Refiners are increasing the production of LCO from their FCCU's to take advantage of the significantly higher value of diesel relative to gasoline. Figure 1 shows how LCO and bottoms shift versus conversion for a high and low zeolite/matrix ratio catalyst. LCO, like gasoline, is an intermediate product increasing with conversion at very low conversion levels, eventually reaching an over-cracking point. Past the over-cracking point, LCO yield declines with increasing conversion. This high conversion regime represents the traditional FCCU operating point. A low Z/M catalyst generally produces higher LCO at the expense of bottoms for a given conversion levels, as suggested by Figure 1.

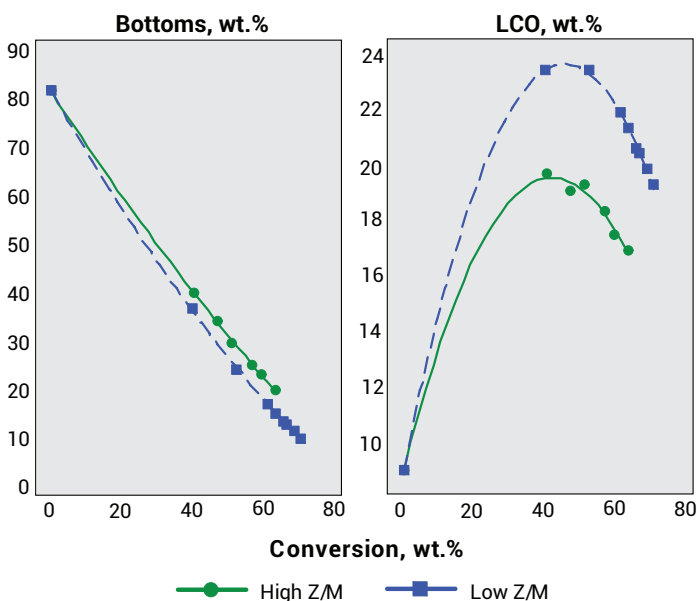


Figure 1. LCO and Bottoms vs. Conversion

Refiners tend to focus on the following strategies to maximize FCC LCO production:

1. Reduced gasoline end point
 - a. Increased gasoline end point
 - b. Higher LCO endpoint
2. Operating conditions
 - a. Lower reactor temperature
 - b. Higher feed temperature
 - c. Lower equilibrium catalyst activity
3. Feedstock
 - a. Removal of diesel range material from the FCC feedstock
 - b. FCC feed hydrotreating severity optimization
 - c. Residual feedstock optimization
4. Catalyst Optimization
 - a. Increasing bottoms conversion
 - b. Lower zeolite to matrix surface area
 - c. Maintaining C3+ liquid yield and gasoline octane
5. Recycle streams
 - a. Heavy Cycle Oil (HCO) or bottoms

Reducing gasoline end point is a simple and effective way to increase LCO production. The LCO flash point specification and main fractionator salting often determine how low a refiner can reduce the LCO initial boiling point (reduce the gasoline end point). The LCO end point should be increased within the maximum main fractionator bottoms temperature, slurry exchanger fouling and diesel hydrotreater constraints.

Maximizing LCO in the FCCU at reduced conversion without producing incremental bottoms oil is the true challenge. Shifts in operating conditions to reduce conversion increase LCO, but also increase bottoms oil yield, as seen in Figure 1. In order to produce increased LCO without producing incremental bottoms, refiners will often reformulate their FCC catalyst to a lower activity with lower zeolite-to-matrix for improved bottoms conversion and to minimize LCO over-cracking.

Recycle is eventually required to minimize bottoms production as the refinery reduces conversion to reach an optimal LCO yield, as suggested by Figure 1. Almost all FCC units operated with large recycle streams prior to the introduction of zeolite catalyst in the 1960's and 1970's. However, since the 1970's, recycle was generally removed from FCC's as the catalyst and equipment technology improved and the FCC operated at high conversion and feedrates to produce gasoline, C₄'s and C₃'s. As a result, our industry has limited recent experience with these recycle streams and their effect on FCC products and coke.

To better understand these recycle effects with the state-of-the-art maximum bottoms cracking catalyst MIDAS®, Grace has

conducted a series of riser pilot plant (Davison Circulating Riser or DCR), ACE, and computer simulation studies.

2.0 Experiments

2.1 DCR Pilot Plant Runs and Preparation of Recycle Streams

A commercially available MIDAS[®] catalyst was deactivated, without Ni or V, at 1465°F for 20 hours, using the Advanced Cyclic Propylene Steam protocol described by Wallenstein.^[3] After deactivation, the catalyst had 94 m²/g zeolite surface area, 83 m²/g matrix surface area, and a unit cell size of 24.30Å. The deactivated catalyst was charged in our DCR pilot plant^[4], where cracking of a resid feedstock was conducted. Reaction severity was varied by adjusting the temperature set points of riser top, regenerator, and feed pre-heat. We obtained four balanced runs with conversion levels of 54, 58, 68, and 75 wt%. The DCR conditions and product yields are listed in Table 1. The C₄- products were analyzed by gas chromatograph, while C₅+ liquid products (syncrude) were analyzed by simulated distillation and expressed as gasoline (C₅-430°F), LCO (430- 650°F) and bottoms (650°F+), as shown in Table 1. The detailed boiling point distribution of the bottoms fraction is also provided in Table 1. These results provide the amount of hydrocarbon in a given boiling range when an ideal distillation is achieved. These results were used as a basis to determine the maximum quantity of each recycle stream.

C₅+ liquid products from each DCR run was first separated by atmospheric distillation on a modified Hempel still (ASTM D295) to obtain the 650°F+ fraction. Each 650°F+ fraction was further separated by vacuum distillation (ASTM 1160) to obtain the desired boiling fractions. The properties of the various boiling fractions are shown in Figures 2 and 3.

Conversion, wt%	54	58	68	75
Rx Exit Temp, °F	950	950	971	970
Regenerator Temp, °F	1350	1350	1270	1270
Feed Temp, °F	701	574	700	299
C/O Ratio	4.3	5.0	5.9	9.4
Dry Gas, wt%	2.0	1.9	2.6	2.2
LPG, wt%	8.2	8.9	11.4	13.3
Gasoline, wt%	38.4	42.0	48.0	51.9
LCO, wt%	22.2	21.7	19.2	16.7
Bottoms, wt%	24.0	20.0	12.8	8.6
Coke, wt%	5.2	5.3	5.9	7.1
Boiling Point Distribution of 650°F+ Bottoms				
650-700°F	5.3	4.8	3.5	2.5
700-750°F	4.8	4.2	2.9	2.0
750-800°F	4.3	3.6	2.2	1.4
800-850°F	3.6	2.9	1.6	1.1
850-900°F	2.5	2.0	1.2	0.7
900-950°F	1.6	1.2	0.8	0.5
950°F+	1.9	1.4	0.8	0.4
650-750°F	10.1	9.0	6.3	4.4
650-800°F	14.4	12.6	8.5	5.9
650-850°F	18.0	15.5	10.1	6.9
650°F+	24.0	20.0	12.9	8.6
750°F+	13.9	11.0	6.5	4.1

Table 1. DCR Runs to Generate Recycle Feedstock

2.2 ACE of Recycle Blends

To simulate HCO and bottoms recycle, we prepared feed samples by blending various boiling range fractions back into the starting resid feedstock. These feed blends, listed in Table 2, can be separated into two groups. One group consists of recycle fractions with various boiling ranges obtained at 54 wt% conversion, while the other group consists of recycles with one boiling range, 650°F-750°F, but obtained at various conversion levels from the DCR runs. The percentage of recycle in each blend was selected based on simulated distillation listed in Table 1 and the strategy to keep the recycle fraction low enough so that one can use

two-pass cracking to simulate steady state operation. The steady state approximation will be discussed further in the Data Analysis section. The HCO streams were blended at two recycle ratios to demonstrate the sensitivity and reproducibility of yield changes due to recycle.

The ACE runs^[5] were conducted using the same laboratory deactivated MIDAS[®] catalyst as above and the same commercial FCC resid feed as the base feedstock. All ACE runs were conducted at a reactor temperature of 950°F using the same amount of feed of 1.5g and a constant feed delivery rate

Continued on Page 49

Continued from Page 48

of 3.0g per minute. In order to achieve desired conversion, catalyst to oil ratio was varied by changing the amount of catalyst charged in the reactor in each run. As in the above DCR study, gas and liquid products were analyzed by gas chromatography and simulated distillation. Coke on catalyst was measured using a LECO analyzer.

2.3 Data Analysis

In steady operation with HCO recycle, it is conceivable that some hydrocarbon molecules could go through the riser multiple times. In our DCR-ACE experiment, we are approximating steady state yields with yields from two-pass cracking. We will use the Feed-Element-Tracking-Approach to discuss the validity of this approximation. Consider 100 grams of oil, which is fed into the FCC unit and cracked into various products, of which the bottoms are partially recycled. For example, 10 grams of bottoms are recycled and fed into the unit again to crack further. Additional products are obtained, and some of the resulting bottoms, e.g., 1 gram, are recycled, and so on. By collecting the products along the route of this 100 gram crude oil, we can get the product yields on the fresh feed basis. The process is shown in Figure 4.

RR is the recycle ratio, defined as the fraction of the recycled HCO stream in the total feed into the unit. RR is equal to 0.1 in the following example.

Using the Element-Tracking- Approach, we can calculate the LCO yield as follows:

$$LCO = LCO_1 + RR \times LCO_2 + RR^2 \times LCO_3 + \dots + RR^{i-1} \times LCO_i \quad (1)$$

where LCO_i is the LCO yield of i -th pass cracking of the recycled portion of $(i-1)$ -th pass bottoms. Since the quality of the feed becomes worse and worse when recycling further, $LCO_i < LCO_{i-1}$. Obviously, if the recycling ratio RR is small, the second order and above term of RR can be safely ignored. In this work, the

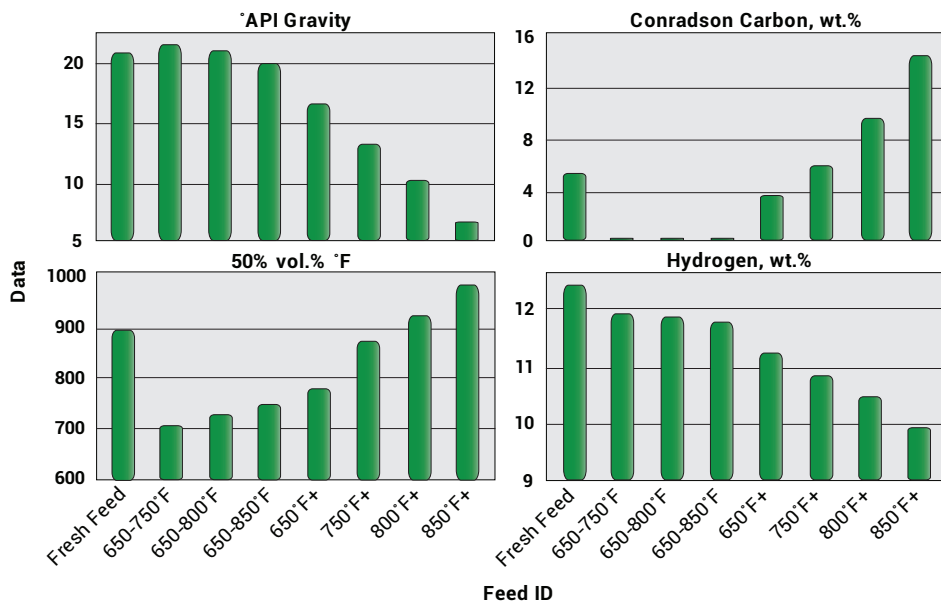


Figure 2. Properties of Recycle Feedstocks Obtained from DCR Run at 54% Conversion

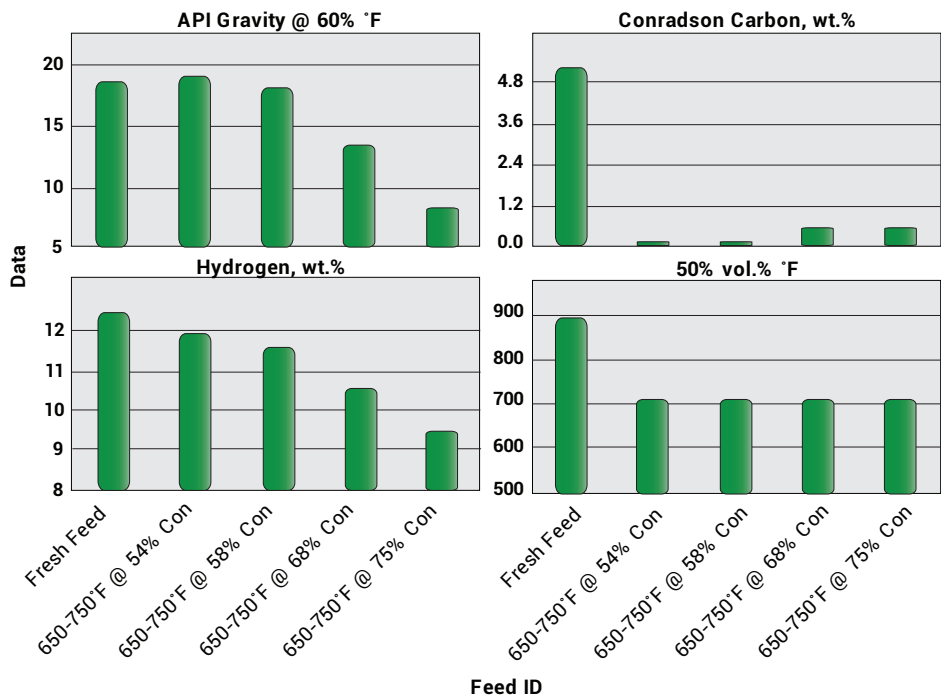


Figure 3. Properties of 650-750°F Recycle Fraction Obtained from DCR Runs

maximum RR is 0.15; so, the third term on the right-hand-side of Equation 1 is only about 2.25% of the first term.

Therefore, if we can get LCO_2 , we will have a reasonable estimate for LCO. Looking at the second pass cracking,

Conversion, wt%	Recycle Stream, °F	Blend Ratio wt%	Original Feed wt%	°API
			100.0	20.60
54	650-750	8.3	91.7	20.42
54	650-750	6.3	93.7	20.39
54	650-800	11.7	88.3	20.37
54	650-800	9.7	90.3	20.38
54	650-850	13.4	86.6	20.29
54	650-850	11.4	88.6	20.30
54	650+	14.7	85.3	19.83
54	750+	7.1	92.9	19.87
58	650-750	8.3	91.7	20.29
58	650-750	6.3	93.7	20.29
68	650-750	7.3	92.7	19.95
68	650-750	5.3	94.7	20.03
75	650-750	5.4	94.6	19.72
75	650-750	3.4	96.6	19.93

Table 2. Combined Feeds Used in ACE Study

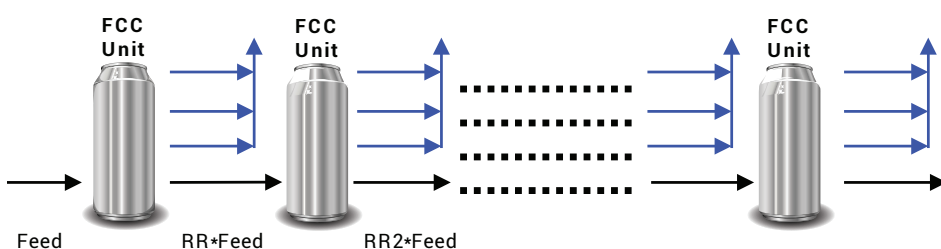


Figure 4. Schematic Diagram of Feed-Element-Tracking-Approach

the total feed in this pass consists of $(1-RR)$ fresh feed and RR recycled HCO from the first pass cracking. This second pass corresponds to the ACE study in our DCR+ACE experiment. Denoting the LCO yield in the ACE study as LCO' , LCO_1 as the LCO yield in the cracking of the base feed (which corresponds to the first pass), and noting that the portion of the fresh feed in the combined feed has the LCO yield of LCO_1 , we have:

$$LCO' = (1-RR) \times LCO_1 + RR \times LCO_2 \quad (2)$$

which can be rearranged to:

$$LCO_2 = LCO_1 + (LCO' - LCO_1)/RR \quad (3)$$

The yields on a fresh feed basis are determined as follows:

$$LCO_{FF} = LCO'/(1 - RR) \quad (4)$$

$$Bot_{FF} = (Bot' - RR)/(1 - RR) \quad (5)$$

The Element-Tracking-Approach predicts that at low (<15%) recycling ratio, two-pass cracking is very close to

the steady state operation because the higher order term in the yield expression is negligible.

3.0 Results and Discussion

3.1 Effect of Recycle Streams

Table 3 shows the interpolated yields of the original feed at 70 and 55% conversion, as well as the yields of the combined feeds at 55% conversion. The yields are expressed as wt% of the total feed (fresh + recycle). To better illustrate the contribution of each recycle stream, the yields of LCO, bottoms, coke, and gasoline, as a function of the recycle ratio, are plotted in Figure 5. With the exception of the 750°F+ recycle feed, all recycle containing feeds made higher LCO and lower bottoms than the original feed. With the exception of the 650-750°F recycle feed, all recycle-containing feeds made higher coke and lower gasoline than the original feed. The data quality confirms that the ACE testing has the sensitivity to measure the yield contribution of the recycle streams at the desired range of recycle ratios.

Using the Element-Tracking-Approach described earlier, we can calculate the theoretical yields derived from the second-pass cracking of each of the recycle streams. This is shown in Figure 6. The recycled streams are less crackable than the base feed, as indicated by the much higher cat to oil ratios required to achieve the same conversion. This is expected, as the easy to crack material of the recycle streams has been cracked in the first pass. The crackability of the recycle streams increases with the API gravity (Figure 7). As expected, the 650-750°F stream made the most LCO and gasoline and the lowest coke for a given conversion, when comparing yields among the recycle streams. The trends in LCO and gasoline yields from the lightest stream (650-750°F) to the heaviest stream (750°F+) appear to be continuous and consistent with the trend in the API gravity (Figure 2). However, the increase

Continued on Page 51

Continued from Page 50

Recycle Boiling Range	None	None	650-750°F	650-750°F	650-800°F	650-800°F	650-850°F	650-850°F	650°F+	750°F+
Recycle Ratio	0.0%	0.0%	8.3%	6.3%	11.7%	9.7%	13.4%	11.4%	14.7%	7.1%
Wt% Conversion	70	55	55	55	55	55	55	55	55	55
Cat-to-Oil Ratio	6.0	3.4	3.5	3.5	3.6	3.6	3.7	3.6	3.7	3.6
Hydrogen, wt%	0.1	0.1	0.1	0.1	0.1	0.1	0.1	0.1	0.1	0.1
Total C ₁ 's & C ₂ 's, wt%	1.4	1.0	1.0	1.0	1.1	1.1	1.1	1.1	1.0	1.1
Propylene, wt%	3.3	2.1	2.2	2.1	2.2	2.2	2.2	2.2	2.1	2.0
Total C ₃ 's, wt%	3.9	2.4	2.5	2.4	2.5	2.5	2.6	2.5	2.4	2.4
Total C ₄ 's, wt%	5.1	3.9	3.9	4.2	3.8	3.9	4.0	4.0	3.9	3.8
Total C ₄ 's, wt%	8.5	5.6	5.7	6.0	5.6	5.7	5.9	5.8	5.8	5.5
C ₅ + Gasoline, wt%	49.4	40.6	40.8	40.4	40.2	40.1	39.8	39.8	39.9	40.0
RON	89.6	89.5	89.3	89.6	89.5	89.5	89.4	89.5	89.5	89.3
MON	78.7	77.6	77.6	77.7	77.7	77.7	77.8	77.7	77.8	77.6
LCO, wt%	20.5	24.7	25.8	25.5	25.6	25.5	25.1	25.0	25.0	24.7
Bottoms, wt%	9.5	20.3	19.2	19.5	19.4	19.5	19.9	20.0	20.0	20.3
Coke, wt%	6.7	5.6	5.6	5.6	5.7	5.6	5.7	5.7	6.1	6.1
Relative Feed Rate										
Coke Burn Limited	1.00	1.20	1.20	1.21	1.18	1.20	1.18	1.19	1.11	1.10
Wet Gas Limited	1.00	1.53	1.49	1.46	1.49	1.48	1.44	1.45	1.48	1.54
Catalyst Circulation Limited	1.00	1.76	1.72	1.71	1.70	1.68	1.62	1.69	1.63	1.68
Fresh Feed Rate										
Coke Burn Limited	1.00	1.20	1.10	1.13	1.04	1.08	1.02	1.05	0.95	1.03
Wet Gas Limited	1.00	1.53	1.36	1.37	1.32	1.33	1.25	1.29	1.26	1.43
Catalyst Circulation Limited	1.00	1.76	1.58	1.60	1.50	1.52	1.40	1.50	1.39	1.56

Table 3. Interpolated Yields of Base and Combined Feeds at 70% and 55% Conversion

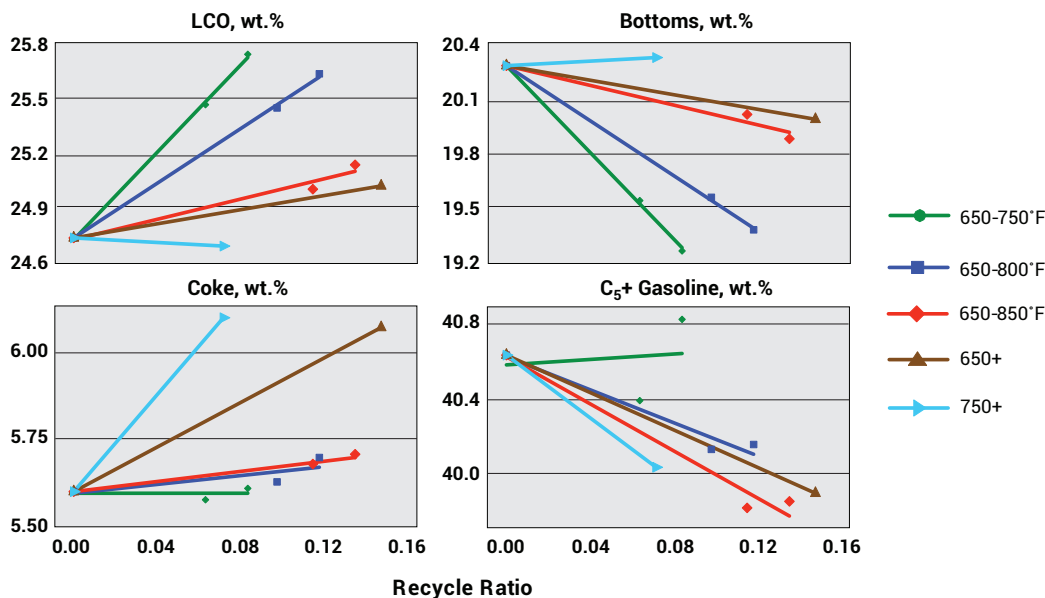


Figure 5. Plots of Interpolated Yields at 55% Conversion vs. Recycle Ratio

of coke appears to be very gradual up to the 650-850°F stream and becomes stepwise higher for the 650°F+ and 750°F+ streams. The coke yield trends very closely with the Conradson Carbon (Figure 7), which is concentrated in the 850°F+ range (Figure 2). These results suggest that during first-pass cracking, coke precursors in the boiling range of 850°F+ are formed. These molecules are responsible for coke production during second-pass cracking.

While the 750°F+ stream is not a practical recycle stream, it does provide valuable insight on the negative impact of recycling heavy bottoms. This stream made more than double the coke yield of the base feed. A close examination of the hydrocarbon compounds by GC Mass Spec (Table 4) shows that the 750°F+ fraction contains higher aromatic compounds, and in particular tetra-aromatic compounds, than the lighter 650-750°F+ fraction. It is likely that the coke precursors formed during first-pass cracking are indeed the tetra-aromatic compounds. We noticed that Ye and Wang^[6] reported slightly less coke formation (0.6%) with recycling of highly aromatics bottoms in FCC unit. However, their recycling ratio was much lower, only 1.5%.

3.2 Modeling Overall Yields

Table 3 also lists the interpolated yields for max gasoline operation at 70 wt% conversion of the base feed. Compared to the yields at 70% conversion, the LCO yield at 55% conversion is higher while the yields of wet gas and coke are much lower and the C/O ratio is lower. If the unit changes from max gasoline (70% conversion) to max LCO (55% conversion) operation, one should be able to increase total feed rate until the unit reaches coke burn, wet gas compressor or catalyst circulation constraint, assuming there are no other limitations. The results of Table 3 suggest that the coke burn constraint will be reached much sooner than the wet gas or catalyst circulation constraint. (Catalyst circulation could

be a limit at reduced catalyst activity.) At a coke burn limitation, the combined feed rate of the max LCO operation is 10 to 20% higher than at the max gasoline operation.

The data analyses so far have been confined to yields on the combined feed basis with the selected recycle ratios.

The following examples demonstrate how to use this data to determine the recycle stream and recycle ratio to optimize LCO production. We will examine a maximum recycle case and a constant bottoms case. A modeling of a commercial unit (heat balanced) will be presented later.

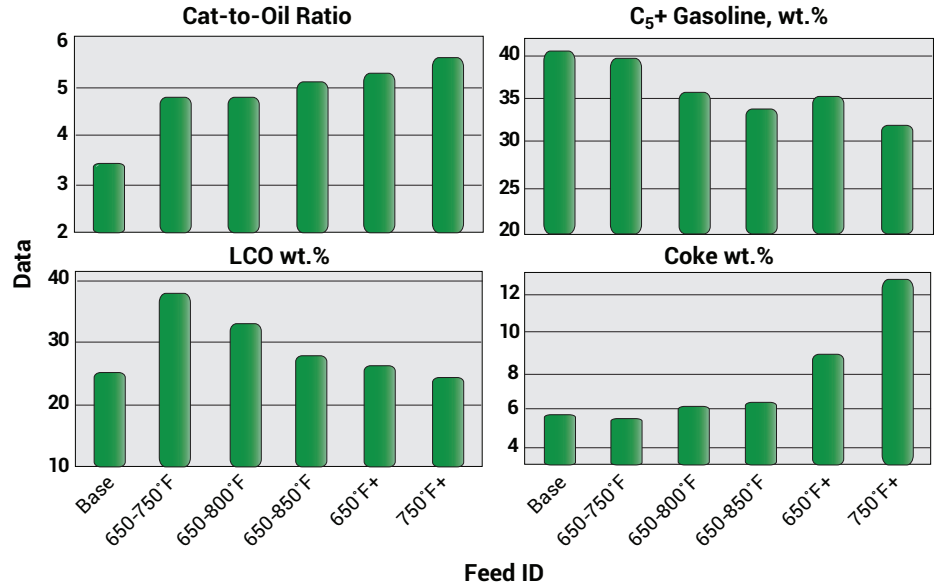


Figure 6. Theoretical Yields of Second Pass Cracking at 55% Conversion of Recycle Streams

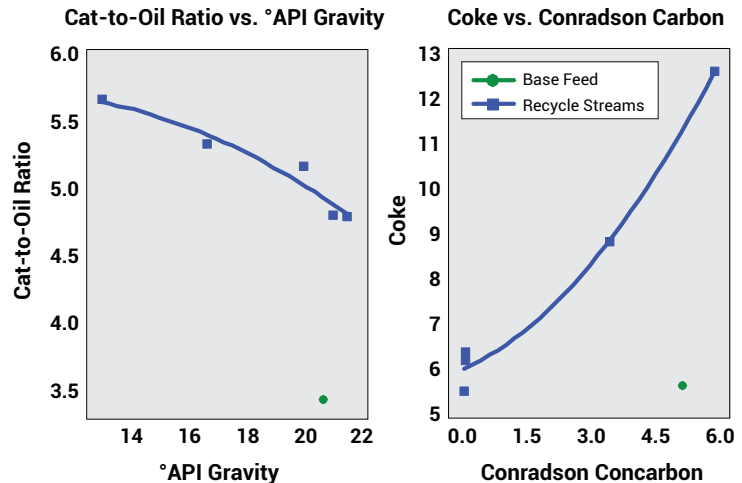


Figure 7. Effect of API Gravity and Conradson Carbon on Catalyst to Oil Ratio and Coke Yield at 55% Conversion

Continued from Page 52

		54 wt% Conversion		68 wt% Conversion	
		650-750°F	750°F+	650-750°F	750°F+
Saturates		Avg., wt%	Avg., wt%	Avg., wt%	Avg., wt%
C(N)H(2N+2)	Paraffins	5.2	4.3	3.4	1.2
C(N)H(2N)	Monocycloparaffins	7.2	8.7	3.6	3.1
C(N)H(2N-2)	Dicycloparaffins	4.9	5.4	2.4	2.7
C(N)H(2N-4)	Tricycloparaffins	3.1	3.9	1.5	2.0
C(N)H(2N-6)	Tetracycloparaffins	0.0	0.2	0.0	0.1
TOTAL SATURATES		20.4	22.4	11.0	9.1
Monoaromatics					
C(N)H(2N-6)	Alkylbenzenes	4.3	6.1	2.6	2.6
C(N)H(2N-8)	Benzocycloparaffins	2.4	2.3	0.6	0.6
C(N)H(2N-10)	Benzodicycloparaffins	1.6	1.1	0.3	0.1
Diaromatics					
C(N)H(2N-12)	Naphthalenes	4.3	2.9	3.4	1.8
C(N)H(2N-14)		14.5	3.2	15.6	1.9
C(N)H(2N-16)		21.2	7.7	24.4	6.4
Triaromatics					
C(N)H(2N-18)		13.9	9.3	18.9	9.8
C(N)H(2N-22)		3.3	25.0	4.2	38.5
Tetraaromatics					
C(N)H(2N-24)		0.0	8.7	0.0	13.6
C(N)H(2N-28)		0.0	1.1	0.0	2.2
TOTAL AROMATICS		65.3	67.4	70.1	77.5

Table 4. GC Mass Spec Analysis of Bottoms Fractions from Resid Cracking in the DCR

Case 1. Maximum Recycle

The goal of the calculation was to maximize recycle ratio of each recycle stream until the coke yield of the base feed at 70% conversion was reached. The hydrocarbon yields, on the fresh feed basis, calculated using the Element-Tracking-Approach are shown in Table 5. In the cases of the 650-750°F and 650-800°F streams, the maximum available recycle levels, based on SIMDIST (Table 1), were reached before the coke yield limit was reached; therefore, the maximum recycle ratio was used.

The highest LCO yield of 30.2% was achieved with maximum recycle (14.4%) of the 650-800°F HCO stream. The next highest LCO yield of 29.9% was achieved with 15.6% recycle of 650-850°F HCO stream. Even though the 650-750°F stream had the best yields by the Element-Tracking-Approach, because it was limited to a maximum recycle ratio of 10.1%, the combined feed with 650-750°F stream made only 28.9% LCO and much higher bottoms. In the case of the 650°F+ bottoms stream, due to coke limitation, only 15% out of the available 24% recycle stream could be recycled. The operation recycling 650°F bottoms made lower LCO throughput and

higher bottoms throughput than the operation with recycling HCO streams of 650-800°F and 650-850°F. Thus, it is advantageous to recycle HCO rather than bottoms. Gasoline yields on fresh feed base for all the recycling streams are about 4-6% higher than that of the case without recycling, which corroborates the results reported by Fernandez et al.^[7]

Case 2. Constant Bottoms

The goal of this calculation was to adjust the recycle ratio of each recycle stream until the bottoms yield of the base feed at 70% conversion was reached. The hydrocarbon yields, on the fresh feed basis, are shown in Table 6. In this case, all the combined feeds with HCO recycle had higher LCO selectivity than bottoms (650°F+) recycle. The difference also comes from the coke yield differences, which allow the feeds with HCO recycle to be processed at higher feed rates than the feed with bottoms recycle. Again, this example shows it is advantageous to recycle HCO rather than bottoms.

	Max. Gasoline Base	Base No Recycle	650-750°F	650-800°F	650-850°F	650°F+
Conversion, wt%	70.0	55.0	61.2	64.2	65.2	64.7
Recycle Ratio	0	0	0.10	0.14	0.16	0.15
Maximum recycle available			0.10	0.14	0.18	0.24
Cat-to-Oil Ratio	6.05	3.43	3.48	3.56	3.59	3.60
Hydrogen, wt%	0.11	0.09	0.10	0.11	0.12	0.12
	1.4	1.0	1.1	1.3	1.4	1.4
C3=, wt%	3.3	2.1	2.4	2.6	2.7	2.7
Total C3's, wt%	3.9	2.4	2.7	2.9	3.1	3.1
Total C4='s, wt%	5.1	3.9	4.5	4.5	4.7	4.8
Total C4's, wt%	8.5	5.6	6.6	6.6	6.9	7.0
C5+ Gasoline, wt%	49.4	40.5	44.6	46.8	47.0	46.4
RON	89.6	89.2	89.4	89.5	89.5	89.7
MON	78.6	77.3	77.7	77.8	77.7	77.9
LCO, wt%	20.5	24.7	28.9	30.2	29.9	29.3
Bottoms, wt%	9.5	20.2	9.9	5.6	5.0	6.0
Coke, wt%	6.7	5.6	6.1	6.5	6.7	6.7
Relative Combined Feed Rate Const Coke	1.00	1.20	1.23	1.21	1.18	1.18
Relative Fresh Feed Rate	1.00	1.20	1.10	1.04	1.00	1.00
Relative Coke Production Rate	6.7	6.7	6.7	6.7	6.7	6.7

Table 5. Case 1 (Max Recycle)—Yields on Fresh Feed Basis (Constant Coke Yield Relative to Max Gasoline Case)

3.3 Effect of Conversion Level

The objectives of this work were to determine how the composition of the HCO stream changed with conversion and how recycling HCO, obtained at varying conversion levels, affected the LCO yield. As described earlier, DCR syncrude samples obtained at 54, 58, 68 and 75 wt% conversion were distilled and the 650-750°F fraction of each syncrude was collected and analyzed (Figure 3). The 650-750°F fractions were blended with the original feed and tested in the ACE.

The theoretical yields of the second-pass cracking on a unit recycle feed basis are calculated using the Element-Tracking-Approach discussed in Section 2.3. The difference in the yields of gasoline, LCO, and coke between the second-pass cracking of the recycle stream and cracking of the fresh feed is shown in Figure 8. The maximum recycle ratio at each conversion, calculated based on simulated distillation, is also plotted in Figure 8. At lower conversion, there is more 650-750°F fraction available for recycle. The low-conversion recycle stream made much higher LCO than the fresh feed, while making about the same gasoline and coke. However, at higher conversion there is less 650-750°F stream available. The high-conversion recycle stream made much lower gasoline, similar LCO and much higher coke. These results can be explained by examining the properties

of the recycle steams in Figure 3. Generally speaking, higher cracking severity in FCC units leads to more gasoline, but a much higher concentration of condensed aromatics in the bottoms.^[8] Although the 50 vol.% boiling points are about the same for each stream, the API gravity and hydrogen content decrease with increasing conversion. This is consistent with the mass spectrometry data in Table 4, which shows the tri-aromatics of the 650-750°F stream, obtained at 68% conversion, is much higher than that at 54% conversion.

Figure 9 shows the yields of gasoline, LCO, bottoms, and coke as a function of conversion for cracking of only the base feed (first cracking). The same figure also shows the corresponding yields, normalized to the fresh feed basis, for cracking of the combined feed (base feed + maximum recycle of the 650-750°F stream at each conversion level). At a given conversion, by recycling the 650-750°F fraction, one can lower bottoms and increase LCO without sacrificing gasoline and with only a minor penalty in coke. This is achieved for two reasons. First, recycling lowers bottoms because part of the bottoms is cracked twice. Secondly, the second-pass cracking of the 650-750°F stream is very selective toward producing LCO, and while coke increases, so does conversion; consequently, coke selectivity is not much higher than that of the first-pass cracking of the base feed.

Continued on Page 55

Continued from Page 54

	Max. Gasoline Base	Base No Recycle	650-750°F	650-800°F	650-850°F	650°F+
Conversion	70.0	55.0	61.2	62.0	62.4	62.5
Recycle Ratio	0.00	0.00	0.101	0.112	0.118	0.120
Maximum recycle available			0.10	0.14	0.18	0.24
Cat-to-Oil Ratio	6.0	3.4	3.48	3.53	3.56	3.56
Hydrogen, wt%	0.1	0.1	0.10	0.10	0.11	0.11
Total C ₁ 's & C ₂ 's, wt%	1.4	1.0	1.1	1.2	1.3	1.3
Propylene, wt%	3.3	2.1	2.4	2.5	2.5	2.6
Total C ₃ 's, wt%	3.9	2.4	2.7	2.8	2.9	3.0
Total C ₄ 's, wt%	5.1	3.9	4.5	4.4	4.5	4.6
Total C ₄ 's, wt%	8.5	5.6	6.6	6.4	6.6	6.8
C ₅ + Gasoline, wt%	49.4	40.5	44.6	45.1	45.1	44.9
RON	89.6	89.2	89.4	89.5	89.5	89.6
MON	78.6	77.3	77.7	77.7	77.7	77.8
LCO, wt%	20.5	24.7	28.9	28.6	28.2	28.0
Bottoms, wt%	9.5	20.2	9.9	9.5	9.4	9.5
Coke, wt%	6.7	5.6	6.1	6.2	6.4	6.4
Relative Combined Feed Rate Const Coke	1.00	1.20	1.23	1.21	1.19	1.19
Relative Fresh Feed Rate	1.00	1.20	1.10	1.08	1.05	1.04
Relative Coke Production Rate	6.7	6.7	6.7	6.7	6.7	6.7

Table 6. Yields on Fresh Basis (Constant Bottoms Yield Relative to Max Gasoline Case)

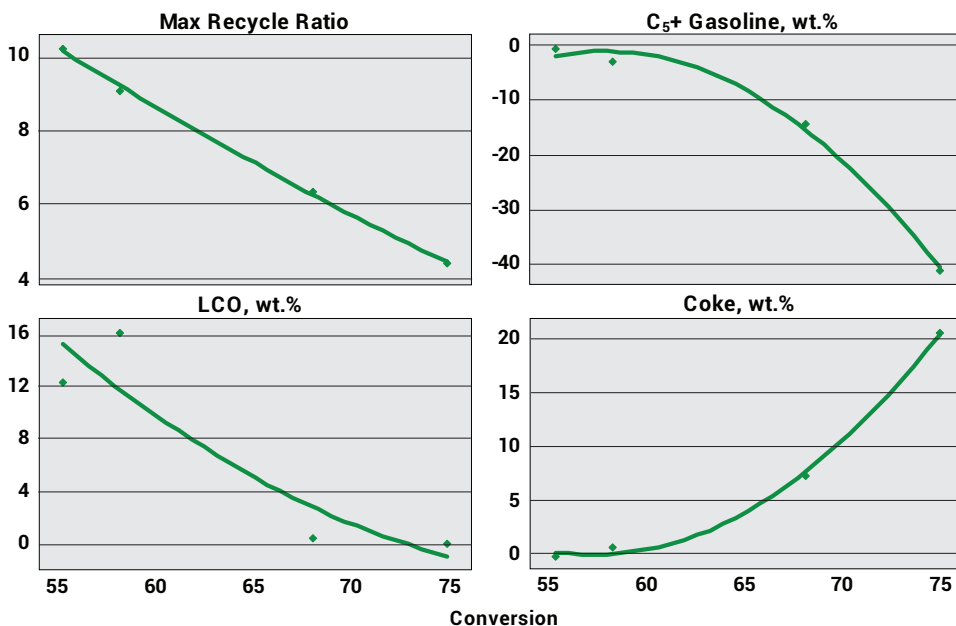


Figure 8. Yields of Second Pass Cracking Minus Fresh Feed Cracking vs. Conversion

The results from Section 3.2, Case 1 (Table 5) of 650-800°F and 650-850°F recycle are also plotted on Figure 8. Compared to recycling with the 650-750°F stream, the LCO gain from recycling these heavier streams is higher; however, the coke penalty is greater. These results suggest that one can achieve the desirable yield shift by lowering conversion on the combined feed basis and selecting the proper recycle stream.

4.0 MIDAS® Catalyst Technology

Application of the correct catalyst technology is critical to ensure high LCO yield and minimal bottoms and coke yield. A balanced approach is required to achieve maximum bottoms upgrading to LCO and other valuable products. Grace Davison MIDAS® catalysts have been proven to minimize bottoms

production^[9]. As a result, a MIDAS[®] catalyst was used for the experiments described here.

Commercialized in 2008, MIDAS[®]-300 catalyst series is specially designed for today's distillate-driven market. MIDAS[®] catalyst has been used in 52 units since its first introduction. Currently in three commercial units, MIDAS[®]-300 catalyst is the latest result of Grace's long commitment to developing industry

leading bottoms cracking catalysts. MIDAS[®]-100 series of catalyst were introduced in 2005 and in 2007 the MIDAS[®]-200 series was commercialized.

MIDAS[®]-300 catalysts offer higher activity matrix surface area, balanced with optimized zeolite content. The majority of matrix porosity in MIDAS[®] technology is found in the crucial 100-600 Å pore size diameter range, ensuring high LCO selectivity.

LCO selectivity is maximized via the three-step bottoms cracking mechanism originally described by Zhao^[10] as shown in Figure 10. Each of these bottoms cracking mechanisms is particularly critical in lower conversion operations to ensure high LCO yield and low bottoms.

It is critical that feed vaporization be maintained when the FCC operates at reduced reactor temperature to maximize LCO. At low operating reactor temperature, optimization of Type I cracking becomes more critical due to the reduction in the riser mix zone temperature. Catalyst design plays a critical role in maintaining the right conditions. Since resid feeds contain a high percentage of molecules boiling above the mix zone temperature, pre-cracking is necessary to achieve complete vaporization. Porosity in the 100-600Å range is essential for the pre-cracking reactions that facilitate vaporization. MIDAS[®]-300 catalysts have the highest porosity in this critical range of any cracking catalyst. MIDAS[®]-300 ensures that feed is properly vaporized even at low severity.

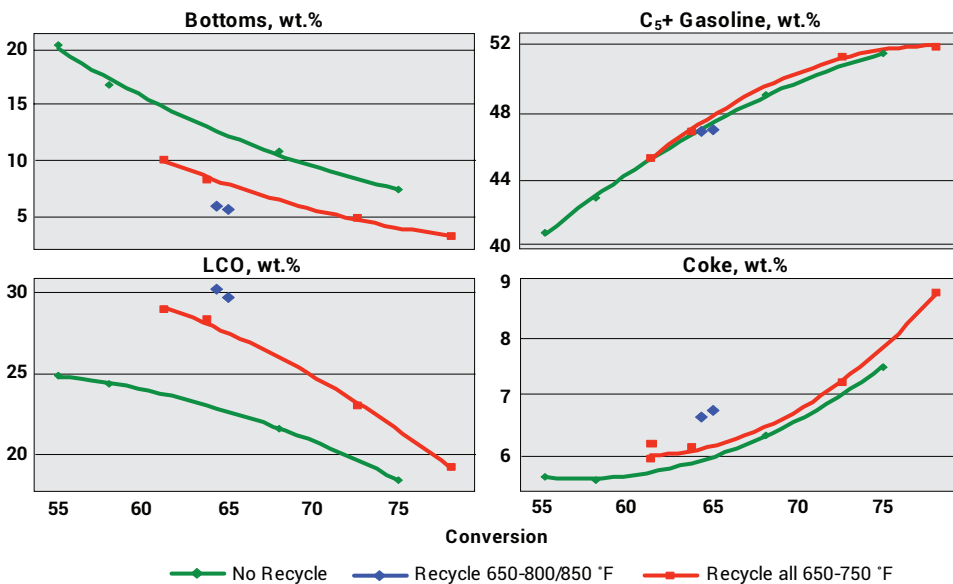


Figure 9. Yields vs Conversion of Base Feed and Combined Feed Normalized to Fresh Feed Basis

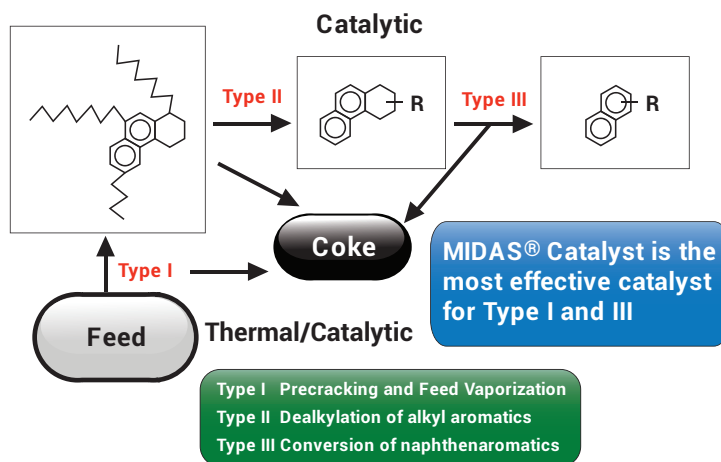


Figure 10. Bottoms Cracking Fundamentals

Most of the LPG and gasoline produced in an FCC comes from dealkylation of aromatics or Type II cracking. Zeolite is much more effective than matrix in cracking long chain alkyl aromatics. Type II cracking is important to reduce the molecular size and promote eventual conversion of bottoms; however, we must prevent any LCO that is produced from being over-converted to lighter components. The zeolite level in MIDAS[®]-300 has been optimized to provide sufficient dealkylation activity, yet maintain the product yield as LCO rather than LPG and gasoline.

Finally, Type III cracking destroys naphthene rings in naphthenoaromatic compounds. The size of typical naphthenoaromatic molecules is too large to easily fit into the zeolite. The cracking of these molecules will occur on the matrix sites or on the external surface of the zeolite. The selective cracking of

Continued on Page 57

Continued from Page 56

this type of molecule requires the proper design of matrix activity and the interaction of matrix and zeolite. The high mesoporosity of MIDAS®-300 catalysts improves LCO selectivity by converting coke precursors into valuable liquid product.

Grace Davison can also deliver enhanced LCO selectivity in an additive form. BX™-450 is Grace's newest catalytic additive offering and is the first of its kind designed specifically for maximum distillate yield. BX™-450 is based on MIDAS®-300 technology and offers high activity matrix surface area balanced with an optimized zeolite level to maximize LCO selectivity. The optimized zeolite level in BX™-450 provides sufficient catalytic activity, enabling 1:1 replacement of fresh catalyst.

5.0 Commercial Maximum Operation Using Recycle and MIDAS® Technology

A commercial operation was modeled using results from the work described earlier together with our new MIDAS®-300 technology. Table 7 shows a maximum gasoline/ conversion FCC operation with a residual feedstock. Two cases are modeled off this base operation. Case 1 is a reduced conversion operation together with a recycle of 11 vol.% HCO (650-800°F). Case 2 represents a fully optimized maximum LCO operation. Cases 1 and 2 were modeled assuming the base maximum gasoline/conversion operation was operating at an air blower and wet gas compressor constraint.

January 2009 FCC product values were used to assess the relative product values for Cases 1 and 2. LCO is valued at 8.00 \$/bbl greater than gasoline. Those product values are shown in Table 8.

Case	Base	1	2
Operating Mode	Max Gasoline	Max LCO	Fully Optimized Max
Catalyst/Additive	MIDAS®-100	MIDAS®-100	MIDAS®-300 & OlefinsUltra®
Recycle, % FF, vol.%	0	11	11
Ecat Activity	68	64	64
Feedstock Properties			
°API	21.6	21.6	21.6
Conradson Carbon, wt%	3.0	3.0	3.0
1050°F+, vol.%	20	20	20
Operating Conditions			
Reactor Temperature, °F	995	950	950
Feed Temperature, °F	400	405	405
Regenerator Temperature, °F	1350	1290	1290
Cat/Oil	7.2	7.8	7.8
Air Blower	Base	Base	Base
Wet Gas Compressor Rate	Base	0.75 Base	Base
Product Yields/Properties			
Dry Gas, scfb	331	235	235
LPG, vol.% FF	23.9	19.3	30.0
Gasoline, vol.% FF	56.7	51.9	44.0
RON/MON	92.6/80.6	90.0/79.5	92.9/80.7
LCO, vol.% FF	22.9	32.0	33.4
Bottoms, vol.% FF	6.8	6.0	5.0
Coke, wt% FF	5.2	5.2	5.2
C ₃ +, vol.%	110.3	109.2	112.4
Incremental Product Value, \$/B	Base	+0.10	+1.40

Table 7. Commercial Maximum Gasoline and Maximum Conversion Modeling Results

C ₃ =, \$/bbl	34.0
C ₄ =, \$/bbl	45.4
Gasoline, \$/bbl	47.9
LCO, \$/bbl	55.9
Bottoms, \$/bbl	29.0
Gasoline Octane, Base 86.9 (R+M)/2	0.49

Table 8. FCC product values January 2009

LCO is increased in Case 1 by reducing conversion via lower reactor temperature, lower equilibrium catalyst (Ecat) activity, higher feed temperature and the incorporation of 11 vol.% recycle. Coke yield is the same as the base operation. Lower reactor temperature and higher feedstock temperature reduce the unit coke demand, allowing the incorporation of recycle at the same air blower demand as the base operation. As described above, coke yield or air blower rate will be the primary constraint reached. The FCC catalyst in the Base and Case 1 operation is MIDAS®-100 catalyst.

Case 1 has a higher cat to oil ratio due to the introduction of recycle and lower catalyst activity and results in increased bottoms conversion to LCO. Wet gas rate is lower in Case 1 as a result of lower LPG and dry gas.

Despite a 9 vol.% increase in LCO yield, the Case 1 product value is only a modest 0.10 \$/bbl greater than the base operation. The reduced C₃+ vol.% and gasoline octane compared to the base operation hinder the total product value.

Case 2 represents a fully optimized operation using MIDAS®-300 catalyst and OlefinsUltra® ZSM-5 additive. LCO is increased at the expense of bottoms due to improved bottoms cracking with MIDAS®-300 catalyst. OlefinsUltra® additive is used to increase the gasoline octane, which dropped sharply from the base operation due to lower reactor temperature. Wet gas rate increases compared to the base operation due to additional LPG production. Air blower and wet gas compressor rates in Case 2 are identical to the base operation.

The optimized Case 2 product value has increased 1.40 \$/bbl relative to the base operation. These product values are achieved despite a low value of propylene and confirm the need to maintain liquid yield and gasoline octane while operating in a maximum LCO mode.

6.0 Conclusions

Maximizing LCO yield is largely a bottoms management process. Operating at reduced conversions by shifting operating conditions and reducing Ecat activity increases LCO, but also increases bottoms. To fully maximize LCO from the FCC, the refinery should consider several strategies in parallel.

Recycle can be employed to fully maximize LCO at reduced conversion, while maintaining bottoms equal to a traditional maximum gasoline operation. The crackability and LCO yield produced by a particular recycle stream are consistent with its API gravity and hydrogen content. Due to the reduced first-pass cracking conversion, the potential of recycle streams to produce LCO with minimal coke production are improved over high conversion operations.

The 650-750°F stream, when recycled, produces the most LCO and gasoline and the lowest coke for a given conversion. However, it is not produced at sufficient quantities to fully maximize LCO. High Conradson Carbon levels consistent with higher tetra-aromatic and heavier compounds limit the yield of LCO when 650+°F or 750+°F streams are recycled. The 650-800°F or 650-850°F recycle stream produces the highest LCO when recycled against a coke burn and bottoms constraint.

MIDAS®-300 is the latest development in Grace's successful MIDAS® series of catalysts. MIDAS®-300 catalyst improves bottoms conversion via high activity matrix surface area balanced with an optimized zeolite level. OlefinsUltra® and OlefinsMax® ZSM-5 additives should be considered to preserve C₃+ liquid yield and gasoline octane.

References

1. R. E. Ritter, J. E. Creighton, "Producing Light Cycle Oil in the Cat Cracker", *Catalagram*® 69 (1984) 5.
2. Energy Information Administration (EIA) short-term outlook January 2009.
3. D. Wallenstein, R.H. Harding, J.R.D. Nee, L.T. Boock, "Recent Advances in the Deactivation of FCC Catalysts by Cyclic Propylene Steaming (CPS) in the Presence and Absence of Metals," *Appl.Catal. A: General* 204 (2000) 89.
4. G. W. Young, G.D. Weatherbee, "FCCU Studies with an Adiabatic Circulating Pilot Unit," AIChE Annual Meeting, November, 1989.
5. J.C. Kayser, Versatile Fluidized Bed Reactor, U.S. Patent 6,069,012.
6. A. Ye, W. Wang, "Cracking performance improvement of FCC feedstock by adding recycle stock or slurry", *Lianyou Jishu Yu Gongcheng* (2004), 34(6), 5-6.
7. M. L. Fernandez, A. Lacalle, J. Bilbao, J. M. Arandes, G. de la Puente, U. Sedran, "Recycling Hydrocarbon Cuts into FCC Units", *Energy & Fuels* 16 (2002) 615.
8. R. Venugopal, V. Selvavathy, M. Lavanya, K. Balu, "Additional Feedstock for Fluid Catalytic Cracking Unit", *Petroleum Science and Technology* 26 (2008) 436.
9. Schiller, R. et al "The Genesis™Catalyst System" *Catalagram*® 102, Fall 2007.
10. Zhao, X., et al, "FCC Bottoms Cracking Mechanisms and Implications for Catalyst Design for Resid Applications" NPRA AM-02-53.
11. A. Corma, L. Sauvinaud, "How can we increase the LCO yield and quality in the FCC: cracking pathways analysis", *Preprints - American Chemical Society, Division of Petroleum Chemistry* (2006), 51(2), 447-451.




The iron tolerance properties of an FCC catalyst can offer a refiner significant flexibility to process heavier and more contaminated feedstocks. For the past several decades, iron tolerance research has been at the forefront of the Grace R&D program, with major insights and learnings contributing to the comprehensive landscape of knowledge available today. One important article, entitled “The Effects of Fe Poisoning on FCC Catalysts” and published at the 2001 NPRA Meeting (now referred to as AFPM), detailed the earlier work and findings from Grace catalyst experts on iron poisoning.


The article discusses the effects of iron on equilibrium catalyst (Ecat) properties, the deposition mechanism and associated surface effects, and strategies for addressing iron poisoning in the FCCU, many of which are still employed today. This foundational and fundamental understanding of iron tolerance has been key in developing some of Grace's recent breakthrough technologies, including MIDAS® Pro, Grace MILLE™ technology, and the Grace Iron Deactivation Protocol (Grace-IDP™).



Gary Cheng
Director, Strategic Marketing
W. R. Grace & Co.

The Effects of Fe Poisoning on FCC Catalysts

 G. Yaluris, W.C. Cheng, M. Peters, L. T. Boock, and L. J. Hunt

 Originally published by the American Fuel and Petrochemical Manufacturers Association (AFPM) at the AFPM Annual Meeting in 2001, AM-01-59, 2001.

Contamination of FCC catalyst with metals, like Ni, Na, V and Fe, coming from feed or other sources has always been a major issue in most FCC units. However, for Ni, V and Na, catalytic and other solutions have been developed over time that have allowed the FCCU to operate at high levels of contamination. Fe has also been known to adversely affect the performance of FCC catalysts, but until recently Fe related problems in FCC units were largely unreported, and unlike Ni, V and Na, little work has been done to understand the effects of Fe on FCC catalysts. Today because of increased processing of high Fe feeds, and the need by many units to process heavy local feeds, the effects of Fe on the unit operation cannot be ignored.

Increasing Fe on the equilibrium catalyst (Ecat) can have serious adverse effects, including loss of activity and bottoms cracking, as well as increased SO_x emissions and CRC (in partial burn units). Ecat ABD has also been reported to decrease. Despite these

dramatic effects, until now, little has been published about how Fe impairs catalyst performance. Thus, Davison Catalysts has undertaken an extensive research program to understand the mechanism by which Fe deactivates FCC catalysts, and to develop practical solutions to address the problem.

It appears that there are two types of Fe. One type consists primarily of particles of inorganic Fe from pipes, storage tanks and other hardware. This type is usually called "tramp" Fe and is generally benign in FCCU operation. The other type is primarily organic Fe coming from feed and/or from hardware corrosion by naphthenic acids and other corrosive feed components. Because of the deleterious effects on unit performance, we have focused our work on the latter type of Fe and investigated the mechanism for Fe-induced catalyst deactivation. In this paper we present the results of our work and we recommend a strategy to deal with FCC catalyst poisoning caused by Fe.

Continued from Page 60

Effect Of Fe On Ecat Properties

Part of the difficulty in studying the effects of Fe on FCC catalysts is that contrary to other metal contaminants, Fe does not have as significant an impact on Ecat properties. Increasing Ni, V and Na has obvious effects on Ecat properties that can be correlated to catalyst performance in the unit. For example, V and Na decrease the zeolite surface area and Ecat microactivity, explaining the observed decrease of unit conversion. Similarly Ni increases the Ecat coke and gas factors, explaining the in-unit increase of coke and hydrogen. However, there are few Ecat properties that are consistently affected by Fe.

One Ecat property that is affected by Fe contamination is ABD. It has been observed in some FCCU's that increasing Fe can result in decreasing Ecat ABD. In Figure 1 we show one example where this is the case. Our analysis of the Ecat data shows that in general, in units where Fe has been shown to have an adverse effect on catalyst performance, increasing Fe will cause a decrease in Ecat ABD, sometimes by as much as 0.15 g/cc. The exact magnitude of the decrease depends on the increase of Fe levels on the Ecat, the unit type and operation and the catalyst used. However, as we show in Figure 2 an increase of Fe levels on Ecat does not always cause a decrease in Ecat ABD. This appears to be particularly the case for units which are able to operate with high Fe levels on Ecat without significant performance debits.

The effect of Fe on other Ecat properties is less clear and, if observable, less severe. Our analysis of Ecat data for many FCCUs shows that in most cases the Ecat pore volume remains unchanged or changes only slightly (<10%) with increasing Fe. Ecat microactivity and zeolite surface area usually cannot be correlated with increasing Fe levels on the Ecat. In most cases either there is

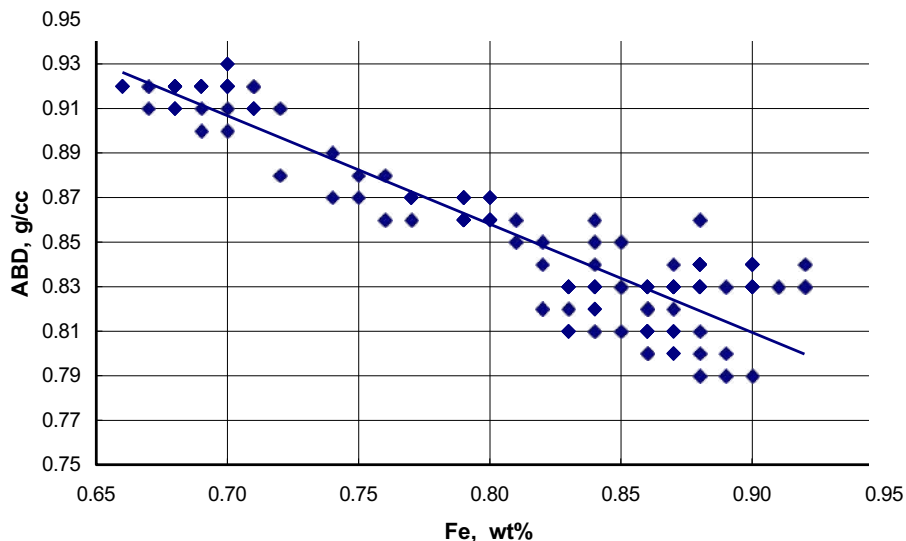


Figure 1. In units where Fe causes catalyst performance deterioration, Ecat ABD decreases with increasing Fe contamination.

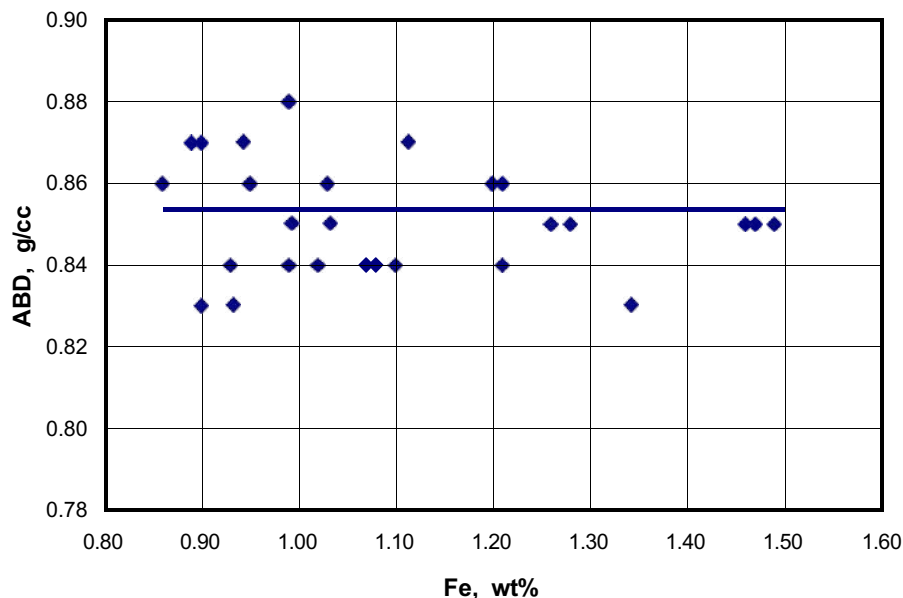


Figure 2. For some units Ecat ABD does not decrease with increasing Fe contamination.

not a significant change with Fe, or if there is, the picture is confused by the fact that other contaminants well known to affect microactivity and zeolite surface area, like V and Na, also increase. Changes in unit operation, like reduced catalyst additions, can also affect Ecat activity and cause an incidental increase of Fe levels on the Ecat. Thus, when

assessing the impact of Fe on unit performance it is important to take into account all changes in the unit, including the levels of other contaminant metals.

Deposition Of Fe On Ecat

We studied the deposition of Fe on various Ecats using EPMA (Electron Probe Micro Analyzer). This technique

can identify the distribution of an element across a polished section of a particle with a resolution of 1 μm . Areas with high concentration of the element probed show as red or yellow, while low concentration areas are purple or blue. We show representative examples of the distribution of Fe on Ecat in Figure 3. The EPMA data unequivocally show that Fe always deposits on the external surface of Ecat particles, creating rings of high Fe concentration around the particles.

We also investigated if Fe can penetrate further inside the FCC particle as Fe levels on the Ecat increase. Analysis of the data like the example shown in Figure 4, suggests that increasing the Fe content of the Ecat increases the concentration of Fe on the particle surface, but not the depth of Fe penetration inside the particle. It appears that Fe does not penetrate inside the Ecat particles much deeper than 1-3 μm . This result explains why the effects of Fe on Ecat properties like surface area, pore volume and microactivity are limited. For a 70 μm particle, a ring of 1-3 μm of Fe is only 4-12% of the total particle volume, leaving the vast majority of the particle unaffected.

These results show that Fe deposits on the first site of the particle it encounters and continues to do so as long as Fe deposition continues. The raw materials used, catalyst manufacturing process, binding system or other differences among catalysts made by the same or different manufacturers do not appear to have any influence on how Fe deposits on catalyst particles. Thus, we conclude that any pore structure differences among the catalysts studied do not have a major impact on the deposition of Fe, and therefore, do not significantly impact catalyst deactivation by Fe.

Ca is another contaminant that has the same deposition profile as Fe. It also forms rings 1-3 μm deep on the external particle surface (Figure 3), and it does not penetrate further when the levels of

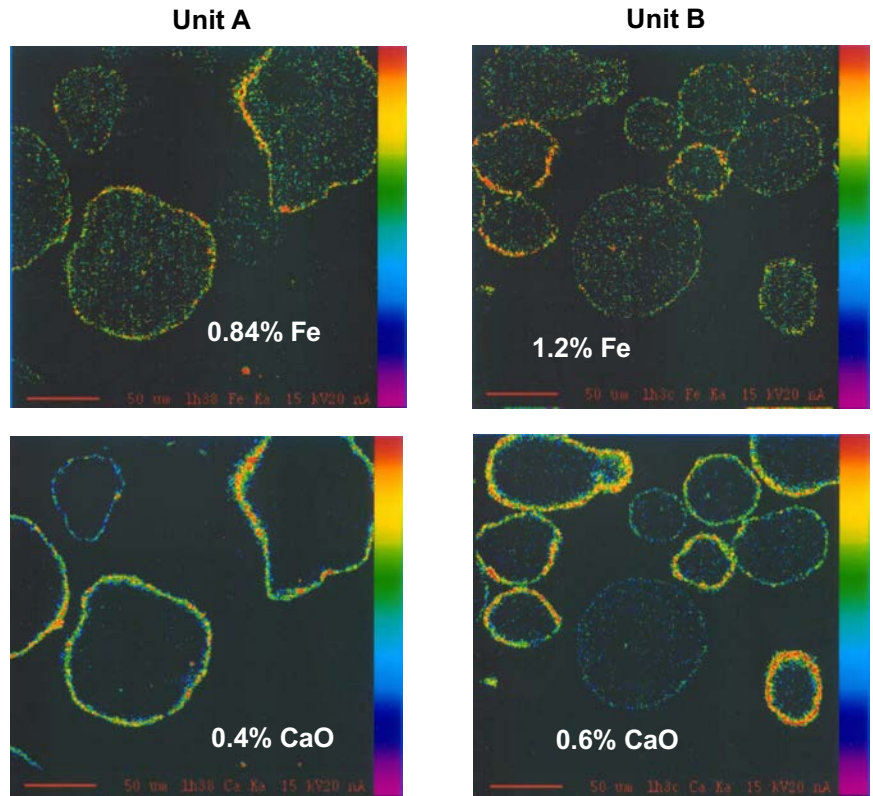


Figure 3. The distribution of Fe and Ca deposited on Ecat particles during catalyst aging in the unit. Ecats from two different units.

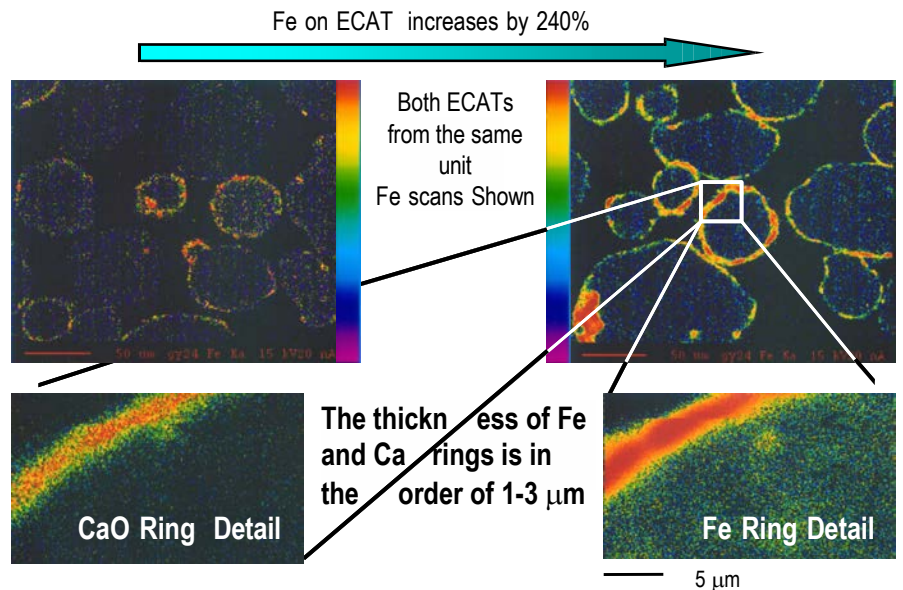


Figure 4. Increasing the amount of Fe or Ca deposited on Ecat does not result in Fe or Ca penetrating deeper into the particle.

Continued from Page 62

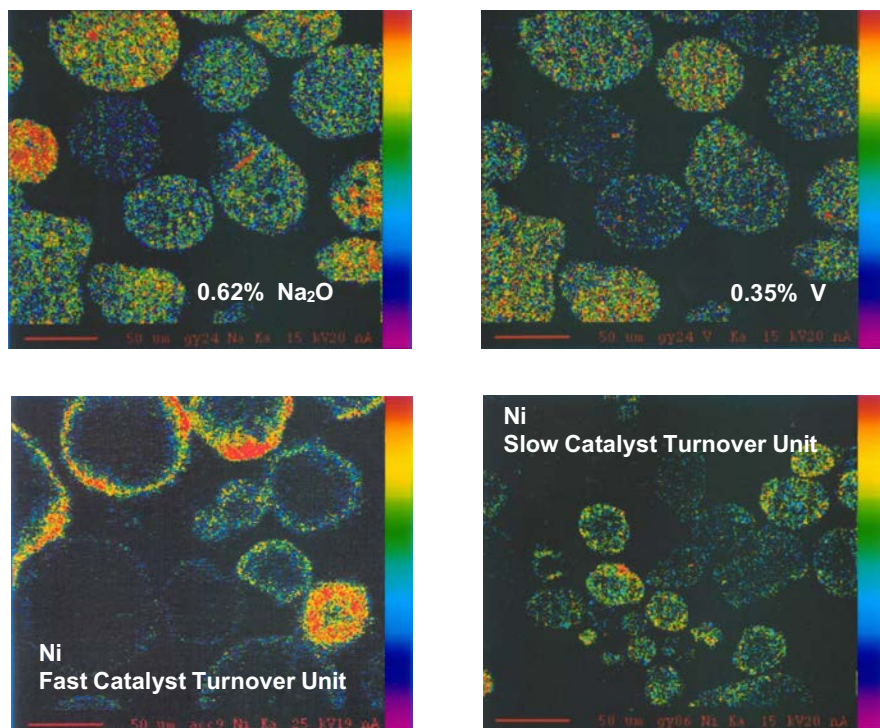


Figure 5. Deposition of Na and V on Ecats particles, as well as Ni deposition on Ecats from two units representing two extreme cases of Ni concentrating on the outward particle areas or distributing throughout the particles.

Ca deposited on the Ecats increase. The presence of Ca in high concentration on the external surface of catalyst particles, often at the same high Fe concentration areas of the particle, suggests that Ca may be involved in the mechanism by which Fe poisons the FCC catalyst.

Of the other contaminant metals, the deposition of V and Na, shown in Figure 5, is distinctly different from that of Fe. Within the accuracy of the technique, both metals deposit throughout the catalyst particle. Ni has a somewhat different deposition profile. The EPMA data in Figure 5 show that Ni can concentrate on the external surface of Ecats particles. However, depending on the unit, the amount of Ni deposited, the average residence time of the catalyst in the unit and the catalyst technology employed, Ni can eventually penetrate throughout the particle, resulting in a deposition profile similar to that of Na or V.

Fe Concentration on Ecats Particles Surface

Since Fe deposits on the external surface of the Ecats particle, it is reasonable to assume that the bulk Fe loading of the Ecats is not important in establishing the extent to which the deposited Fe will affect catalyst performance. Much more critical is the surface concentration of Fe as well as its oxidation state.

Using X-ray Photoelectron Spectroscopy (XPS) we measured the surface concentration of various Ecats mostly from units reporting problems with Fe poisoning of their catalyst, but also from a few units which have not reported any Fe related problems. From the XPS data and the bulk composition measured by ICP, we calculated surface enrichment ratios for many of the elements present in Ecats. We

have compiled those data in Table 1. In general, the surface enrichment ratios in Table 1 show that there seems to be little difference between the surface and bulk concentration for Na and Si. This result is not unexpected considering the well known mobility of both of these elements. On the other hand Al is not very mobile and in general it is covered by the depositing elements (primarily Fe), resulting in a surface enrichment ratio well below 1. As expected based on the EPMA results, Fe is greatly enriched on the surface by as much as 10-18 times. Because XPS probes all of the particle exterior surface, these data do not exclude the possibility of local areas with even higher than the average surface concentration of the elements measured.

Since Si and Na are not covered by the depositing Fe, we conclude that on the Ecats particles external surface Si and Na are well mixed with the deposited Fe. Ca is also present in the Fe-rich ring formed around the particles, as it deposits in a fashion similar to that of Fe. Aluminum does not appear to mix with Fe and the other elements. Thus, solid phases that contain silica, iron, calcium and sodium oxides form easily on the surface of Ecats particles with Fe contamination. Similar low melting phases containing alumina and Fe oxides seem to be much harder to form.

The XPS data show that the Fe on the Ecats is in the form of Fe³⁺. However, this is not necessarily the state of Fe in the riser or the regenerator. Ecats are typically discharged hot from the unit and it is exposed to the atmosphere which most likely will oxidize any reduced iron to the Fe³⁺ state. Our experiments show, that Fe can easily be reduced in the unit to Fe²⁺ and perhaps even further. In our partial burn cyclic propylene steaming lab deactivation protocol¹, Fe³⁺ is easily reduced to magnetite (Fe₃O₄).

	Surface Weight (%)	Surface Enrichment Ratio
Na	up to 1%	1-2
Al	Varies	0.4
Si	Varies	0.8 - 1.2
Ca	up to 1.2%	2 - 30*
Fe	up to 26%	10 - 18

* Ratios of species in small amounts can change significantly from Ecat to Ecat depending on the amount of them present on the fresh catalyst

Table 1. Surface enrichment ratios for elements present in Ecat. The ratios are calculated by dividing the concentration of the element on the surface by its concentration in the bulk.

Morphology and Surface Texture of Fe-Poisoned Ecats

We studied the morphology and surface texture of Fe poisoned Ecats using Scanning Electron Microscopy (SEM) and optical microscopy. The SEM data in Figure 6 clearly show that Fe has a distinct effect on the Ecat morphology and texture. Nodules and valleys form on the surface of Ecat particles poisoned with Fe. Nodules appear to be present on the surface of Ecat particles from different units and different catalyst technologies. As we show in Figure 6, these characteristic nodules are present even on Ecat particles from a unit using a purportedly 'high accessibility' competitive technology.

However, we have found examples of catalysts with significant levels of Fe contamination on Ecat, but with little evidence of nodule formation.

The results of the SEM analysis of various Ecats have shown many examples of catalyst particles that appear to "stick" together or have irregular shapes. We show an example in Figure 7. However, as we show in the same figure, we have been able to find similar examples of catalyst particles "stuck" together or with irregular shapes in fresh FCC catalyst samples. Given the limitations of SEM, there is not sufficient evidence at this time to unequivocally conclude that Fe poisoning results in particles sticking together or having irregular shapes. Thus, claims made² based on SEM data that Fe contamination can cause catalyst particles to agglomerate, must be considered as unproven at this time.

Optical microscopy shows that the texture of Fe contaminated Ecat changes in another important way. In Figure 8, we show one example of the optical microscopy pictures of Ecats from the same unit taken at different times as the Ecat Fe levels changed. The data show that a lab deactivated sample of the same catalyst as the one used in the unit with no added Fe has a dull texture that does not reflect light very well. As the catalyst ages in the unit with Fe, the Ecat appears to acquire a "glassy" cover which under optical microscopy gives the Ecat particles a sharper definition and glossy appearance making them more reflective of light. Increasing levels of Fe on the Ecat particles further enhances the observed glassy layer and, as expected, changes the particles color to red/brown similar to the known color of iron oxide.

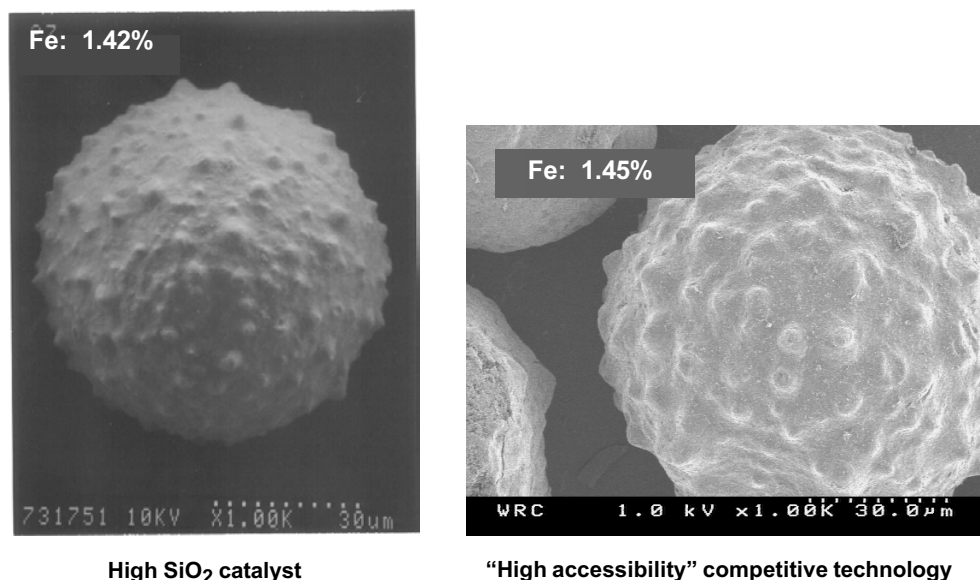


Figure 6. SEM pictures of Ecat particles from two different high Fe units.

Continued on Page 65

Continued from Page 64

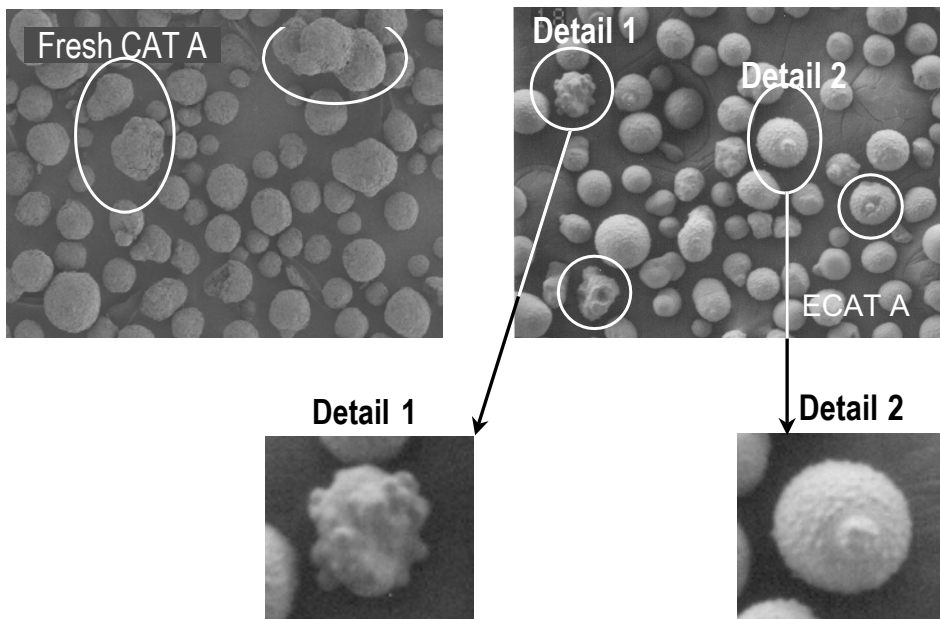


Figure 7. SEM pictures of Ecat particles as well as fresh catalyst particles (steamed for 4 h at 1500°F). Both samples are from the same manufacturer.

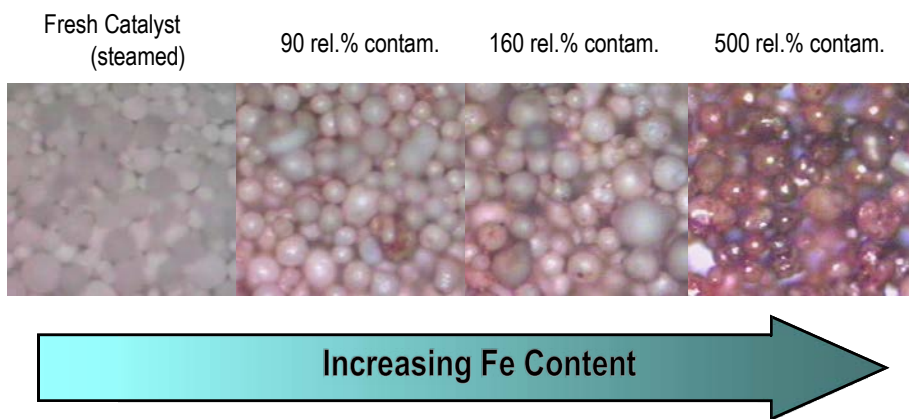


Figure 8. Optical microscopy pictures of lab deactivated catalyst with no added Fe, and three Ecat samples of the same catalyst from the same unit taken at different times as Fe levels changed. All pictures taken under the same conditions.

Laboratory Evidence of the Effects of Fe On FCC Catalysts

As part of our comprehensive research program on the effects of Fe poisoning, we have expended significant effort to duplicate in the lab some of the deactivation phenomena that occur in an FCC unit. Studying the effects of Fe

on FCC catalysts in the laboratory has proven challenging at best because the standard methods for studying the effects of metals like Ni and V on catalyst activity and stability can not be applied to Fe. Iron deposits on the exterior surface of the particles, having in most cases marginal effects on bulk catalyst properties, and making it difficult to confirm that Fe effects

have been successfully replicated in laboratory studies. In addition, few surface sensitive techniques can be easily applied in the study of FCC catalysts and Ecats. To our knowledge, no lab studies of the effect of Fe on FCC catalysts have been published.

To overcome the problems of studying the effects of Fe on FCC catalysts in the laboratory, we utilized our measurements of the chemical composition of the external area of the particles and prepared catalysts that have in the bulk of the particles the same composition that Fe contaminated Ecat particles have on the external surface. For the purposes of this experiment we prepared two sets of catalysts, one with a proprietary Al-sol binding system and 0, 5 and 20% Fe, and the other with a proprietary Si-sol binding system and 0, 5, and 20% Fe. We also added the necessary Na and Ca to simulate the presence of these elements on the surface of Fe poisoned catalysts. We then studied these catalysts both after calcination and after various deactivation treatments.

The data in Figure 9 show that without some deactivation treatment there are no differences between Al-sol and Si-sol catalysts. The surface area of the catalysts is reduced almost proportionally to the amount of Fe added, probably because iron oxide is a low surface area oxide contributing weight to the samples, but not as much surface area as the other constituents of the catalyst (e.g., zeolite, matrix, and binder). When the catalysts are treated using the Davison partial burn Cyclic Propylene Steaming¹ deactivation protocol (CPS), both the Al-sol and the Si-sol catalysts without any added Fe have the same surface area stability. However, as the Fe on the catalysts increases, the surface area of the Al-sol catalysts is much more stable than that of the Si-sol catalysts. In fact, after the deactivation treatment, the Al-sol catalyst with 20% Fe has almost double the surface area retention of the Si-sol catalyst with the same amount of Fe.

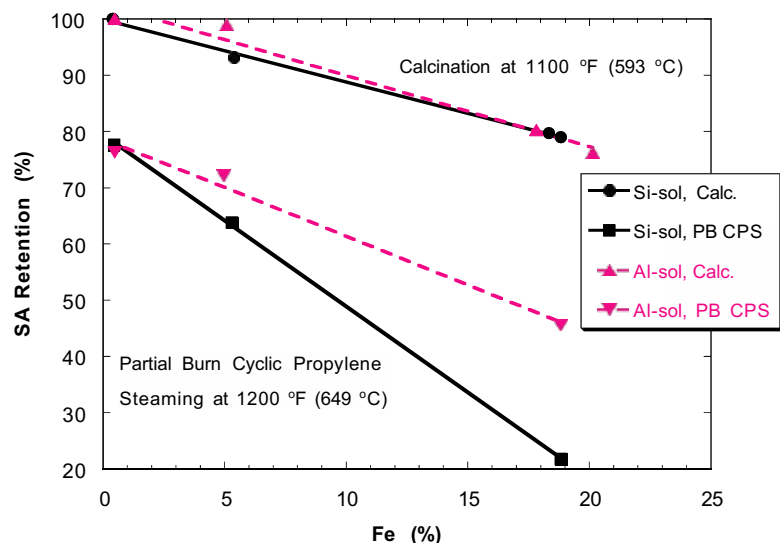


Figure 9. Laboratory evidence of the effects of Fe on FCC catalysts. When Fe is deposited throughout the catalyst particle, surface area retention after partial burn cyclic propylene steam deactivation decreases more for Si-sol than it does for Al-sol catalysts.

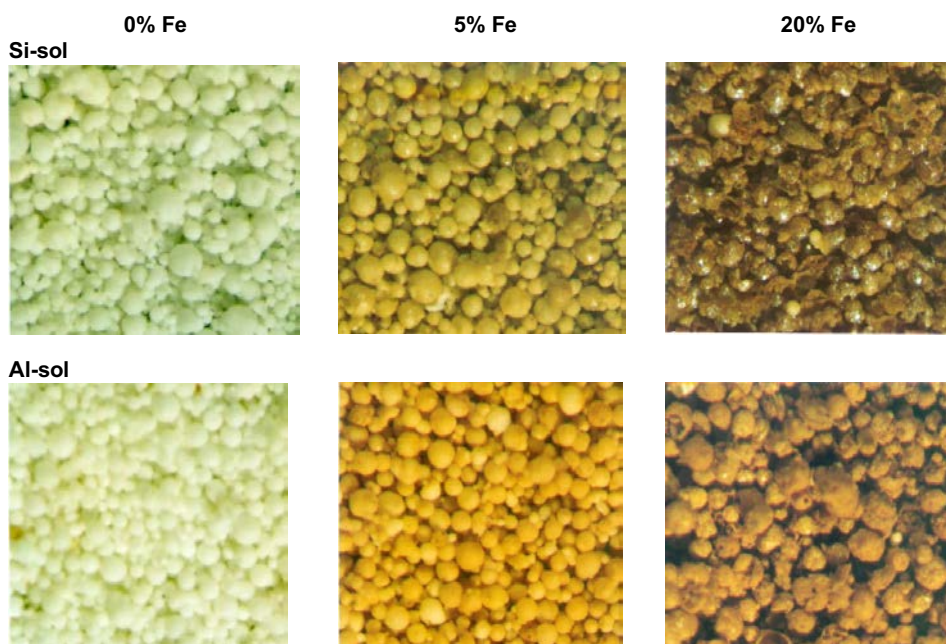


Figure 10. Optical microscopy images of lab-made Si-sol and Al-sol catalysts with 0, 5 and 20% Fe, partial burn CPS deactivated at 1200°F, showing the differences in texture and color between the two classes of catalysts when poisoned by Fe. All images taken under the same conditions.

Using optical microscopy, we studied the color and texture of these catalysts. The CPS deactivated Al-sol catalysts maintain the same texture regardless of the amount of Fe on the catalyst (Figure 10). Only the color changes from white to a light ferric oxide red/brown and finally to a darker red/brown. However, for the Si-sol catalysts as the Fe level increases, the particles change texture and a shiny-glassy texture can be identified covering the catalyst particles. In addition, with the increasing Fe the color changes from white to dark green-brown.

At high Fe levels, SEM pictures of the same deactivated catalyst particles have features indicating that while for Al-sol catalysts the constituent particles which make up the catalyst microspheres retain their integrity, for Si-sol catalysts these constituent particles lose their integrity and become less well-defined. This observation is confirmed by XRD data. As we show in Figure 11, the crystal structure of the components of the Si-sol catalysts gradually becomes amorphous as the Fe content increases to 20%, leaving only some magnetite peaks from the excess iron oxide showing. In contrast, the Al sol catalyst with 20% Fe maintains much more of its original crystallinity than the Si-sol catalyst with the same amount of Fe.

These data clearly show that in the external area of the catalytic particle affected by Fe poisoning (Fe rings) there is a loss of surface area and crystallinity, probably due to melting or accelerated sintering that gives the catalyst particles a glassy appearance. The data also convincingly show that these effects of Fe are more severe for Si-sol than Al-sol catalysts. Because the Fe rings formed on Ecat particles constitute only a small portion of the particles, the overall loss of crystallinity and surface area due to Fe on Ecats is too small and cannot be observed.

Continued from Page 66

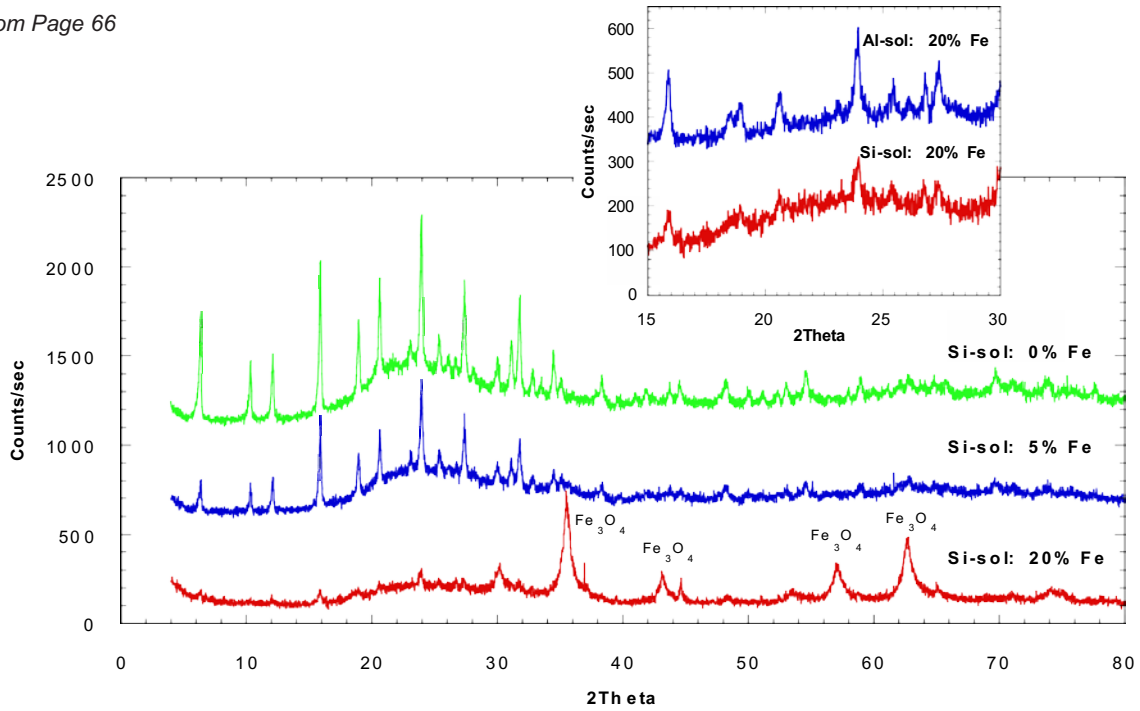


Figure 11. XRD analysis of lab-made Si-sol and Al-sol catalysts with 0, 5 and 20% Fe, partial burn CPS deactivated at 1200°F, showing the effect of Fe on crystallinity. After depositing 20% Fe, Al-sol catalysts have double the crystallinity of Si-sol ones.

System	SiO ₂ (%)	Al ₂ O ₃ (%)	FeO/Fe ₂ O ₃ (%)	Na ₂ O (%)	CaO (%)	(°C)	(°F)
SiO ₂	100					1713	3115
Al ₂ O ₃		100				2050	3722
SiO ₂ -Na ₂ O ⁴	Balance			0*-25		780	1436
SiO ₂ -CaO ⁵	Balance				0-36	1436	2617
Al ₂ O ₃ -Na ₂ O ⁶		Balance		0*-5.5		2000	3632
				5.5-9.2		1580	2876
				>9.2		1410	2570
SiO ₂ -FeO ⁷	Balance		0*-62				
SiO ₂ -FeO•Fe ₂ O ₃ ⁸	Balance		0*-85				
Al ₂ O ₃ -FeO ⁹		Balance	0*-35				
SiO ₂ -FeO-Na ₂ O ¹⁰	Balance		0*-57*	25-0*,†		<500	<932
Na ₂ O-Al ₂ O ₃ -SiO ₂ -Fe ₂ O ₃ ¹¹	71.3	4	6.2	18.4		771	1420
	58.5	9	17.3	15.1		943	1729
	59.3	16.4	9	15.3		998	1828
	47.9	24.1	9.7	18.4		1248	2278

* 0% is not included in the composition range with the indicated first liquid temperature.

† The combination of high FeO and high Na₂O concentrations leads to phases that have slightly higher melting temperatures (~ 667°C/1233°F).

Table 2. Initial melting temperatures for phase systems containing SiO₂, Al₂O₃, FeO/Fe₂O₃, Na₂O and/or CaO at ranges of concentrations which include those that can be found on the surface of FCC Ecats.

The Thermodynamics of Fe-Poisoned FCC Catalyst Surfaces

Of the two major components of FCC catalysts, alumina has the highest melting point, higher than 3722°F (2050°C) after α -alumina is formed. Silica (quartz) melts at lower temperatures, 3115°F (1713°C). However, when Na, Ca and Fe are present, the melting points of both silica and alumina decrease substantially. In Table 2 we show a compilation of the temperatures at which the first liquid appears (initial melting temperatures) for phases that silica or alumina can form with Na, Ca and Fe present on the catalyst surface. For ranges that contain the Na concentrations we have measured on the surface of FCC Ecats both Na and Ca dramatically reduce the initial melting temperature of silica. However, Na is a much more effective fluxing agent for SiO_2 than Ca. The effect of FeO on the initial melting point of phases with SiO_2 is not as severe as that of Na, but it is more severe than that of magnetite or Fe_2O_3 . The combination of Na with Fe is particularly destructive. Combining Na with FeO and SiO_2 at concentrations similar to the ones we measured on the surface of Ecats can lower the initial melting point to less than 932°F (500°C). This temperature is lower than the operation temperature of virtually every FCC riser.

Contrary to silica, the melting temperature of alumina is not affected as severely (Table 2). While the mere presence of Na in SiO_2 can lead to the formation of small amounts of liquid at 1436°F (780°C), it takes more than 7% Na to decrease the melting temperature of alumina to 2570°F (1410°C). Like Na, Fe is also less effective in decreasing the melting temperature of alumina than silica. Even a combination of alumina and unrealistically high amounts of Na with silica and Fe does not bring the melting point of the phases richer in alumina (>15% Al_2O_3) below 1830°F (1000°C). Thus, for alumina-rich areas of the Ecat surface, and for the levels of Fe, Na, and Ca we can expect to find on the catalyst surface, the initial melting temperatures of such alumina-rich surfaces are expected to be hundreds of degrees higher than similar silica-rich phases.

The Mechanism of FCC Catalyst Poisoning By Fe

Every FCC catalyst microsphere is constituted of smaller particles of zeolite, matrix, clay, and the binder that holds everything together. As a result, the exterior surface of the particle is not homogeneous. Rather it has areas of zeolite, clay and matrix (typically added alumina), mostly coated with the binder used. Since clay has a low surface area and few pores, and zeolite has mainly micropores and some mesopores, many of the large pores responsible for allowing large hydrocarbon molecules inside the particle for cracking come from the binder, the matrix, and the voids between the particles that constitute the catalyst microspheres. TEM analysis of fresh and deactivated FCC

catalyst confirms the heterogeneity of the surface of FCC catalyst particles. In addition, spot analysis of the binder areas by EDS shows that Si-sol binder areas of the particle are essentially silica containing only traces of alumina. Similarly, Al-sol binder and alumina matrix areas are essentially alumina containing only traces of silica.

Si-sol Catalysts

In Figure 12, we show a schematic diagram of the process of catalyst deactivation by Fe deposition for catalysts employing a Si-sol binding system. As the catalyst ages, Fe, Ca, Na and other contaminant metals deposit on it. Fe and Ca remain on the catalyst surface, and on Si-sol catalyst they mix with the binder silica (or silica from other silica-rich areas) and sodium oxide, forming phases that have initial melting temperatures as low as the operation temperature of the riser and/or the regenerator. The oxidation state of the Fe on the catalyst surface changes as the catalyst circulates in the unit, but it probably spends most of the time in a reduced state (Fe^{2+}), further decreasing the melting point of Fe containing phases. The formation of these low melting temperature phases facilitates the fluxing of silica in the binder, thus filling and closing the pores and giving the surface the "glassy" texture we have observed. Even if outright melting does not occur, accelerated sintering, due to the decrease of the material melting temperature, will have a similar effect. The result is again the destruction of the surface pores that are largely responsible for carrying the large hydrocarbon molecules inside the particle for cracking. As the Fe accumulates on the surface of Si-sol catalysts, these low melting temperature phases cover a larger and larger area of the particle external surface, thus closing more and more pores.

The collapse of the surface pore structure where the Fe deposits causes the surface to rescind as the melting and sintering decreases the volume of the affected material. The result of this process is the shrinkage of the catalyst surface. In areas where the Fe does not mix well with the underlying components or if it does the resulting phases have high melting points (alumina-rich areas), the integrity of the structure is retained. The combination of areas where the particle structure collapses with the areas where it is maintained gives rise to the formation of nodules and valleys we observed on the surface of Ecat particles. Because of the way they are formed, nodules are rich in Fe and Ca which cover the underlying structure, while in the valleys Fe is diluted by mixing with silica and other compounds. We have been able confirm this conclusion by measuring the concentration of Fe, Ca, Si, and Al in nodules and valleys of an Fe poisoned Ecat using SEM/EDS, a technique that allows for quantitative elemental analysis of small areas on the particle surface (Figure 13).

Continued from Page 68

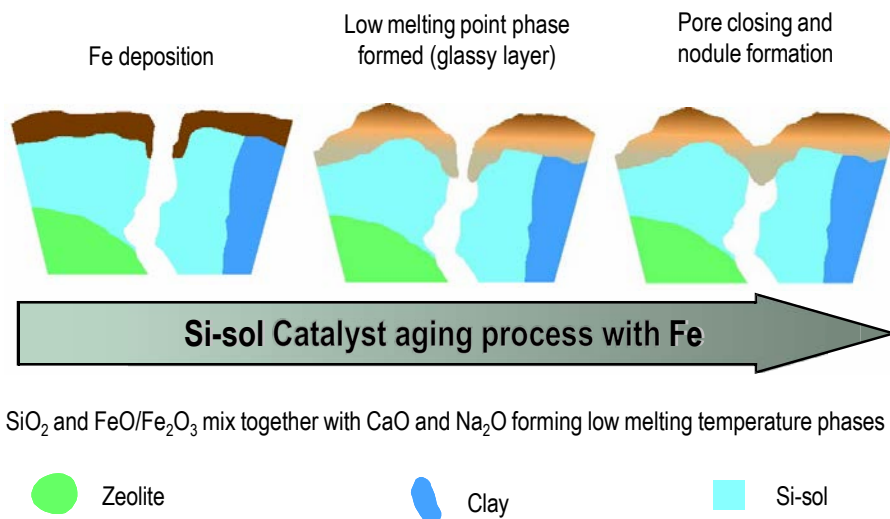


Figure 12. Schematic representation of Si-sol catalyst deactivation by Fe poisoning, showing Fe deposition, the formation of low melting temperature phases, and pore closing and nodule formation in a small section of the surface of the spherical catalyst particle.

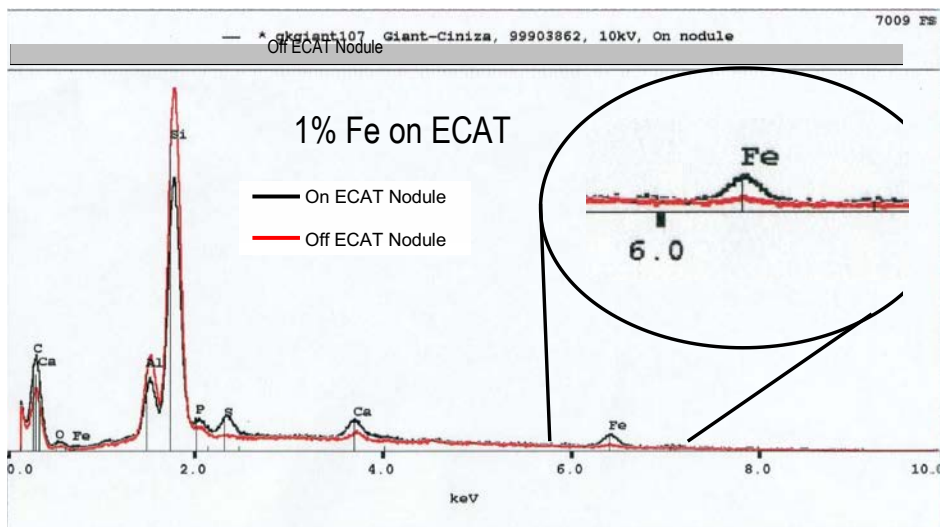


Figure 13. Relative Fe concentration on nodules and valleys formed on an Ecat poisoned by Fe as measured by SEM/EDS.

Continuous collisions between the fluidized particles may further shape the softened particle surface, pushing the softened area further inside. Although there is no conclusive evidence to support this assertion, it is possible that particles may also stick together and then break apart forming particles of irregular shape. All these processes

either create or facilitate the creation of nodules and valleys on the catalyst surface that we observed by SEM. This morphology of Fe poisoned catalysts and the increased likelihood of particles sticking together and forming particles of irregular shape result in less efficient packing of Ecat particles causing the ABD to decrease.

Since in most cases Fe does not deposit deeper than 1-3µm, the formation of low melting temperature phases only affects a small portion of the particle volume and surface area (typically less than 10%). However, in the FCC unit it is critical that during the time the feed molecules spend in the riser, they diffuse inside the particle and the products diffuse out. Closing of pores by the processes set in motion by Fe deposition on the catalytic particle restricts the diffusion of the feed molecules into catalyst particles, thus decreasing activity. Since large feed molecules are the ones most affected by pore closing, bottoms cracking is the catalyst property more severely affected by Fe poisoning.

Al-sol Catalysts

The formation of high Fe low melting temperature phases may also occur at high silica areas of the particle surface of catalysts employing the Al-sol binding system. Nodule formation and some pore closing may occur on these catalysts as well. However, in Al-sol catalysts the alumina binder and the active matrix component are dispersed throughout the particle, and contribute surface area and cracking activity. The alumina binder and active matrix are also where much of the bottoms cracking occur. These components provide many of the pores needed to transport feed molecules inside the catalytic particle, and these components are essentially pure alumina.

Our XPS data show that alumina is largely covered by the deposited Fe contamination and it does not mix with it to form low melting temperature phases. Even if alumina could mix with the depositing Fe, our thermodynamic analysis shows that alumina phases containing FeO, Na₂O and/or CaO require high temperatures to melt. These temperatures are much higher than the riser and regenerator temperatures. Thus it is not likely accelerated sintering can occur. As a result of the resistance of alumina to Fe poisoning, the surface pores in binder and active matrix

areas remain essentially open allowing the feed molecules to transport inside the catalytic particle for cracking. Hence, these catalysts are resistant to Fe-poisoning offering good activity maintenance even in the face of high Fe contamination, good bottoms cracking, and little or no change in Ecat ABD.

The mechanism of FCC catalyst deactivation we described here is consistent not only with Ecat and laboratory data, but also with in-unit catalyst performance data. Refinery experience has proven that unlike other types of catalysts, Al-sol catalysts are resistant to increasing levels of Fe poisoning. A unit using Davison Al-sol catalysts can operate with high levels of Fe on Ecat and no loss of conversion or bottoms cracking selectivity. One of the Davison Catalysts Al-sol catalyst users³ has been able to operate the FCC unit with high Fe levels over a period of more than 4 years. During this time Fe levels on Ecat have remained consistently among the industry's highest (ca. 1% Fe), and at times reached record levels (2.6% Fe). Yet despite these extraordinarily high levels of Fe, the unit has not experienced a loss of activity, bottoms yield changes, or a decrease of Ecat ABD.

Strategies for Addressing Catalyst Iron Poisoning in the FCCU

For the FCC units that are faced with the problem of Fe poisoning, the key question is how to maintain or improve catalyst performance when Fe levels in the catalyst inventory start increasing or are chronically high. For these units, a strategy for solving the effects of Fe poisoning is critical in improving unit economics. Having identified the mechanism via which Fe affects FCC catalysts, we recommend the following strategy:

- 1. Establish that any catalyst performance deterioration observed is indeed due to rising iron levels on the Ecat.** Sometimes Fe may rise after a feed change accompanied by a loss of activity and bottoms cracking. Before concluding the increased iron levels have poisoned the catalyst, the refiner should establish that the performance deterioration is not due to a change in feed crackability and increases of other metals (e.g., Na, V, Ni) deleterious to catalyst performance. SEM, EPMA, XPS, and optical microscopy analysis of the Ecat can be used to look for the surface composition and texture characteristic of Fe poisoned catalyst.
- 2. Try to reduce the Fe coming into the unit.** Measures that can be employed to reduce iron coming with the feed is to stop using high Fe feeds and/or to buy a low iron feed to blend with the high Fe one. It is possible that acids in the feed (e.g., naphthenic acids) can corrode hardware increasing the iron content of the feed. Reducing the acid content, or purchasing low acid content feeds can reduce hardware corrosion, and thus decrease the amount of iron in the feed.

- 3. Reduce the Na and Ca content of the feed.** Na and Ca act as fluxing agents severely aggravating the catalyst poisoning effect of Fe. It is therefore critical that either low Na and Ca feeds are used, or that the amounts of these metals in the feed are reduced by using desalting or other suitable processes.
- 4. Minimize the regenerator temperature, if possible, and improve catalyst coke selectivity.** High temperatures accelerate catalyst deactivation by Fe. However, lowering the temperature of the regenerator can have a significant impact on unit operation, and may not be an option for most units. A more coke selective catalyst may help reduce the catalyst temperature in the regenerator while minimizing any adverse effects in unit operation.
- 5. Use an appropriately designed iron resistant Al-sol catalyst.** When the unit does not have the flexibility to implement other solutions, or other solutions fail, Al-sol catalysts have been proven to provide excellent resistance to iron contamination³, and maintain activity and bottoms cracking even at iron levels on Ecat which are the highest in the industry. In addition to having appropriate chemical/physical properties and structure for providing high activity, bottoms cracking and excellent coke selectivity, catalysts made with the Davison Al-sol binding system are designed to inhibit the chemical processes that lead to pore closing and the loss of activity and bottoms cracking.

References

1. L. T. Boock, T. F. Petti, and J. A. Rudesill, Ch 12, "Contaminant-Metal Deactivation and Metals Dehydrogenation Effects During Cyclic Propylene Steaming of Fluid Catalytic Cracking Catalysts" in Deactivation and Testing of Hydrocarbon Processing Catalysts, P. O'Connor, T. Takatsuka, and G. Woolery Eds., *ACS Symposium Series 634, Ch. 12, p. 171*, Washington, DC, 1996.
2. E. Rautiainen and P. van Krugten, *Catalyst Courier*, **40** (2000).
3. B. Niess, Bayernoil Raffineriegesellschaft mbH, "Impact of Fe on FCC Resid Processing" in FCC • Additives • Hydroprocessing • Refining Technology Grace Davison Conference, Singapore, August 16-18, 2000.
4. F. C. Kracek, *J. Phys. Chem.*, **34**, 158 (1930)
5. B. Phillips and A. Muan, *J. Am. Ceram. Soc.*, **39** [4], 5 (1915).
6. M. Rolin and P. H. Thanh, *Rev. Hautes Temp. Refractaires*, **2** [2], 178 (1965).
7. N. L. Bowen and J. F. Schairer, *Am. J. Sci., 5th Ser.*, **24**, 200 (1932)
8. B. Phillips and A. Muan, *J. Am. Ceram. Soc.*, **12** [9], 415 (1959).
9. I. A. Novokhatskii, B. F. Belov, A. V. Gorokh, and A. A. Savinskaya, *Russ. J. Phys. Chem.*, **39** [11], 1498 (1965).
10. P. T. Carter and M. Ibrahim, *J. Soc. Glass Technol.*, **36**, 156 (1952).
11. D. K. Bailey and J. F. Schairer, *J. Petrol.*, **7**, Pt. 1, 125&126 (1966).



The coke selectivity of an FCC catalyst underpins the unit's operability and profitability with wide ranging impacts to catalyst circulation rates, product yields, and regenerator combustion kinetics. In the 1987 *Catalagram* article "Coke Selectivity Fundamentals," Charles Wear explains coke selectivity in plain terms and touches on how it can have profound effects on the unit's heat balance, operating window, and overall product yield slate. Wear's write up also emphasizes that a "one-size-fits-all" approach to catalyst design is destined to fall flat.

These insights from the late 1980s continue to ring true today. A refiner's ability to work with industry partners to optimize FCC operation, feedstock and catalyst selection will be imperative to successfully navigate shifts in product demand and refined product margins. Grace's collaborative relationships with customers enable our technical experts to design catalysts that maximize operational flexibility and product value. For example, latest innovations offering improved coke selectivity, including FUSION® and PARAGON™ technologies, incorporate novel metals trapping functionality and to help optimize customer operation.



Victor Bartarseh
Strategic Marketing Manager, FCC
W. R. Grace & Co.



Coke Selectivity Fundamentals

 Charles C. Wear

 Originally published in *Catalagram* #75 in 1987 and reprinted in #106 in 2009 (3)

Coke selectivity is a term that often means different things to different people. So to lead off our discussion, let's focus on a definition: Coke selectivity is the relative coke-making tendency of any given cracking catalyst. In the vernacular, a catalyst that has "good coke selectivity" means it produces lower coke compared to some reference catalyst. This is usually considered a favorable characteristic, since liquid yields are preferred.

That seems fairly straightforward, but the often misunderstood part is just what the phrase "coke-making tendency" really means. Many times it is confused with coke yield as expressed in say, weight percent of fresh feed. However, the coking tendency of a catalyst in the context of "coke selectivity" is actually its tendency to produce delta coke.

Continued from Page 72

The Concept of Delta Coke

The concept of delta coke is neither novel nor complicated. It is simply the difference between coke on spent catalyst (at stripper outlet) and coke on regenerated catalyst, expressed as a weight percent of catalyst.

More correctly, delta coke can be thought of as the amount of coke formed on the catalyst for a single pass of the catalyst through the reactor which, in the continuous steady-state operation of a commercial FCCU, is also equal to the amount of coke burned off the catalyst in the regenerator.

Delta coke also has kinetic significance, especially on the reactor side of the process where it formed. The coke on catalyst per pass is a combustion function of many variables, including but not limited to: feed quality and dispersion at the nozzle, reactor temperature and pressure, catalyst activity and contact time, and last but not least, catalyst coke selectivity.

Therefore, when all other variables affecting delta coke are more or less constant, a catalyst that possesses "coke selectivity" will exhibit lower delta coke at any given activity.

A "coke balance" around the regenerator results in a useful expression for delta coke. The coke yield must equal the difference in coke entering and leaving the regenerator. Therefore, note that

$$\text{Coke Yield} = C/O \text{ (CSC-CRC)}$$

or

$$\text{CSC-CRC} = \frac{\text{Coke Yield} = \text{Delta Coke}}{C/O}$$

where:

Coke Yield is wt.% Feed

C/O is Cat Circulation,
lb. Cat/lb. Feed

CRC is Coke on Spent Catalyst,
wt.% Catalyst

CSC is Coke on Regenerated Catalyst,
wt.% Catalyst

coke yield and cat/oil must be expressed on the same feed basis, fresh or fresh plus recycle, to yield a meaningful number.

Since coke yield and cat/oil are related to delta coke in the above mentioned manner, it follows that a coke "selective" catalyst can decrease coke "yield", but not necessarily. For instance, in many cases, coke selective catalysts will operate with higher cat/oil ratios with little or no change in coke yield. An understanding of this requires examination of the FCCU heat balance and the interaction of process operating variables.

Heat Balance Effects

A commercial unit, like all steady state processes, must be in energy balance. This means that the total energy coming

into the process must equal the energy leaving the process, as shown in Figure 1. The energy to heat the fresh feed, recycle feed and stripping steam to reactor outlet temperature, to heat the air to flue gas temperature, to supply the endothermic heat of reaction and any losses to the atmosphere—all of this must come from the coke's heat of combustion. A portion of the feedstock is therefore "consumed" to supply the energy requirements of the process.

One consequence is that the coke yield as weight percent feed is determined by the sum of these energy requirements, not by the catalyst coke selectivity (or feed coking tendency for that matter). This is the key concept that distinguishes delta coke, which is catalyst and feed related, to coke yield, which is not. We will return to this concept in a moment.

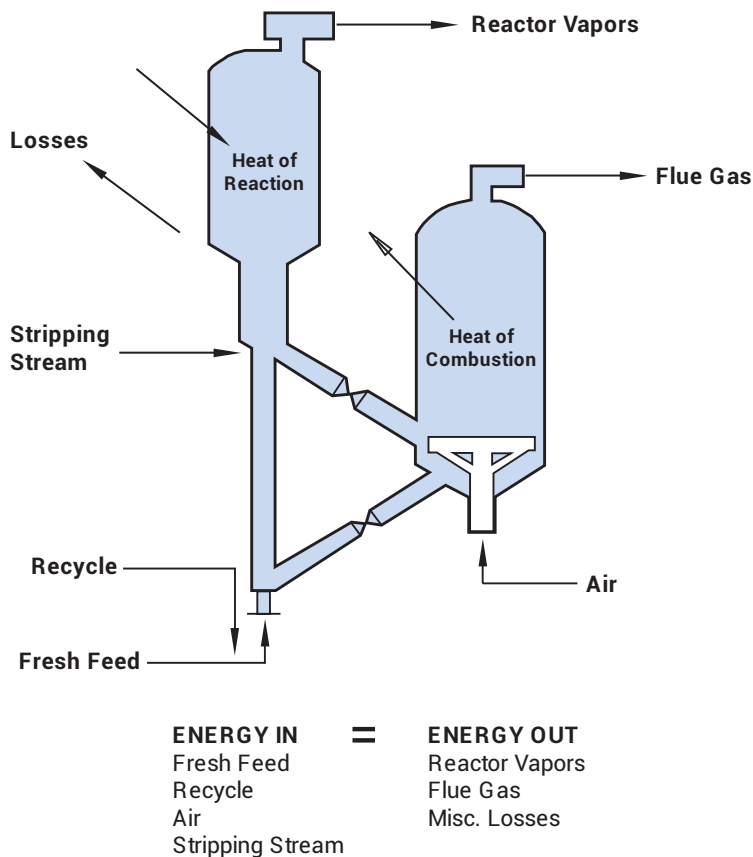


Figure 1. Simplified Overall Energy Balance

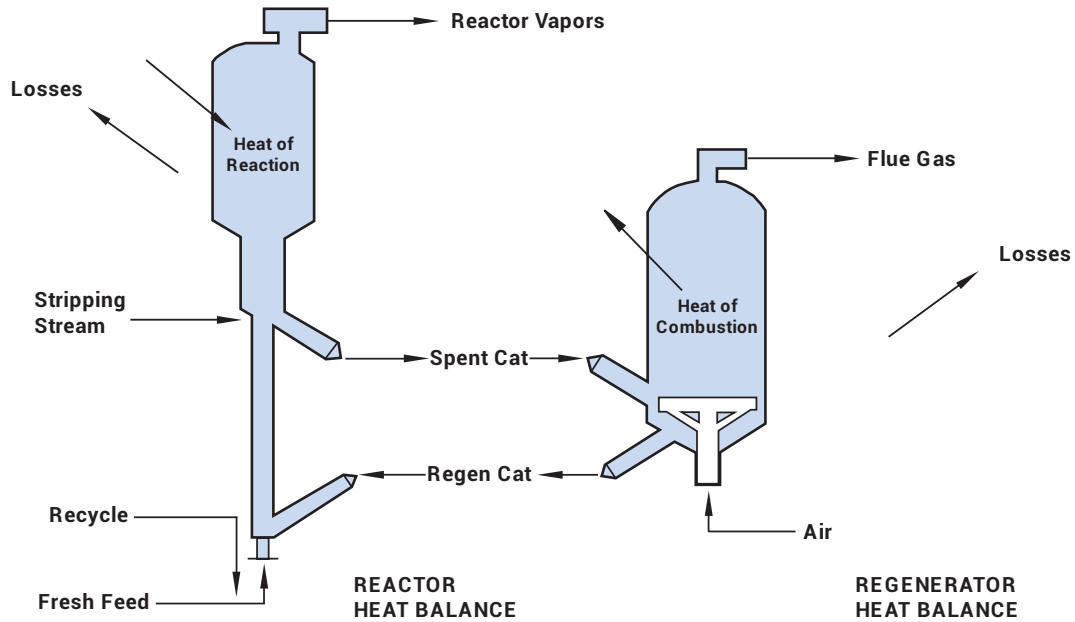


Figure 2. Energy Balance of Reactor and Regenerator Involves Catalyst Circulation Rate

The principle of energy balance holds for the individual reactor and regenerator as well as the overall process, as shown in Figure 2. Table 1 lists the simplified components to balance each vessel. By equating the regenerator heat production to the heat transferred by catalyst, a useful relationship can be derived:

Heat of Coke Combustion + Other Terms = Heat Transferred by Catalyst

Coke Yield (ΔH_c)
 $\cong C/O \text{ Cp}^{\text{Cat}} (T_{\text{Regen}} - T_{\text{Rx}})$

Delta Coke =
 $\frac{\text{Coke Yield}}{C/O} \cong \frac{\text{Cp}^{\text{Cat}}}{\Delta H_c} (T_{\text{Regen}} - T_{\text{Rx}})$

Noting that the catalyst heat capacity (Cp^{Cat}) is constant for any particular case, along with the coke's specific heat of combustion (H_c) when hydrogen in coke and degree of CO combustion are constant, the following proportionality holds:

Delta Coke $\propto (T_{\text{Regen}} - T_{\text{Rx}})$

Reactor Heat Requirements	Regen Heat Production	Heat Transferred by Catalyst
+ Heat of Reaction	+ Heat of Coke Combustion	$(C/O) \text{ Cp}^{\text{cat}} (T_{\text{Regen}} - T_{\text{Rx}})$
+ Heat Up Feed	- Heat Up Air	
+ Heat Up Recycle	- Heat Up Coke	
+ Heat Up Strip Stream	- Heat Up Rx Entrainments	
+ Account for Losses	- Account for Losses	
- Heat from Regen Entrainments		

Table 1. Energy Balance Relationship

This implies that a coke selective catalyst will, for a constant reactor temperature, reduce regenerator temperature. This is exactly what is observed commercially. Consider the unit in full combustion that has changed to a catalyst with different coke selectivity. Depending on the shift in delta coke, the changes shown in Figure 3 occur.

Of course, unit response to coke selective catalysts is not limited to regenerator temperature reductions. Consider the

unit in partial CO combustion, where a drop in regenerator temperature could possibly result in an undesirable increase in regenerated catalyst carbon level. For this case, it would be wise for the operator to intervene—via increased promoter additions and/or air rate—to burn more CO to CO₂ and thus return the dense bed to original temperature.

In this example, these “external stimuli” from the operator directly affect the overall heat balance by increasing the

Continued on Page 75

Continued from Page 74

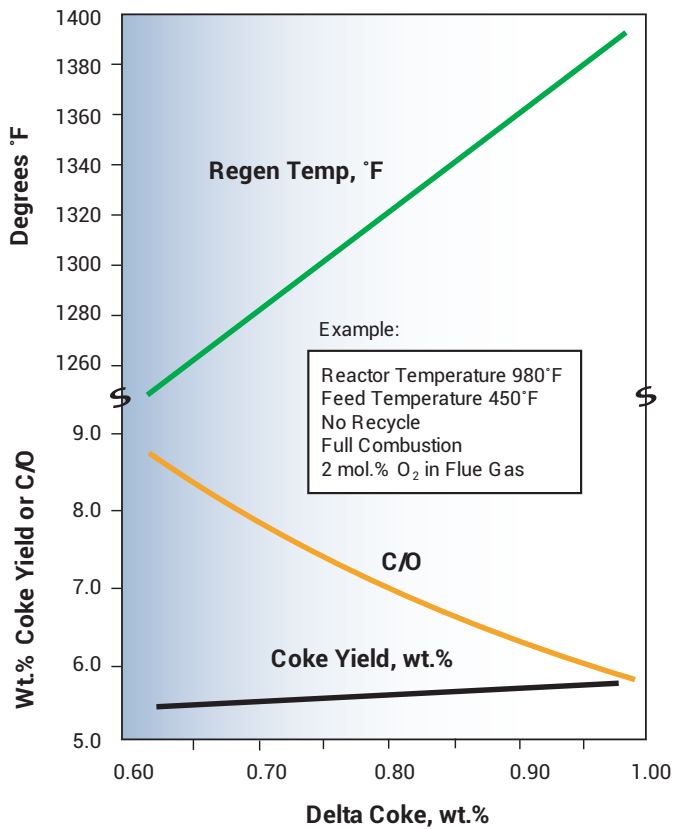


Figure 3. Typical Effect of Delta Coke on FCC Operation

heat release per pound of coke burned (higher CO₂/CO). It therefore takes the combustion of less coke to satisfy the energy demand of the process. So, for this partial combustion case, coke yield will drop at the same or nearly the same reactor/regenerator temperatures (and therefore cat/oil). It has to, because the catalyst caused a reduction in the delta coke, and by definition coke yield must be lower if delta coke drops at constant cat/oil!

Remember earlier in this discussion it was stated that catalyst (and feed quality) have a direct effect on delta coke, but that the unit heat balance determines coke yield. As the preceding example showed, sometimes it's difficult to separate what changes were caused directly by catalyst (or feed) as opposed to heat balance changes made by the operator.

In reality, the difference is not very important in many cases. The important point is that coke selective catalysts will, in more cases than not, allow an operator to have more flexibility in running his plant. Here are some of the ways we have seen operators use Davison coke selective catalysts to their fullest extent, and thus alleviate operating constraints and improve refinery profitability:

- Increase reactor temperature to produce maximum gasoline octane.
- Increase cat circulation for increased conversion.
- Increase resid content for additional bottoms destruction.
- Increase feed rate to satisfy increased product demand.
- Increase CO₂/CO for lower coke yield.

As with many things in life, "more" catalyst coke selectivity in all cases does not necessarily mean "better". A thorough review of the base operation, including goals and constraints, should be performed before any catalyst change is considered. For example, some operations are precluded from the use of incremental catalyst coke selectivity. Consider the unit in full combustion, at maximum catalyst circulation and feed temperature, that cannot "heavy-up" the feed nor accept a lower reactor temperature. This obviously is not a unit that would profit from catalyst coke selectivity. It is a unit, however, which could greatly benefit by removing these limitations, and many have done exactly that via revamps.

A Check on Data Consistency

The fact that delta coke can be measured directly by comparing the difference in coke levels between spent and regenerated catalyst samples was discussed earlier. Delta coke determined in this manner, versus the calculations of delta coke from the unit heat balance, can be a useful tool to check data consistency.

Most process engineers will calculate coke yield using air rate and flue gas composition, and then calculate catalyst circulation rate by heat balance. These coke yield and cat/oil results can then be used to calculate a delta coke. If this "heat balance method" to obtain delta coke differs substantially from the direct sampling method, it could mean one or more of the following:

- Incorrect flue gas analysis or air rate (the most common problem).
- Nonrepresentative catalyst samples (also a common problem).
- Error in heat balance method, data or assumptions.
- Excessive entrainment of interstitial hydrocarbons through the stripper.

Types of Delta Coke

It is convenient to define components of delta coke as to source, and several proposed breakdowns have been published. A sampling is listed in Table 2. The three components of delta coke defined here can be influenced by proper catalyst design:

1. Catalytic—the coke deposit formed when hydrocarbon is cracked via acid site catalysis.

Unit	A		B	
Catalyst	Zeolite-Low Metals		Zeolite-High Metals	
Feed Type	Gas Oil		Resid	
Delta Coke Types	Wt% Cat	% Total	Wt% Cat	% Total
Catalytic	0.52	65	0.40	29
Cat/Oil	0.12	15	0.10	14
Contaminant	0.12	5	0.40	29
Feed/Nondistillable	0.04	15	0.50	28
Total	0.80	100	1.40	100

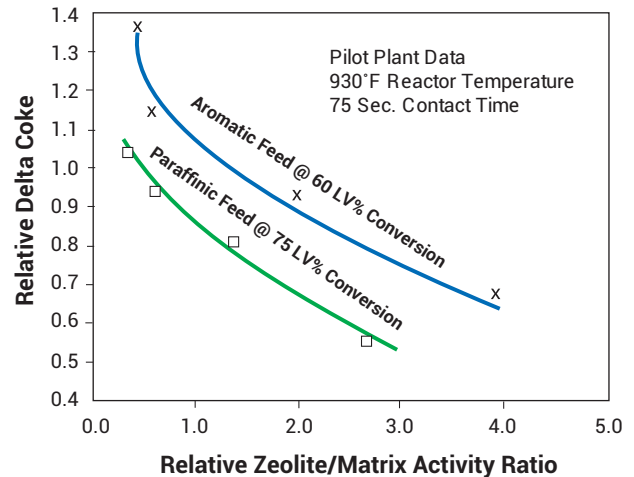


Table 2. Typical Delta Coke Breakdowns^(1, 2)

2. Cat/Oil-adsorbed/unstripped hydrocarbons entrained by catalyst flowing through the stripper.
3. Contaminant-coke produced as byproduct of contaminant metal (V, Ni, Cu, Fe) dehydrogenation activity.

Catalytic Delta Coke

Most cracking catalysts have two sources of acid sites, and therefore two types of activity-zeolite and matrix. Zeolite is crystalline silica/alumina with a specific structure. In the usual case it is where most of the overall catalyst activity resides.

The balance of the catalyst particle is defined as the matrix. It may be similar to the zeolite in composition (silica/alumina), but does not have the particular crystalline structure unique to zeolites. Many of today's matrices resemble the amorphous catalysts of the 1950's and 60's.†

The activity associated with the zeolite and the matrix have very different selectivity patterns, especially in regard to coke. This is illustrated in Figure 4. As matrix activity relative to zeolite is minimized, delta coke at constant activity decreases—the catalyst becomes more “coke selective”.

Differences in zeolite type also affect coke selectivity. The key issue is the chemical composition (Si/Al ratio) of the equilibrated zeolite, which is measured by X-ray as the unit cell size. Zeolites that equilibrate with high Si/Al ratios (low cell sizes) exhibit retarded hydrogen transfer rates which, among other things (such as increasing gasoline octane), reduce catalytic coke make. Davison's experience with these zeolites, generically referred to as “ultrastable” or USY types, is unmatched in the industry. The premium form of USY, patented by Davison as “Z-14US”, is the core technology behind Davison's current octane catalyst product line. The coke selective properties of these octane

Figure 4. Effect of Zeolite/Matrix Activity on Catalyst Coke Selectivity

catalysts have been thoroughly treated in earlier *Catalagram* magazines (Numbers 73 and 74).

Cat/Oil Coke

Cat/oil coke is perhaps the most insidious component of delta coke because¹ it is totally independent of any beneficial chemical reaction taking place, such as making gasoline, and² it has the highest heat of combustion (highest hydrogen content) which leads to high intraparticle temperatures during regeneration.

A properly designed and operated catalyst stripper will minimize the amount of hydrocarbons that flow into the regenerator along with the circulating spent catalyst. Stripping steam rates of at least two lb. per 1000 lb. of catalyst circulated are typically recommended. Increasing catalyst level (residence time) in the stripper can also be effective in minimizing carry-over. The common commercial practice is to increase steam rate and/or stripper level until no further reduction in regenerator temperature is observed, providing, of course, reactor-side catalyst losses do not increase.

Steam injection displaces hydrocarbon vapor between catalyst particles – it is not very effective in reversing surface adsorption or pore condensation. In some cases, higher reactor (stripper) temperatures have been found to reduce cat/oil coke. The mechanism may involve volatilizing and/or further cracking of desorbed material.³

Cat/oil coke is also influenced by catalyst matrix pore size and surface area. Catalyst “strippability” can be measured in the lab by subjecting an inert porous material to heavy oil, followed by nitrogen stripping at typical reactor operating conditions. The results is shown in Table 3 as a function of stripping time and temperature.

Continued on Page 77

† In the 1980's most high matrix catalysts were neither selective nor metals tolerant. Today's high MSA MIDAS® catalysts have been known to improve coke selectivity by eliminating and cracking coke precursors.

Continued from Page 76

Surface Area, M²/g	439	389	105
Pore Volume, cc/g	0.89	1.8	1.14
Volume Avg. Pore Diameter, A	72	184	436
Stripping Temperature	Unstripped Coke (Wt% FF) After 1 Minute		
900°F	17.3	17.7	6.4
990°F	2.0	1.7	1.3
Stripping Temperature	Unstripped Coke (Wt% FF) After 15 Minutes		
900°F	1.5	1.3	1.1
990°F	1.7	0.9	0.8
Conditions: MAT REACTOR: 5 gm. Charge, 16 WHSV, 3 C/O, WEST COAST FEED, N ₂ STRIPPING AT 30 SCCM, Volume Avg. Pore Diameter: $\frac{40,000 \text{ (pore Volume)}}{\text{Surface Area}}$			

Table 3. Effect of Surface Area on Hydrocarbon Stripping

Catalyst	500 ppm Ni (Impregnated After Steam Deactivation ¹)		500 ppm Ni + Sb
	Fresh	Aged ²	Aged ²
Super-D (50 m²/gm)³			
MA, V%	68.5	69.5	69.0
H ₂ , Wt%	0.21	0.08	0.075
Coke, Wt%	2.6	2.5	2.45
Competitor B (115 m²/gm)³			
MA, V%	70.0	68.0	69.5
H ₂ , Wt%	0.42	0.38	0.145
Coke, Wt%	4.15	4.2	2.8
Competitor A (220 m²/gm)³			
MA, V%	79.0	78.0	77.0
H ₂ , Wt%	0.45	0.35	0.14
Coke, Wt%	4.0	3.9	3.8
¹ Deactivation Conditions: 1350°F, 100% Steam, 15 psig, 8 Hrs.			
² Aged 13 Cycles in Cyclic Fixed-Fluid Bed Pilot Units; 40 WHSV, 3 c/o, 1000°F Reaction/1100°F Regeneration			
³ Typical Matrix Surface Area			

Table 4. Metal Aging Study Results⁽¹⁰⁾

High intraparticle temperatures associated with adsorbed hydrocarbon have been the subject of several studies,^{4,5} which showed that high surface area (hence, more adsorptive) catalyst particles are prone to deactivate rapidly when regenerated. Particle temperatures several hundred degrees higher than average regenerator bed temperatures were calculated.

To summarize, catalysts designed to minimize the cat/oil component of delta coke should have low surface area, large average pore diameter matrices to discourage hydrocarbon adsorption and enhance "strippability".

Contaminant Delta Coke

The hydrogen-producing effect of feed metals-particularly that of nickel, copper, and vanadium-deposited on the cracking catalyst is well known. Coke is a companion product of dehydrogenation, and from Table 2 it is clear that contaminant coke can be a substantial percentage of the overall delta coke for metals-laden catalysts.

The passivation of nickel by antimony (licensed by Phillips Petroleum Co.) and of vanadium by tin additives is being practiced commercially. f Claims of a 50% reduction in hydrogen and coke produced by contaminant metals have been published.^{6,7,8,9}

We have found that the level of hydrogen and coke production due to contaminant metals is also a function of catalyst matrix composition. Matrices with low alumina content and low surface areas are more effective in minimizing contaminant metal dispersion and dehydrogenation activity√ (Table 4).

f Tin passivation is no longer practiced in the industry. Integral vanadium traps, such as those in IMPACT, are much more effective for selectivity preservation in high metals operations.

Coke Selective Catalyst Properties

As can be seen from the preceding discussion, catalyst design has a direct bearing on the formation of various components of the overall "delta coke". Certain catalyst properties, associated with the true "coke selective" catalyst system, act to minimize delta coke for any given activity level. The essential ingredients are¹ a zeolite that will equilibrate at low unit cell size, while retaining the appropriate activity level to dominate that of the matrix and² a matrix of controlled surface area with large pores to maximize strippability and control dispersion and dehydrogenation activity of contaminant metals.

Davison has used these principles for years to design a wide range of catalysts. Current examples are members of the Octacat, GXO, and Nova families that have led the industry in coke selectivity, as well as octane enhancement. Davison R&D is focused on a continuous program of improving these products, as well as on the design of new coke selective grades such as the DXB family.

References

1. Cimbalo, R.N., Foster, R.L., and Wachtel, S.J.; *O&GJ*; May 15, 1972; p. 112.
2. Mauleon, J.L., and Courcelle, J.C.; *O&CJ*; October 21, 1985; p. 64.
3. Schuurmans, H.A.J.; *Ind. Eng. Chem. Process Des. Dev.*; 19(2); 1980; p. 267.
4. Bondi, A., Miller, R.S., and Schlaffer, W.G.; *Ind. Eng. Chem. Process Des. Dev.* 1(3); 962; p. 196.
5. Wilson, W.B., Good, G.M., Deahl, T.J., Brewer, C.P., and Appleby, W.G.; *Ind. Eng. Chem.*; 48(11), November 1956; p. 1982.
6. Johnson, M.M. and Tabler, D.C.; US No. 3,711,422.
7. Dale, G.H. and McKay, D.L.; *Hydrocarbon Processing*; September 1977; p. 97.
8. English, A.R. and Kowalczyk, D.C.; *O&CJ*, July 16, 1984; p. 127.
9. Barlow, R.C.: "Commercial Application of Vanadium Passivation Technology", NPRA Spring Meeting, 1986.
10. Ritter, R.E.; *Catalagram No. 73*; 1985; p. 14.



One of Grace's most frequently requested articles, Raymond W. Mott's "Troubleshooting FCC Standpipe Flow Problems," has withstood the test of time. It was originally published in *Catalagram* No. 83 in 1992, and later republished in *Catalagram* No. 106 in 2009. This classic article reviews common symptoms and causes of FCC standpipe flow problems and clearly explains how these problems should be systematically diagnosed. While significant improvements have been made in areas such as advanced process control, modeling, and digitalization since the original print of this article, troubleshooting standpipe flow issues remains one of the most difficult challenges that an FCC operator can face. With larger FCC units being designed and coming online in the coming years, we expect FCC standpipe flow problems to remain a very relevant topic. Grace's experienced technical service representatives are very familiar with standpipe flow issues and troubleshooting, and they can help get your standpipes flowing smoothly again.




Clint Cooper
Sr. Principal Technologist, Global Customer Technology
W. R. Grace & Co.



Trouble-Shooting FCC Standpipe Flow Problems

 **Raymond W. Mott**

 Originally published in *Catalagram* #83 in 1992
and republished in #106 in 2009 (11)

Troubleshooting the performance of an ill-behaved FCC standpipe can present one of the most difficult challenges that the FCC process engineer faces. Not only is the nature of the catalyst circulation problem very nebulous, but the existence of a catalyst circulation problem places a great deal of technical and economic pressure on the process engineer's shoulders.

This paper will discuss how to systematically diagnose the operation of an FCC standpipe with chronic problems. In the process, some of the causes for the behaviors observed in standpipe operation will be investigated, and some engineering bench marks against which the operation of the FCC standpipe can be compared will be presented.

Continued from Page 80

Symptoms of Standpipe Flow Problems

There are a whole range of catalyst circulation symptoms that show up in FCC standpipes. Many of these symptoms are interrelated, and there are several distinctly different problems that exhibit the same symptoms. All of this makes troubleshooting standpipe flow problems extremely challenging.

Some of the symptoms of catalyst circulation problems that commonly occur in standpipes include:

- Low slide valve (or plug valve) differential pressure.
- An inability to circulate additional catalyst despite changes in slide valve position. Often this is accompanied by an inability to control reactor temperature.
- Erratic slide valve differential pressure that threatens the loss of catalyst circulation.
- Physical bouncing or hopping of catalyst standpipes.

Any of these symptoms can make smooth FCC operations impossible. However, before we dive into trouble shooting, it is worth looking into the detailed mechanics of catalyst flow in standpipes to establish a framework for investigation.

Pressure Profiles in the FCC Standpipe

One way to glimpse into the workings of the FCC standpipe is to conduct a pressure survey along its length. Usually, the most readily available way to do this is to conduct a single gauge survey. In this type of survey, a single calibrated pressure gauge is carried up and down the FCC structure to measure the pressure at various locations along the length of the vessels and standpipes. This helps reduce the errors that reading many separate gauges would introduce.

In principle, the FCC standpipe is expected to behave analogously to a pipe full of water. The pressure measured at any depth in the standpipe should be roughly proportional to the density of the fluidized catalyst and the height of the catalyst above the point where the pressure is being measured. Figure 1 shows the "idealized" pressure profile that would be observed in a perfectly behaved FCC standpipe. The pressure is linearly increasing with respect to depth in the standpipe.

In practice, when a standpipe is experiencing operating difficulty, the pressures observed at any point along the length of the standpipe may be going through wild gyrations. So, taking a meaningful single gauge pressure survey will require patience.

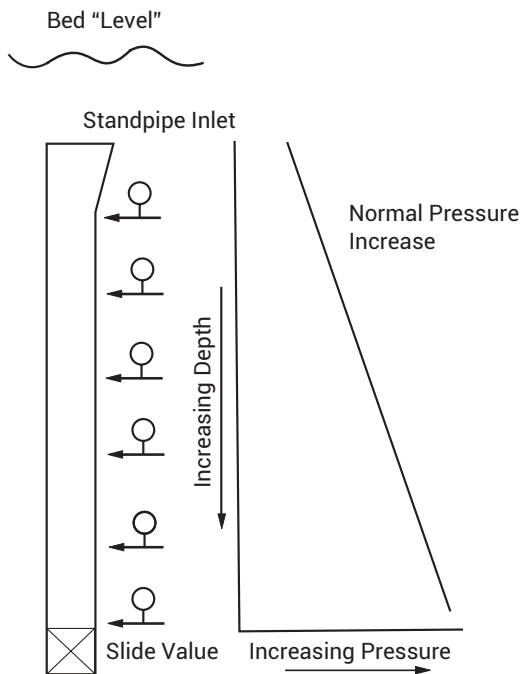


Figure 1. Idealized Pressure Profile in a Standpipe

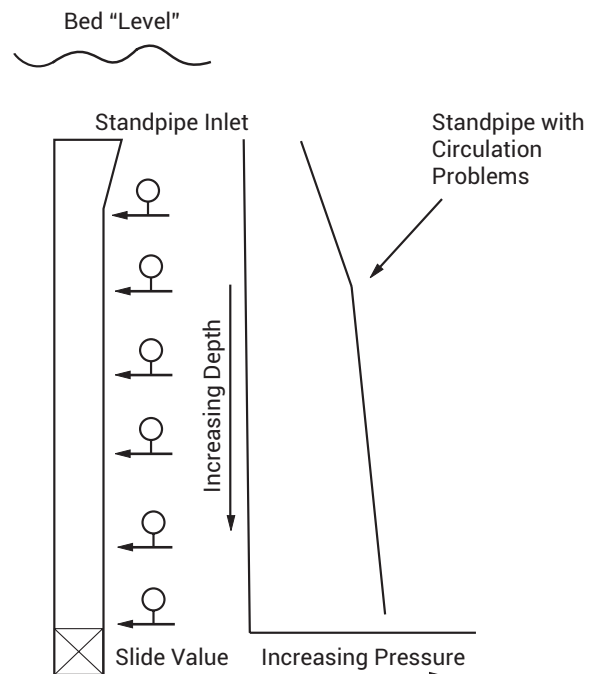


Figure 2. Idealized Pressure Profile in a Standpipe

Obviously, FCC catalyst differs from water in the important sense that it is actually a fluidized solid. Less obvious is the fact that non-fluidized powders can support their own weight against the walls of their container. For example, as an empty storage silo is filled with corn or wheat, the pressure on the floor of the silo initially increases as the height of grain in the silo increases. However, when the grain reaches a depth of approximately three times the diameter of the silo, the pressure on the floor of the silo stops increasing. The grain in the upper levels of the silo supports most of its own weight against the silo walls instead of the floor!

The implications for FCC catalyst flow in a standpipe are dramatic. If the catalyst loses its fluidization, it, too can start supporting a portion of its weight against the standpipe walls, and the slide valve at the bottom of the standpipe will see a reduced pressure buildup. A pressure survey will provide a better idea of what is going on inside the standpipe, and may help isolate where such local problems as defluidization are occurring.

Figure 2 shows the pressure profile for a standpipe that is experiencing moderate circulation difficulties. At first, the pressure is increasing normally as you descend the standpipe; however, this standpipe has trouble building additional pressure below the second aeration tap (counting from the top down).

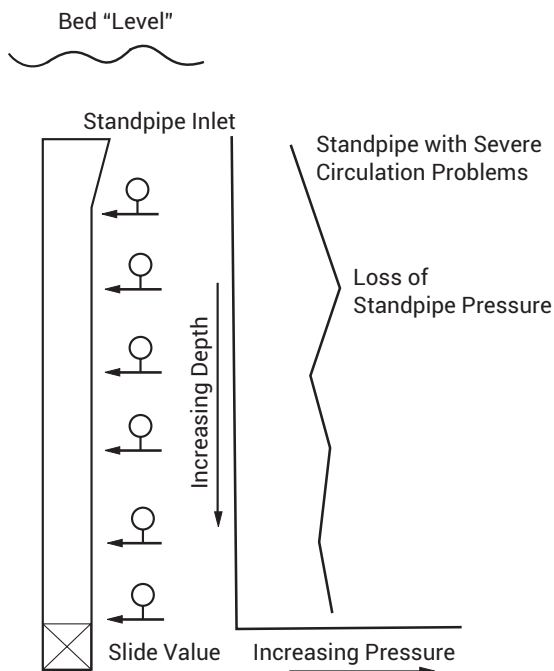


Figure 3. Idealized Pressure Profile in a Standpipe

A more extreme problem is shown in Figure 3. In this standpipe, the pressure profile actually shows a loss of pressure below the second aeration tap, and an inability to build up much pressure below this point.

The single gauge pressure surveys shown in Figures 2 and 3 suggest that the catalyst flow may be obstructed by a foreign object or by bubbles. Another possibility is that the catalyst may be losing its fluidization in some sections of the standpipe so that a portion of the catalyst weight is supported against the walls.

The Narrow Operating Window of the FCC Catalyst

FCC catalyst only has a narrow range of conditions under which it will flow well in standpipes. At one end of this operating range, the catalyst is at the point of incipient bubbling. If any more gas were present in the fluidized catalyst emulsion, then there would be a tendency for the system to generate bubbles. In standpipes, bubble formation tends to impede catalyst flow because the bubbles act as obstacles that the catalyst must flow around.

Incipient fluidization represents the other end of the well-behaved operating spectrum. If there were any less gas present in the catalyst emulsion at this point, the fluidized catalyst would then revert back to a packed bed.

These two extremes of fluidization are often measured in terms of velocity, and many articles have been written on measuring the superficial gas velocity at incipient bubbling (U_{ib}) and the superficial gas velocity at incipient fluidization (U_{if}) in beds of FCC catalyst. In an operating FCC standpipe, however, gas velocity has only a very nebulous meaning because it is difficult to determine what the relevant gas velocity is.

Fortunately, the well-behaved operating range can also be defined in terms of the density of the fluidized emulsion. Thus, the range of densities between the density of the emulsion at its point of incipient fluidization (ρ_{if}), and its point of incipient bubbling (ρ_{ib}) can be considered the range of densities over which a fluidized FCC catalyst will be well-behaved in a standpipe.

The catalyst beds encountered in commercial FCC units do not generally operate as quiescent fluidized beds that are confined to operate within the range of densities mentioned above. The typical catalyst bed found in the average FCC regenerator, for example, is usually operating as a very active bubbling bed. In open fluidized beds, bubbles do not present a fluidization problem. However, in a standpipe, bubbles need to be avoided. Thus, as the bubbling bed of catalyst begins to enter an FCC standpipe, it needs to shed itself of the excess gas bubbles to avoid dragging them down into the standpipe. The standpipe

Continued from Page 82

inlet geometry and location of the standpipe inlets should be carefully designed to allow this initial shedding of excess gas to take place in an orderly fashion.

It is beyond the scope of this paper to go into how the specific inlet geometry should be arranged; however, from the troubleshooting point of view, the process engineer needs to be aware that this process of shedding excess gas is taking place at the inlet to the standpipe. Thus, introducing aeration right at the standpipe inlet often causes more problems than it solves.

The Compression of Catalyst in a Standpipe

After the fluidized FCC catalyst emulsion enters the top of the standpipe and begins its descent, it starts to undergo a form of compression. As the catalyst descends the standpipe, the pressure head that is seen at any given depth in the standpipe increases. This increasing pressure compresses the interstitial gas that is surrounding the catalyst particles, as well as the gas that is in the pores of the catalyst particles. The net result of all this gas compression, is that the volume of the fluidizing gas surrounding the catalyst particles is reduced. So the catalyst particles move closer together, and the density of the emulsion increases.

If the standpipe is long enough, and if no aeration is introduced along the length of the standpipe, then this process of compression will continue as the catalyst travels deeper and deeper into the standpipe. This will cause the density of the catalyst emulsion to continue to increase until the catalyst emulsion reaches its incipient fluidization density. If the catalyst emulsion is compressed past this point, the emulsion will change phase from a fluidized bed to a packed bed, and the catalyst will have trouble circulating.

On FCC units that use standpipe aeration, the purpose of the standpipe aeration is to supply just enough additional gas to the catalyst as it passes each aeration tap to restore the catalyst emulsion to its original volume, as in Figure 4.

The ration of ρ_{if}/ρ_{ib} is known as the "Stable Expansion Ratio" for a fluidized catalyst. The higher this ratio, the more forgiving the fluidized catalyst is to changes in density, and the more easily it will tend to circulate in an FCC unit.

Another way of interpreting this ratio is to realize that it represents the maximum compression factor that the catalyst emulsion can be expected to tolerate as it descends the standpipe before losing its fluidization.

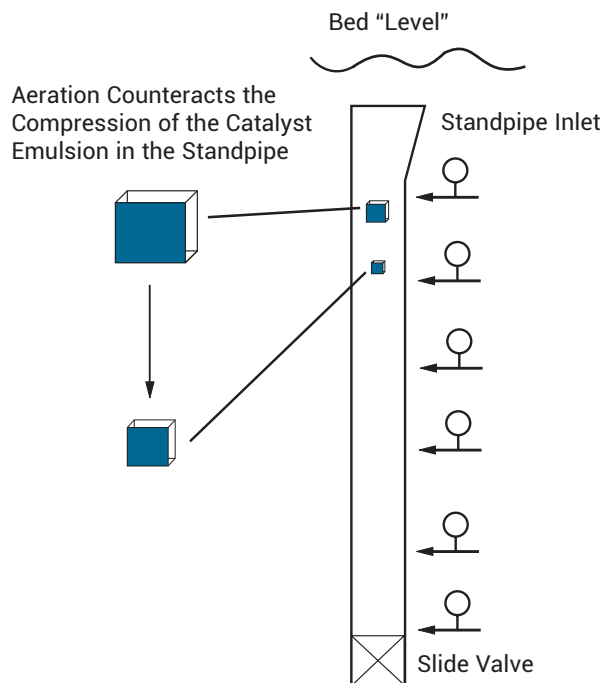


Figure 4. Compression of Catalyst in a Standpipe

Abrahamsen and Geldart¹ have shown that the ratio of the superficial gas velocity at incipient bubbling to the superficial gas velocity at incipient fluidization is a function of the physical properties of the catalyst as shown below.

$$\frac{U_{ib}}{U_{if}} = \frac{2300 \rho_g^{0.126} \mu^{0.523} e^{(0.716 F)}}{d_p^{0.8} g^{0.934} (\rho_p - \rho_g)^{0.934}} \quad (1)$$

Where:

U_{if} = Superficial Gas Velocity at Incipient Fluidization, m/sec.

U_{ib} = Superficial Gas Velocity at Incipient Bubbling, m/sec.

ρ_g = Gas Density, kg/m³

ρ_p = Particle Density, kg/m³

μ = Gas Viscosity, kg/m sec.

F = 0-45 micron Fines Fraction in Catalyst

d_p = Mean Particle Diameter, meters

g = Gravitational Constant, 9.81m/sec²

They also show that the Maximum Stable Expansion Ratio (MSER) can be estimated from the equation below:

$$MSER = \frac{\rho_{if}}{\rho_{ib}} = \left(\frac{U_{ib}}{U_{if}} \right) \quad (2)$$

Inspection of Equations 1 and 2 shows the following:

- Very low fines content in the equilibrium catalyst greatly reduces the maximum stable expansion ratio. Thus, standpipes that normally operate well will often fail when the cyclone performance deteriorates and the 0-40 micron fines content of the equilibrium catalyst falls.
- Catalyst with a very high equilibrium apparent bulk density (ABD) also can aggravate standpipe circulation problems because the maximum stable expansion ratio decreases with increasing catalyst particle density¹.

Both of these effects are clearly illustrated in Figure 5 which is taken from work published by Magnussun². Figure 5 shows the measured Maximum Stable Expansion Ratios for a series of equilibrium FCC catalysts at room temperature and pressure. The sensitivity of the measured MSER in Figure 5 to changes in ABD and the 0-40 micron fines fraction appears to be significantly greater than what Equation 2 would predict. This lack of precise agreement is common in the field of fluidization. It is mentioned here to illustrate that published correlations and measurements need to be applied cautiously.

Equation 2 and Figure 5 both provide estimates of the MSER for FCC catalyst under "ideal" conditions. In actual practice, the effective MSER of the catalyst in the FCC standpipe appears to be only a fraction of this estimated number, so the MSER should not be taken at full face value when looking at standpipe compression. However, the relative changes predicted in MSER by Equation 2 and Figure 5 due to particle size, ABD, viscosity, and gas density are very real effects. It is these relative movements in MSER that are very useful for troubleshooting.

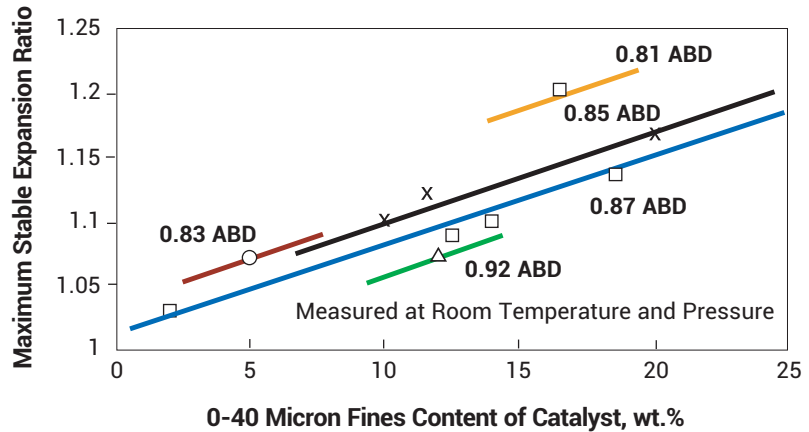


Figure 5. Maximum Stable Expansion Ratio Versus Fines Content of Equilibrium Catalyst

In an operating FCC unit, one of the ramifications of Equations 2 and Figure 5 is that the ability of the equilibrium catalyst to tolerate compression can change dramatically due to subtle effects like a loss of fines, or an increase in ABD that might accompany a catalyst change out.

The limited ability of equilibrium FCC catalyst to tolerate compression places a great deal of importance on proper standpipe design and aeration practices.

With these ideas in mind, let's move on to troubleshooting standpipe circulation problems.

Assess the Situation; Gather Facts and Figures

When troubleshooting, a good way to get started is to gather some facts about the status of the standpipe's operation for comparison against useful benchmarks. In the process, ask as many questions as possible about the history, and recent operation of the troubled standpipe. Some of the typical avenues of investigation are outlined below.

Catalyst Flux

A quick calculation of the catalyst flux passing through the standpipe will help indicate how high the duty of the

standpipe is. Calculate the catalyst flux rate (kg/m² second) at which the standpipe is operating.

How does this compare with past operating experience for the unit in question? Many FCC standpipes will operate with a flux as high as 980- 1220 kg/m² second (200-250 lbs/ft² sec). Some standpipes have been observed operating as high as 1465 kg/m² second (300 lbs/ft² sec). If your catalyst flux is up at these levels you may be operating near the practical capacity of your FCC standpipe. If, on the other hand, the catalyst flux is significantly lower than this, then it is likely that something other than a sheer capacity limitation is causing the catalyst circulation problem.

Look at the Standpipe Pressure Profile

Conduct a single gauge pressure survey along the length of the standpipe and the vessel from which it is coming. What type of pressure profile is the standpipe generating? How does this compare with the idealized profiles discussed earlier? Usually, you are looking for a section of standpipe that is not generating the expected pressure head as a clue to where the problem is located.

Sometimes it is difficult to visualize what is going on inside those sections

Continued on Page 85

²Unlike the gas contained in the continuous emulsion phase, bubbles can arise at velocities that are competitive with the velocity of the descending catalyst emulsion in the standpipe. Thus, if bubbles form in the FCC standpipe, they can rise against the flowing catalyst, be pulled down by the flowing catalyst, or remain stationary in the standpipe, depending on the relative bubble and catalyst emulsion velocities involved.

Continued from Page 84

of the standpipe that are not building pressure. There are really several different phenomena that can create this type of pressure profile.

- The catalyst might be defluidized so that it is supporting its weight against the walls.
- There may be stationary bubbles² in the standpipe that are acting as obstructions.
- There may be a real obstruction like a piece of dropped refractory or a workman's shovel.

In any case, the section of the standpipe immediately below an obstruction will have a tendency to operate with a dilute rain of catalyst falling through an essentially empty standpipe. This type of flow does not generate the pressure buildup that the standpipe needs to produce.

Check the Standpipe Aeration Practices

The aeration rates being used on the standpipes should be checked against the theoretical aeration rates calculated in the next section. Defluidization of the catalyst from under-aeration, or obstructions in the form of bubbles from over-aeration, can both be caused by errors in the standpipe aeration. Unfortunately the symptoms for both these problems are very similar, so it is necessary to use a theoretical aeration rate as a point of reference.

It is very important to calculate the aeration required by each individual aeration tap location along the length of the standpipe. This information provides a great deal of insight into how the standpipe wants to operate, and provides a basis for comparing the actual aeration rates. Not calculating the individual aeration tap requirements is a serious mistake because the opportunity to look at the operating requirements for each section of the standpipe may be missed.

Also, ask as many questions as possible about the standpipe aeration. Some questions that come to mind are:

- How much aeration is being used in the standpipe?
- Is steam, air, or some other gas being used for aeration? Why is this particular media being used?
- If the standpipe is being aerated with steam, is it absolutely dry steam, or could there be condensate slugging into the standpipe?
- How much aeration is being supplied to each individual tap?
- How does the aeration rate compare with the theoretical aeration rate calculated for each individual tap?
- Could some of the aeration taps be plugged?

- How is the aeration being distributed to the taps?
- Does the aeration system use rotometers for each tap, or are orifices being used to obtain distribution?
- How confident are you that the aeration is going where you think it is going?
- How does the aeration rate compare with theoretical and historical bench marks? (More on these later.)
- Are the aeration tap locations correct? Don't automatically assume that they are. (More on this later also.)

If the standpipe does not have aeration, read on, since this is where the plot thickens.

Calculation of Standpipe Aeration Requirements

The calculation of the aeration, needed at any one of the pressure taps, is relatively straightforward. The steps required are outlined below, followed by a worked example.

1. Calculate the volume of catalyst that is descending the standpipe.
2. Calculate the volume of voids that are circulated with the catalyst³.
3. Calculate the absolute pressure that should be observed at the stand-pipe inlet and at the various aeration taps along the standpipe length using an assumed emulsion density.
4. Calculate the change in gas volume due to the pressure increase between adjacent aeration taps.

This is the theoretical volume of gas that should be introduced into the tap under investigation. However, in practice only about 60-70% of this quantity of aeration is usually needed.

The example discussed below is illustrated in Figure 6.

Example 1

Calculate the steam required to aerate the first aeration tap in a regenerator standpipe that is operating at the following conditions:

Catalyst circulation:

12 metric tons per minute

Regenerator Temperature:

682°C (1260°F)

Regenerator Dilute Pressure:

82.7 kPa gauge (12 Psig)

Molecular Weight of Aeration Gas:

18.0 (Steam)

³The circulation of the catalyst in the standpipe actually pumps the gas that occupies the spaces between (and inside) the particles down the standpipe with the catalyst.

The minimum fluidization velocity of FCC catalyst is on the order of 0.003m/second, while the velocity of the catalyst descending the standpipe is several orders of magnitude higher than this. So the gas that is in the continuous emulsion phase between and inside the catalyst particles is, in effect, dragged down the standpipe with the catalyst.

Trouble-Shooting FCC Standpipe Flow Problems

The distance from the surface of the catalyst bed in the regenerator vessel to the inlet of the standpipe is 1.83 meters (6 feet).

The distance from the inlet of the standpipe to the first aeration tap below the inlet is 2.85 meters (9.35 Ft).

You will need to assume a density for the fluidized catalyst inside the standpipe. For the sake of these calculations, it is customary to assume a density of 560.65 kg/m³ (35 lbs/ft³).

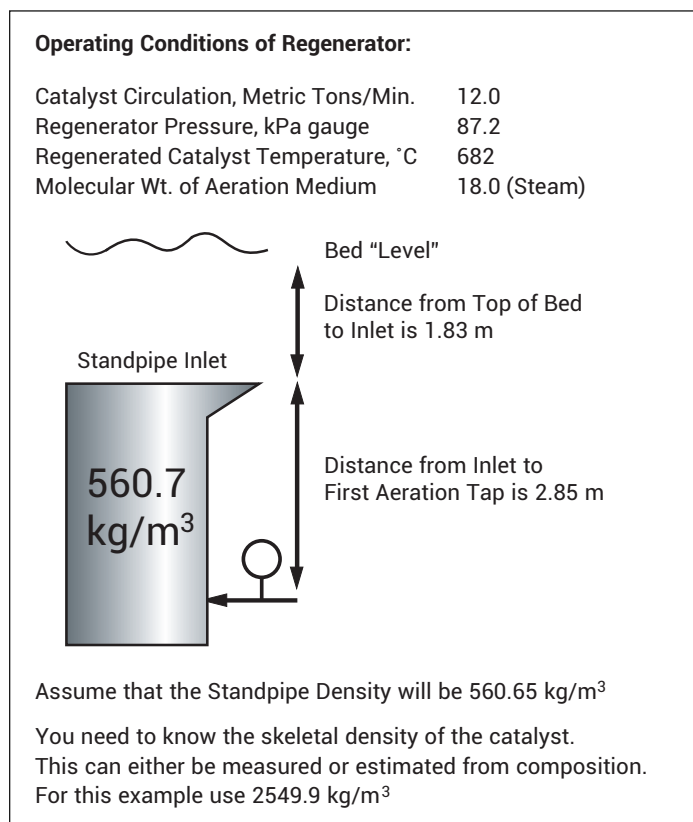


Figure 6. Calculation of Aeration Requirements

You will also need to know the skeletal density of the equilibrium (not fresh) FCC catalyst being used. This can either be measured using helium pycnometry, or the skeletal density can be approximated from the calculation below:

$$\rho_{\text{skeletal}} = \frac{1000}{\frac{\text{Al}_2\text{O}_3}{3.4} + \frac{\text{SiO}_2}{2.1}} \quad (3)$$

Where:

- ρ_{skeletal} = Skeletal density of catalyst, kg/m³
- Al_2O_3 = Weight fraction Alumina in catalyst
- SiO_2 = Weight fraction silica in catalyst

For this example, a skeletal density of 2549.9 kg/m³ was measured using the equilibrium catalyst.

1) Calculate the volume of the catalyst emulsion that is traveling down the standpipe per minute:

$$1000 \frac{Q_{\text{catalyst}}}{\rho_{\text{emulsion}}} = V_{\text{emulsion}} \quad (4)$$

Or

$$V_{\text{Emulsion}} = 1000 \frac{(12.0)}{560.65} = 21.40 \text{ m}^3/\text{min}$$

Where:

Q_{Catalyst} = Catalyst circulation, metric tons per minute.

V_{emulsion} = Volume of fluidized catalyst emulsion m³/min.

ρ_{emulsion} = The assumed stand pipe fluidized density of 560.65 kg/m³.

2) Calculate the total volume of interstitial and intraparticle gas that is circulated with the catalyst:

$$V_{\text{gas}} = V_{\text{emulsion}} \left(1 - \left(\frac{\rho_{\text{emulsion}}}{\rho_{\text{skeletal}}} \right) \right) \quad (5)$$

Or

$$V_{\text{gas}} = 21.40 \left(1 - \left(\frac{560.65}{2549.9} \right) \right)$$

Where:

V_{Gas} = Volume of gas circulated down the standpipe with the catalyst, m³/min.

3) Calculate the absolute pressure at the standpipe inlet, and the first aeration tap:

The pressure at the Inlet is:

$$P_{\text{Inlet}} = P_{\text{Dilute}} + \frac{(\rho_{\text{emulsion}})(g)(\Delta H_{(\text{Inlet} - \text{Surface})})}{1000} \quad (6)$$

Or

$$P_{\text{Inlet}} = (82.74 + 101.32) + \frac{(560.65)(9.81)(1.83)}{1000} = 194.12 \text{ kPa Absolute}$$

Continued on Page 87

Continued from Page 86

The pressure at Tap 1 is:

$$P_{\text{Tap 1}} = P_{\text{Inlet}} + \frac{(\rho_{\text{emulsion}})(g)(\Delta H_{\text{(Tap-1 Inlet)}})}{1000} \quad (7)$$

Or

$$P_{\text{Tap 1}} = 194.12 + \frac{(560.65)(9.81)(2.85)}{1000} = 209.80 \text{ kPa}$$

Where:

- P_{Inlet} = Pressure at the standpipe inlet, kPa absolute.
- $P_{\text{Tap 1}}$ = Pressure in the standpipe at the location of the first aeration tap down from the standpipe inlet, kPa absolute.
- P_{Dilute} = Pressure in the dilute phase of the vessel, above the catalyst bed, kPa absolute.
- $\Delta H_{\text{Inlet Surface}}$ = Height of the catalyst bed above the inlet to the standpipe, meters.
- $\Delta H_{\text{Tap 1-Inlet}}$ = Difference in depth between the location of the standpipe inlet and the first aeration tap, meters.
- ρ_{Emulsion} = Assumed density of the fluidized emulsion (560.65 kg/m³).
- g = Gravitational Constant, 9.81m/sec².

4) The change in gas volume due the pressure increase can then be calculated:

$$\Delta V_{\text{gas}} = V_{\text{gas}} \frac{P_{\text{Inlet}}}{P_{\text{Tap 1}}} \quad (8)$$

Or

$$\Delta V_{\text{gas}} = 16.70 \frac{(16.70)(194.12)}{209.80} = 1.25 \text{ m}^3/\text{min}$$

Where:

- ΔV_{Gas} = The change in gas volume at the temperature and pressure of the standpipe due to compression.

In order to counteract the compression effect and restore the needed volume to the catalyst emulsion, an incremental 1.25m³ of gas per minute (at 682.2°C., 209.80 kPa absolute) must be

injected into the standpipe at Tap 1. Using a molecular weight of 18.0 and PV=nRT this works out to 0.59 kg/min of steam at this tap location.

The theoretical aeration requirement serves as a useful benchmark to judge aeration rates when first examining the operation of the standpipe. However, few FCC units actually operate with exactly this quantity of aeration. In the real world, the actual aeration rate should initially be set to approximately 60-70% of this theoretical aeration requirement. Subsequent adjustment of the aeration rates from this initial point can then be used to seek out additional improvements. Some FCC units will end up operating somewhat above the theoretical aeration requirement, while others will operate below this theoretical aeration rate. In any case the best place to start is with an aeration rate that is 60-70% of theoretical.

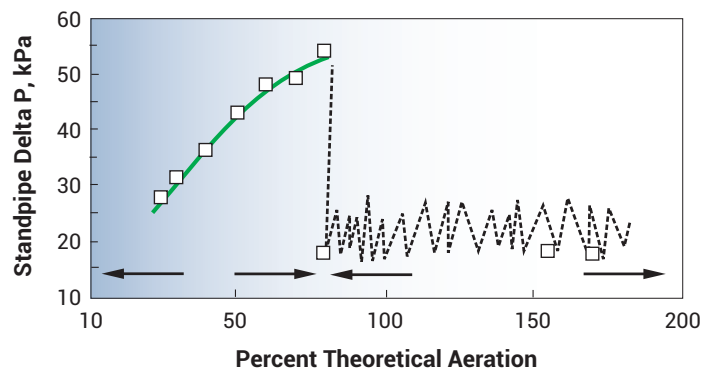


Figure 7. Standpipe Delta P

Figure 7 which is taken from a paper by R.E. Wrench, J.W. Wilson, and G. Guglietta³ shows how the pressure generated in a standpipe responds to variations in aeration rates. Note that over-aeration produces a dramatic loss of standpipe pressure. This behavior provides another good reason to use less than the full theoretical aeration rate when first setting up standpipe aeration.

It should be expected that as the physical properties of the equilibrium catalyst change, the shape of the aeration response curve shown in Figure 7 will also change. As the MSER of the equilibrium catalyst increases, the more tolerant it becomes to improper aeration.

Note that the aeration requirements of a standpipe is dependent on the catalyst circulation rate. So it is convenient to calculate the aeration requirement in terms of kg aeration per metric ton of catalyst circulated. In this example, the theoretical aeration at the first tap is 0.049 kg steam/metric ton of catalyst circulation.

Tap #	Tap Location, Meters Below Bed Surface	ΔH, Meters	Aeration Required, kg/min of Steam
Inlet	1.83	1.83	None
1	4.68	2.85	0.59
2	8.18	3.50	0.73
3	11.68	3.50	0.73
4	15.18	3.50	0.73
5	18.68	3.50	0.73
6	22.18	3.50	0.73
7	25.68	3.50	0.73
8	29.18	3.50	0.73
9	32.68	3.50	0.73
10	36.18	3.50	0.73

Table 1

The aeration calculation should be repeated incrementally from tap to tap down the length of the entire FCC standpipe. All of the actual aeration rates can then be compared to the theoretical bench marks provided by the calculation. Often this exercise will reveal that some portion of the standpipe is being improperly aerated.

When doing these aeration calculations along the length of the standpipe, it is handy to know that if the distances between the taps are equal, then the theoretical aeration required by the equally spaced taps will all be the same. Table 1 illustrates this for the regenerator used in the example above. Aeration taps 2 through 10 are all equally spaced at a distance of 3.5 meters from each other.

Standpipe Compression Requirements

Calculating the change in catalyst emulsion density that is taking place in the standpipe from tap to tap is also very revealing. As was mentioned earlier, there is only a very limited range of densities over which FCC catalyst will remain fluid. If the increase in pressure from tap to tap is too large, the catalyst

will be compressed past its point of incipient fluidization.

Using data from the previous example, the percent change in catalyst density required from tap to tap can be calculated from:

$$\Delta\rho_{Emulsion} \% = 100 \frac{\Delta V_{Gas}}{V_{Emulsion}}$$

Or using the numbers from Example 1:

$$\Delta\rho_{Emulsion} = 100 \frac{1.25}{21.40} = 5.84\%$$

Where:

$\Delta\rho_{Emulsion}$ = The percent change in emulsion density that is taking place from tap to tap.

What we are really doing here is calculating the amount of compression that the standpipe is requiring the catalyst to undergo. The greater the required percentage increase in density from tap to tap, the more prone the standpipe is to circulation difficulties. Calculating the percentage compression from tap to tap, often pinpoints where the FCC standpipe will be most likely to experience compression problems. FCC units that are suffering from catalyst over-compression, and

the subsequent loss of fluidization that it brings on, will often find that these problems are occurring in the upper half of the standpipe because this is where the greatest amount of compression per meter of descent takes place in the standpipe.

This standpipe compression requirement is a function of the FCC design pressure, and the spacing between the taps on the FCC standpipes. For example, it is commonly observed that lower pressure FCC units, where the regenerator may be designed to operate at 82 kPa gauge (12 psig), generally have much more difficulty circulating catalyst in standpipes than do higher pressure designs where the regenerator may be operating at 207 kPa gauge (30 psig). A quick calculation of standpipe compression requirements reveals that the low pressure designs inherently have much higher standpipe compression requirement, per meter of standpipe descent, than do the higher pressure designs.

Table 2 shows how the compression requirements for a standpipe change dramatically with respect to the dilute phase pressure of the vessel from which they are drawing catalyst.

The standpipe that is operating at the lower design pressure requires the catalyst to undergo significantly more compression between the aeration taps. In fact, at the top of the standpipe where the compression requirements are greatest, the low pressure design shown here requires 58% more catalyst compression per meter of standpipe descent.

One way to mitigate this compression requirement when the unit is designed for lower pressure, is to place the aeration taps closer together along the length of the standpipe.

As a rule, the aeration taps for low pressure standpipes should normally be spaced so that less than 4.5-5.0 percent compression is required between the taps.

Continued on Page 89

Continued from Page 88

Tap #	Tap Location, Meters Below Bed Surface	ΔH , Meters	Percent Compression Required in Standpipe	
			Dilute Pressure 82.7 kPa Gauge	Dilute Pressure 206.0 kPa Gauge
Inlet	1.83	1.83		
1	4.68	2.85	5.84	3.67
2	8.18	3.50	6.56	4.26
3	11.68	3.50	6.05	4.04
4	15.18	3.50	5.61	3.84
5	18.68	3.50	5.24	3.66
6	22.18	3.50	4.91	3.50
7	25.68	3.50	4.62	3.35
8	29.18	3.50	4.36	3.21
9	32.68	3.50	4.13	3.08
10	36.18	3.50	3.92	2.97

Table 2

By keeping the compression requirement low, the standpipe circulation will be more tolerant of the changes in catalyst particle size distribution that accompany cyclone deterioration at the end of a run.

In terms of absolute numbers, 4.5 or 5.0 percent compression does not seem very high. However, if the unit is circulating a catalyst with a low stable expansion ratio (Low 0- 40 fines content and high ABD), then a 5.0 percent compression requirement in the standpipe can create catalyst circulation problems very quickly.

Choice of Aeration Media

Inspection of Equations 1 and 2 suggests that if the aeration media has a higher density and a higher viscosity, then the MSER for the system will be higher. Air is significantly higher than steam in both viscosity and density.

Thus, changing the aeration media from steam to air in regenerator standpipes that are suffering from compression problems has sometimes produced a dramatic improvement in catalyst circulation. If, due to poor

cyclone performance, the particle size distribution and density of the catalyst have moved into a region where the catalyst has trouble circulating in a standpipe with a 5.0 percent compression requirement, then changing the aeration media from steam to air can increase the compression tolerance (Effective MSER) to almost 1.08. This type of change in compression tolerance from 1.05 to 1.08 represents almost 60 percent improvement.

The possibility of condensate slugging into the standpipe is also greatly reduced by using air instead of steam.

The refiner should be aware that there are occasional gasoline gum or stability problems that can arise from the additional oxygen that is carried into the reactor by air in the regenerator standpipe. But these problems are relatively infrequent, and if they do occur, then the standpipe can be switched back to steam.

Note that this change in aeration medium is only appropriate in units that are operating with complete combustion in the regenerator.

Catalyst Design

In order to help mitigate a refiners' catalyst circulation problems, there are a number of things that the catalyst manufacturer can do to the catalyst.

First of all, if the FCC unit is limited in the amount of catalyst that it can circulate, then an increase in equilibrium catalyst activity should be considered. This will allow the refiner to achieve his best possible conversion with the limited catalyst circulation that is available. Increasing the activity of the equilibrium catalyst will also raise the regenerator temperature, which in turn will reduce the amount of catalyst that must be circulated at a given set of operating conditions. These two effects complement each other nicely.

Equations 1 and 2 along with Figure 5 clearly show that the Maximum Stable Expansion Ratio of the equilibrium FCC catalyst is a function of catalyst ABD and the 0-40 micron fines content of the inventory. Manufacturers of FCC catalyst have a great deal of flexibility in their manufacturing process which allows them to modify the ABD of the equilibrium catalyst without changing the chemical composition, or the catalytic selectivity patterns of the catalyst. Thus, a reduction of the equilibrium ABD can be designed into the fresh catalyst so that the MSER of the equilibrium catalyst can be enhanced.

In addition, the particle size distribution of the fresh catalyst can be modified in favor of a smaller average particle size with a higher 0-40 micron fines content which also tends to aid circulation.

Attrition resistance of the catalyst is another feature that can be modified so that the tendency to generate 0-40 micron fines can be enhanced. This is sometimes helpful when the cyclones have deteriorated and the ability of the FCC unit to hold the necessary 0-40 micron fines in its inventory is diminished.

By judicious application of these principles, the catalyst manufacturer can provide the refiner with a great deal of relief from standpipe circulation problems.

Pulling it All Together

From the foregoing discussion it should be clear that there are really four disciplines that need to be examined when trouble-shooting catalyst circulation problems in standpipes:

1. The Design of the FCC Unit Itself.
2. The FCC Unit Operations.
3. The Fluidization properties of the Equilibrium FCC Catalyst.
4. The Design of the Fresh Catalyst.

The FCC standpipe design needs to be looked at to confirm that its compression requirements are reasonable, to determine where the standpipe is making the most demands on the circulating catalyst, and to determine what the theoretical aeration bench marks are.

FCC operations need to be looked at to insure that the standpipe is being operated properly, and to insure that the rest of the FCC hardware is really doing what it is suppose to be doing. For example, a false level reading can trigger circulation difficulty by upsetting the bed levels which may uncover the cyclone diplegs, etc. One thing leads to another, and soon the fines have been lost from the inventory, and the standpipe circulation is in jeopardy.

Since the cyclone operation determines the particle size distribution of the equilibrium catalyst, an examination of cyclone performance should be considered an integral part of trouble-shooting standpipe circulation problems.

As shown above, the equilibrium catalyst properties provide much indirect information about how compression tolerant the catalyst will be in the standpipe. Thus, the equilibrium catalyst properties should be closely scrutinized for any subtle changes that may have triggered the standpipe upset.

Since a great deal of relief can often be obtained by modifying the fresh catalyst design, the catalyst manufacturer should be consulted to determine how much latitude is available for changing physical properties or activity. Modification of the fresh catalyst design to mitigate circulation difficulties is just another example of the benefits that accrue from close cooperation between the refiner and the FCC catalyst manufacturer.

References

1. Abrahamsen, A.R., and Geldart, D., Powder Technology, Vol 26, 1980, pp 35-55.
2. Magnussun, J.E.: "Fluidization Properties of Equilibrium FCC Catalyst", Paper presented at the 1985 Katalistiks Seminar.
3. Wrench, R.E., Wilson, J.W., Guglietta, G.: "Design Features for Improved Cat Cracker Operations", Paper presented at "The First South American Ketjen Catalyst Seminar, Rio de Janeiro, Brazil, September 1985.



"Understanding and Minimizing FCC Slurry Exchanger Fouling" was published by Grace in *Catalagram* 101 in 2007. Slurry exchanger fouling was a frequent problem our customers faced early in my career at Grace as a technical service representative. With limited experience of my own, I turned to Grace's wider expertise and the insights and advice of industry publications along with NPRA Q/A responses on the topic to assist our customers.


This *Catalagram* article pools the insights of 15 references to holistically review all aspects of FCC slurry exchanger fouling together with solutions in a single source. Increased understanding together with improved bottoms cracking catalyst like Grace's MIDAS® technology, introduced in 2002, allowed many of our customers to reduce or eliminate slurry exchanger fouling from their operations.

Today, it maintains its relevance as slurry exchanger fouling continues to be a risk due to increasing contaminant iron levels in FCC feedstocks around the globe. Along with the insights offered, recent Grace FCC technology advancements such as MIDAS® Pro and Grace MILLE™ catalyst increases bottoms cracking despite higher levels of contaminant iron, ensuring excellent slurry exchanger performance and improved profitability for our customers.



David A. Hunt
Sr. Principal Technologist, Global Customer Technology
W. R. Grace & Co.

Understanding and Minimizing FCC Slurry Exchanger Fouling

 David A. Hunt, Bill Minyard, Jeff Koebel

 Originally published in *Catalagram* #101 in 2007 (30)

Slurry exchanger fouling is often considered the worst fouling service in the FCC process. ⁽¹⁾ The primary problem that results from slurry exchanger fouling is reduced heat exchanger duty in the slurry/FCC feed preheat exchanger or the steam generators. The reduction in feed preheat temperature that can result from just mild fouling of the FCC slurry/feedstock exchangers can result in reduced unit feed rate or conversion.* Additionally, excessive pressure drop or inability to cool the slurry to the necessary rundown temperature can also require reducing the feed rate. Certainly excessive slurry exchanger fouling can be very costly to the refinery in

terms of lost feed rate, lower conversion and higher maintenance expenses.

The purpose of this article is to present potential sources of slurry exchanger fouling and suggestions on how to prevent or minimize fouling. We Understanding and Minimizing FCC Slurry Exchanger Fouling will draw on industry experience from several sources to present a broad review of the subject. Our readers may consider this information and case study experience as they work to understand and minimize slurry exchanger fouling at their refinery.

*For those FCC units that do not have a fired feed heater and are air blower limited.

Continued from Page 92

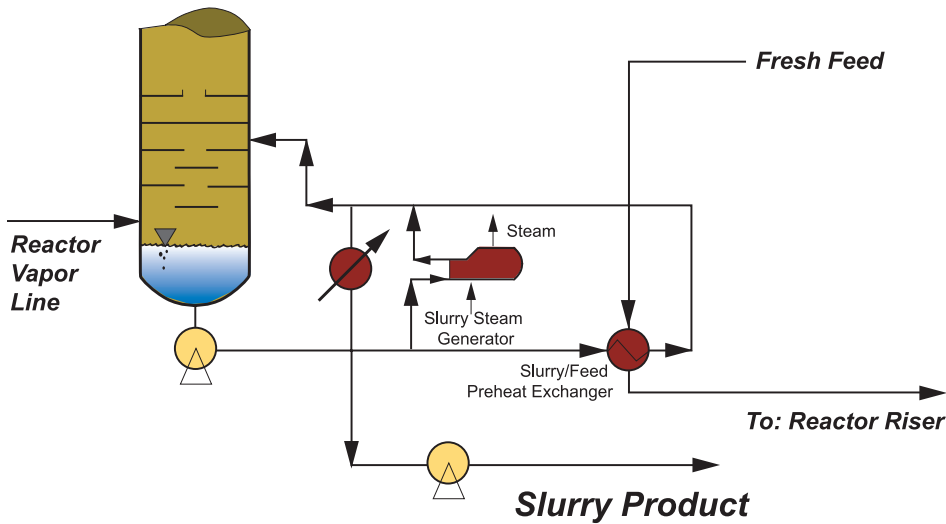


Figure 1. Typical Main Fractionator Slurry Circuit

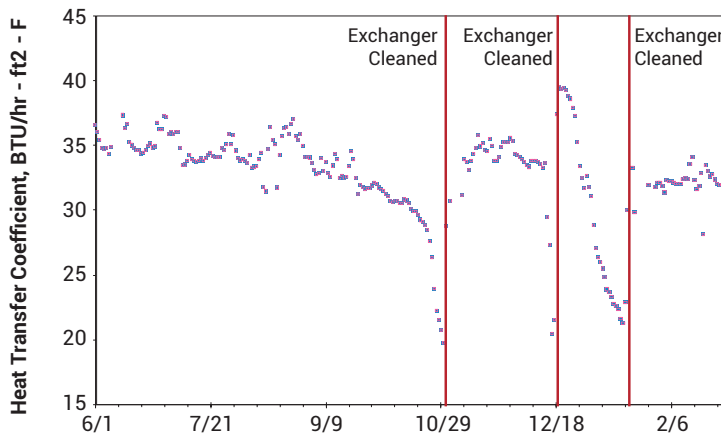


Figure 2. FCC Slurry Exchanger Heat Transfer Coefficient Deterioration

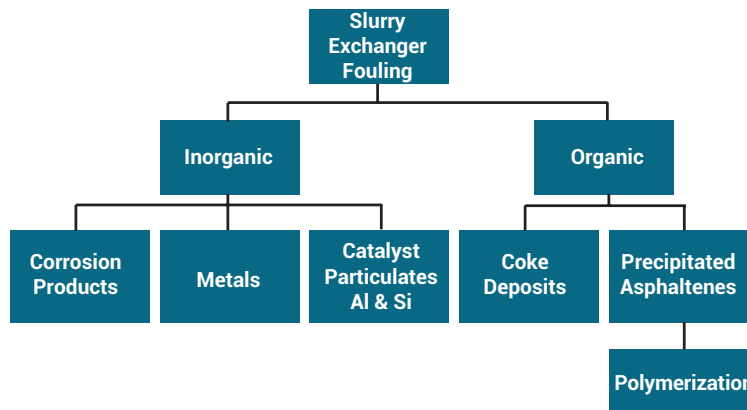


Figure 3. Root Causes of Slurry Exchanger Fouling

Figure 1 illustrates a typical FCC Main Fractionator Slurry circuit. Superheated FCC product vapor is quenched as it enters the main fractionator using the reflux from the slurry pumparound circuit. Slurry exchangers, which recover this energy by heating the feedstock and generating steam, are often subject to fouling through a number of mechanisms. When slurry exchangers foul, feed rate or reactor temperature must often be reduced.

Figure 2 shows how quickly a slurry/feed exchanger heat transfer coefficient can deteriorate. Over a ten-week period, this refiner needed to clean their FCC slurry exchanger three times. During each cleaning cycle they were forced to significantly reduce feed rate.

Potential causes of FCC slurry exchanger fouling are shown in Figure 3. Fouling can be generally classified as either “organic” or “inorganic” based. Several organic or inorganic slurry fouling mechanisms are possible. Each of these possible fouling sources will be discussed and suggestions to prevent or reduce each type will be presented.

Organic Based Fouling

Organic based fouling is the most common fouling type. The potential causes of organic based fouling are very broad. It is helpful to classify organic fouling into two general sub-types: “hard” and “soft” coke fouling.

Hard Coke Fouling

Solid coke fragments circulating to the slurry exchanger tubes that restrict the flow through the exchanger is an example of hard coke fouling. This type of fouling results in excessive pressure drop and a loss of heat transfer duty. These shiny coke fragments generally accumulate on the exchanger tube sheets at the inlet to the tubes. Figure 4 shows how pieces of coke can block the exchanger tubes, increasing exchanger pressure drop.

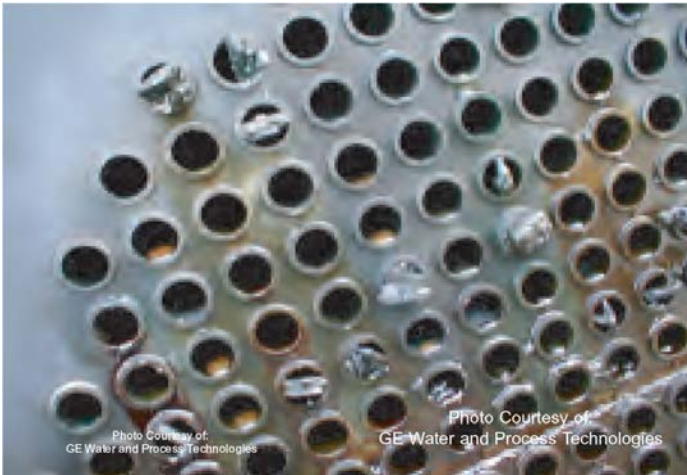


Figure 4. Hard Coke Deposits

These coke fragments can originate in the reactor overhead line or the main fractionator. The coke often becomes dislodged following an FCC shutdown because of the thermal cycling of the surface that the coke is adhered to. If the coke fragments are small enough to pass through the suction strainers on the slurry pumparound pumps, they can eventually foul the first slurry exchanger in the pumparound loop. Another scenario that can result is excessive hard coke accumulation in the bottom head of the main column that restricts the suction of the circulating slurry pumps.

Smaller coke fragments that pass through the exchanger tubes can still be problematic. These coke particles are either smaller coke particles from the main fractionator or are formed by polymerization reactions in the slurry pumparound circuit at high main fractionator bottoms temperatures. Small coke fragments can settle onto the tube surface and further polymerize, resulting in a barrier to heat transfer and slurry flow.

In some cases, formation of a very thin, hard layer of deposit has been observed on the tube walls. This type of deposit has a hard, shiny appearance similar to varnish. These deposits are formed by polymerization reactions on the tube surface. This type of fouling can reduce the heat transfer coefficient.

Preventing Hard Coke Fouling

Poor feed/catalyst contacting can be a significant source of hard coke formation in the vapor line. This is particularly true in units that process resid feeds. Feed /catalyst contacting can be improved in several ways:

- Improve feed atomization;
- Increase feed dispersion steam within the limits of the feed distributor design;

- Repair damaged feed distributors or replace with a more modern design;
- Increase the feed temperature to avoid high feed viscosity at the injection distributors. This is particularly applicable to resid operations.
- Increase the catalyst/oil mix zone temperature. This is most critical in resid or low reactor temperature operations where incomplete vaporization of the feed is more likely. Mix zone temperature can be increased using Mix Zone Temperature Control (MTC) ⁽²⁾ and/or higher reactor and regenerator temperatures;
- Optimal catalyst matrix design can improve feedstock vaporization. ⁽³⁾

A hot wall reactor vapor line must be properly insulated to reduce the likelihood of liquid condensation at cool spots. Insulation must be properly anchored and should be watertight. Once oil droplets form, they eventually dehydrogenate to form coke. The reactor vapor line blind flange and all the vapor line pipe supports should also be insulated if the designs allow, as coke can accumulate at these locations. Do not insulate the bolts of the blind flange, however, as this can result in the flange opening due to bolt creep.

Reactor vapor line vapor velocities less than 100 fps should be avoided to minimize coke formation. The exception to this is the velocity right at the inlet nozzle to the main column, where lower velocities are permitted. ⁽⁴⁾ Higher velocities will reduce the likelihood of un-vaporized oil accumulating along the wall of the vapor line and eventually forming coke. Vapor line velocities between 100 to 120 fps are a good compromise to minimize both coke formation and pressure drop. ⁽⁴⁾ Self-draining reactor overhead lines are a design feature often used to minimize coke formation and subsequent slurry exchanger fouling.

The maximum main fractionator bottoms temperature is typically between 680°F and 700°F to avoid coke formation and slurry exchanger fouling. The maximum safe bottoms temperature for any unit is unit and feedstock specific. It is also important to note that the bottoms temperature is often based a single temperature indicator (TI) at the outlet line of the main fractionator. Poor pumparound distribution and liquid mixing may result in locally hotter temperatures than what is actually measured in the bottoms outlet line, increasing the likelihood of coking. This can be particularly true in operations where quench is used to cool the bottom of the main column.

Long liquid residence time in the slurry circuit will also influence coking. Reducing bottoms liquid level can minimize slurry residence time. Also note that increasing main fractionator bottoms temperature and slurry pumparound rate both increase the liquid residence time. ⁽⁵⁾

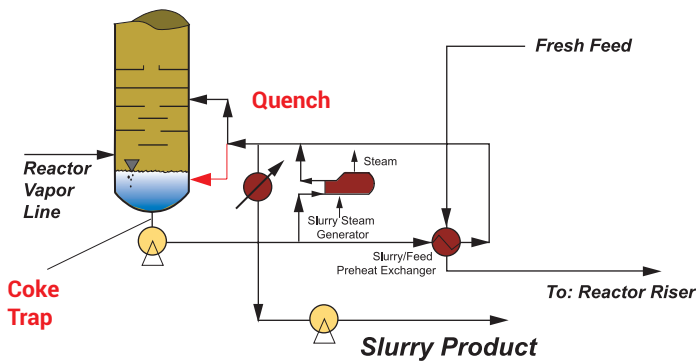
Continued on Page 95

Continued from Page 94

FCC feedstock, particularly feed containing resid, can form coke at typical main fractionator bottom temperatures. As a result, refiners should ensure that no feedstock is leaking into the slurry pumparound circuit through an emergency feed by-pass valve or slurry/feed exchanger.⁽⁵⁾

The slurry pumparound return should be properly distributed to minimize hot spots. The pumparound rate should be sufficient to ensure the grid zone is well wetted. Local areas devoid of liquid flow will allow hard coke to form. A minimum flux rate of 6 gpm/ft² has been recommended.⁽⁶⁾ A slurry pumparound rate of 1.2 to 1.5 times the feed rate is a rule of thumb that has also been suggested to ensure good liquid distribution in the bottom of the main fractionator.⁽⁷⁾

Slurry quench, as shown in Figure 5, can be used to sub-cool the main fractionator bottoms temperature and reduce hard coke formulation.⁽⁶⁾ A quench distributor should be used to minimize hot spots. Slurry quench, however, is commonly injected from a nozzle that terminates near the wall of the fractionator. As a result, the returning quench liquid is often not well distributed. Therefore, do not rely on perfect mixing of the slurry quench, as zones of high temperature could still be present. The refiner may consider monitoring bottoms temperature on a quench-free basis to account for potential high temperature zones.⁽⁶⁾



Main Fractionator Slurry Circuit

Figure 5. Slurry Quench and Coke Trap in the slurry circuit

Maintaining slurry exchanger tube velocities greater than 6 fps will help minimize any settling of small coke fragments or FCC catalyst onto the tube service.⁽⁸⁾ Units often have spillback valves on the slurry product exchangers to help maintain minimum slurry flows during times of turndown operation. Tube velocities should be less than 10 fps to avoid erosion.⁽⁸⁾

Using an elevated slurry exit nozzle can reduce the likelihood of coke being entrained into the slurry pumparound loop.⁽⁸⁾ However, this results in the bottom head of the main column

filling with accumulated coke and catalyst. On units where the liquid draw is on the bottom head, a coke trap should be employed in the bottoms suction nozzle on the column and/or upstream of the slurry exchanger as shown in Figure 5 to trap any entrained coke particles before they can foul the exchanger. G. Walker discussed application of a coke trap and resulting reduction in slurry exchanger fouling.⁽⁹⁾

Soft Coke Fouling

Soft coke fouling is organically based where commonly an insulating barrier is deposited inside the exchanger tubes, reducing the exchanger heat transfer coefficient. The insulating barrier can be found throughout the tube service.⁽¹⁰⁾ Figures 6 and 7 show examples of soft coke fouling. Just a thin layer of material can result in a costly reduction of the exchanger heat transfer coefficient. In some cases, soft coke fouling can also result in increased exchanger pressure drop.⁽¹⁰⁾ Generally, however, reduced heat transfer is apparent before excessive pressure drop with this type of fouling.



Figure 6. Soft Coke Precipitation Fouling



Figure 7. Soft Coke Precipitation Fouling

Precipitated asphaltenes are a common source of soft coke fouling. Asphaltenes are highly condensed polyaromatics typically insoluble in a saturated hydrocarbon such as heptane.⁽¹¹⁾ The concentration of these multiring aromatics in the slurry can be increased by thermal condensation reactions in the slurry circuit.

Asphaltenes can become insoluble in the slurry oil and begin to precipitate onto the tube surface. The tar-like layer on the tube service can also trap coke and catalyst particles that are present in the slurry.⁽¹²⁾ Figure 8, an abbreviated version of Figure 3, illustrates the sequence. Analyzing such tube deposits and slurry for fused aromatics can be insightful. Higher amounts of fused aromatics in the deposit relative to the slurry can confirm asphaltene precipitation.⁽¹³⁾

Slurry viscosities increase at the tube wall due to the locally cooler temperature. The higher viscosity can cause material to adhere to the tubes, resulting in exchanger fouling.⁽¹²⁾ Slurry with a higher paraffinic content may be more prone to fouling due to the inherently higher viscosity.

Preventing Soft Coke Fouling

Two sources suggest minimizing asphaltene content of the slurry in order to minimize fouling.^(5,14) ASTM D3279 can be used to determine asphaltene content. The asphaltene content is defined as those components in the sample that are not soluble in n-heptane. This procedure gives the combined amount of asphaltenes and particulate matter.

Maintaining asphaltenes in solution is key to preventing soft coke fouling. The composition of the slurry will affect the solubility of the asphaltenes. Generally higher aromatic content of the slurry tends to keep asphaltenes in solution. As such, changing the slurry composition by dropping some LCO down the tower can increase the

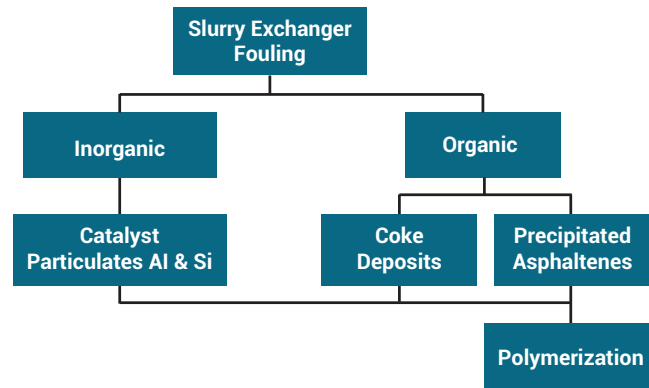


Figure 8. Catalyst and Coke Interaction with Precipitated Asphaltenes

solubility of asphaltenes in the bottoms material. This also has the benefit of reducing the temperature at the bottom of the main column.

It is often necessary to adjust the bottoms composition and temperature in this manner during changes in feed composition. For example, slurry produced from paraffinic feedstocks tends to be more prone to fouling and requires lower main fractionator bottoms temperature to minimize fouling.

Many refiners will also adjust bottoms temperature with conversion shifts to minimize fouling. A drop in conversion could result in higher slurry exchanger fouling. Slurry with higher API gravity, generally due to lower conversion, contains more saturated compounds, which can reduce asphaltene solubility and increase soft coke fouling. Slurry with a high API gravity is also more viscous and more prone to fouling.

Feedstock leaking into the slurry circuit can cause asphaltene precipitation. This occurs because the feedstock is more paraffinic than the slurry and reduces the solubility of the slurry asphaltenes. The refiner should take all precautions necessary to ensure that the feed emergency by-pass valve and the slurry/feed preheat exchangers do not leak feedstock into the slurry circuit.

The FCC catalyst can be formulated with features to minimize fouling. Catalyst matrix design can be optimized to improve slurry exchanger fouling by increasing Type III cracking as described by Zhou.⁽³⁾ Minimizing naphthoaromatics and paraffinic content of the slurry by increased Type III cracking may improve asphaltene solubility and reduce slurry exchanger fouling. Using a catalyst with proper tolerance to contaminant metals will help avoid fouling as well. Increased catalyst contaminants that result in a loss of FCC conversion can increase the likelihood of fouling as discussed above.

Hot Cycle Oil Flush at the inlet of the slurry exchangers can help keep asphaltenes in solution and increase tube velocity, both of which will help reduce slurry exchanger fouling.⁽⁵⁾

Inorganic Based Fouling

Inorganic fouling can include fouling prompted from corrosion or iron scale, catalyst or precipitated metals. Catalyst is often found in tube deposits and can be identified by the presence of alumina, silica, and rare earth. Catalyst in the deposits is often a result of organic based fouling, since catalyst generally accumulates onto viscous precipitated asphaltenes or other hydrocarbons already present on the tubes.

Continued on Page 97

Continued from Page 96

Another inorganic foulant in FCC slurry service is antimony. Antimony present in the slurry has been found on tube deposits. In one instance, 20 wt% antimony was found in a deposit.⁽¹⁵⁾ The antimony source was from antimony injection into the FCC feedstock to passivate equilibrium catalyst nickel.

Preventing Inorganic Based Fouling

Catalyst losses to the main fractionator should be minimized by proper reactor cyclone operation and good reactor cyclone mechanical integrity. The catalyst itself can also be designed to minimize losses to the main fractionator. To maximize catalyst retention, the following catalyst design parameters should be considered:

- Low Attrition Index (Low DI);
- Low 0 to 40 micron content;
- High Particle Density.

Antimony levels in the slurry should be closely monitored to minimize the possibility of antimony depositing onto the tube service. FCC equilibrium catalyst antimony to nickel ratio is generally between 0.10 and 0.60 by weight. The antimony chemical should be injected to maintain the target level on the equilibrium catalyst without significant overfeed.

Proper metallurgy in the main fractionator, slurry piping and slurry exchanger should be used to minimize corrosion. Below is a summary of suggested materials.⁽⁶⁾

- Main fractionator internals TP 410 SS ;
- Exchanger tubes TP 405 or TP 410SS ;
- Slurry Lines 5 Cr - 1/2 Mo with 1/4" CA.

Antifoulants

Antifoulants have been successfully used to prevent FCC slurry exchanger fouling. Antifoulants can be generally classified as follows:

- **Organic dispersants** – prevent the agglomeration and deposition of asphaltenes;
- **Inorganic dispersants** – prevent the deposition of catalyst fines or other inorganic foulants such as Fe compounds;
- **Coke suppressants** – inhibit condensation reactions, which lead to hard coke-like deposits in exchangers.

A combination of antifoulants can be used. However, the likely source of the fouling should be identified before a specific antifoulant is applied.

Note that there can be some downstream effects when using an antifoulant. For example, in some cases catalyst fines settling in slurry tanks can be impacted if an inorganic dispersant is used.

Additional Design and Operation Considerations

There are many design considerations for exchanges in slurry service that can help to minimize the potential for exchanger fouling.

Slurry exchanger tube velocities should be 6 to 10 fps.⁽⁸⁾ Velocities below six fps can result in catalyst, coke or other particulates settling onto the tube surface, resulting in fouling. The minimum slurry exchanger tube diameter should be one inch.⁽⁵⁾ Smaller tubes can be subject to excessive fouling and are difficult to clean.

Spill back control can be used on net product exchangers in turndown conditions to keep tube velocities above minimum values.

Slurry should be present only on the exchanger tube side. With slurry on the shell side, it is impossible to prevent catalyst settling in the exchanger because of low local velocities.

Vertical and Spiral slurry pumparound exchanger designs tend to be less prone to slurry exchanger fouling.

Finally, having spare slurry exchangers should be considered to minimize turndown during exchanger cleaning.

Case Study

An FCC unit began observing severe fouling of their Slurry Steam Generator exchangers. The fouling began suddenly and continued for approximately two weeks and then stopped. During that time, it was necessary to clean the exchangers several times. The exchangers exhibited a reduction in heat transfer coefficient. Exchanger pressure drop was not affected.

The FCC was a modern design employing a modern riser termination device and state-of-the-art feed injection nozzles. The reactor temperature operated at 980°F and main fractionator bottoms temperature was typically 690°F. Conversion normally was ~78 vol.% with a slurry API gravity of -2 API.

The feedstock was a vacuum gas oil and resid blend with the following nominal feedstock properties:

- API 22° to 24°;
- K Factor 11.7 to 11.8;
- Conradson Carbon ~1.0 wt%;
- 10% Greater than 1050°F.

A deposit was taken from the fouled exchanger. Analysis of the deposit showed the following:

- 87% Carbon, 94% Organic Based (C, H, N);
- <1% Alumina;
- 1 wt% Antimony;

- <1 wt% Iron;
- 52% of the sample was Asphaltenes.

The refinery does use antimony to passivate nickel. However, antimony had been used for several years without any previous issues. No recent change in antimony injection was made and consequently antimony was likely not the cause of the fouling.

The deposit itself did not contain catalyst, as evident by the low amount of alumina.

The high amount of asphaltenes in the deposit confirmed asphaltene precipitation as the likely fouling mechanism.

A review of feedstock properties showed the feedstock had recently become more paraffinic, as evident by the higher API gravity and K Factor during the same time as the exchanger fouling. Figure 9 shows how feedstock API and K factor shifted. When the refinery changed the feed source the feedstock properties returned to typical values and the fouling stopped.

Many refineries recognize that some feed and crude sources can result in increased FCC slurry exchanger fouling. Those sources are either avoided, the main fractionator temperature is reduced, and/or antifoulants are used to minimize fouling while those feedstocks are processed.

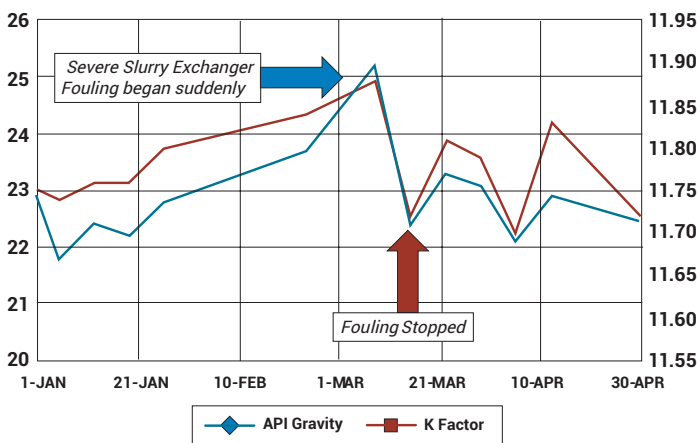


Figure 9. Feed Shift Property Shift Impacts Slurry Exchange Fouling

Final Remarks

Continuous monitoring of the overall heat transfer coefficients is critical to catch a slurry exchanger fouling problem early. Monitoring slurry properties such as API gravity, ash content, asphaltene content, and viscosity can also alert the refiner when the FCC unit may be more susceptible to slurry exchanger fouling. A shift of feedstock properties or unit conversion may also increase slurry exchanger fouling.

Slurry exchanger fouling often occurs during start-up or at turndown conditions when feedstock and operating conditions may be atypical. Special precautions may be considered during these unusual operations.

Reducing slurry exchanger fouling by lower main fractionator bottoms temperature and higher slurry product rate can be costly in terms of lower product value. Grace Davison can work with the refiner to adjust catalyst properties and operating strategy to minimize fouling and any subsequent yield loss.

References

1. Barlow, R., Reduce FCC Fouling, Hydrocarbon Processing, July 1986 pg 37-39
2. Meyers, R., Handbook of Petroleum Refining Processes 2nd Edition, McGraw Hill 1996, pg 3.95
3. Zhao, X. FCC Bottoms Cracking Mechanisms and Implications for Catalyst Design, 2002 NPRA Annual Meeting, San Antonio, TX, AM 02-53
4. Wilson, J., Fluid Catalytic Cracking Technology and Operation, Penwell Publishing 1997, pg 225
5. Sadeghbeigi, R., Fluid Catalytic Cracking Handbook 2nd Edition, Gulf Publishing Co. 2000, pg 251 to 253
6. Walker, P., NPRA FCC Principles and Practices, 2004 NPRA Q&A, Anaheim CA
7. Wilson, J., Fluid Catalytic Cracking Technology and Operation, Penwell Publishing 1997, pg 257
8. Wilson, J., Fluid Catalytic Cracking Technology and Operation, Penwell Publishing 1997, pg 229-230
9. Walker, G, A Case Study in Slurry Fouling, 2003 NPRA Annual Meeting, San Antonio TX, AM 03-63
10. Fouling in FCC Units & Purification Trains, GE Infrastructure Water and Process Technologies Presentation
11. Dickakian, G., Asphaltene Precipitation in Primary Crude Exchanger Fouling Mechanism, Oil and Gas Journal, Mar. 7, 1988, pg 47-50
12. Falker T. et al., Modeling of FCC unit Main Fractionator Bottoms Pumparound Fouling, 1995 NPRA Annual Meeting, San Francisco CA, AM-95-71
13. Shawney, K et al., The FCCU Slurry Loop Fouling Mitigation, 2002 AIChE Spring Meeting, New Orleans LA
14. NPRA Q&A Transcripts 1989, pg 68
15. NPRA Q&A Transcripts 1986, pg 54



"Nitrogen Chemistry and NO_x Control in a Fluid Catalytic Cracking Regenerator" was published in 1997 in *Industrial and Engineering Chemistry Research* and has been subsequently cited in more than 100 scientific papers. This fundamental work developed a complete nitrogen balance around the FCC and demonstrated that NO_x from the FCC regenerator is derived from feed nitrogen and not "thermal NO_x." This work was done in Grace's DCR™ Pilot Plant. The pilot plant scale allowed for studying process conditions not possible in a commercial unit, such as the elegant solution of using an oxygen/argon mix in the regenerator instead of air (oxygen/nitrogen) so the only nitrogen input to the FCC was feed nitrogen.

Today, refineries around the globe look to Grace to reduce NO_x and support environmental compliance, through both our operational insights and our products such as our DENOX® additive for standalone NO_x reduction.



Ken Bryden
Director, Catalyst Evaluation Research & Services
W. R. Grace & Co.

Nitrogen Chemistry and NO_x Control in a Fluid Catalytic Cracking Regenerator

 Xinjin Zhao, A. W. Peters, G. W. Weatherbee

 Originally published in *Industrial and Engineering Chemistry Research* in 1997 (36, 4535-4542)

Emission of NO_x from the fluid catalytic cracking (FCC) regenerator is increasingly controlled by various state and local regulations. The FCC regenerator poses a very challenging environment for controlling NO_x. Other than NO, the high-temperature flue gas contains O₂, CO, CO₂, SO₂, SO₃, H₂O, and possibly other nitrogen or sulfur species. In this paper, we will first present a complete nitrogen balance around the fluid catalytic cracking unit by using a circulating pilot plant with continuous regeneration. We will also discuss the transformation of nitrogen species during the cracking and catalyst regeneration process, which has direct implications on the formation and reduction of NO_x in the regenerator. Pilot plant or commercial data on the effect of operating conditions, cracking feedstocks,

and CO combustion promoter usage on NO_x emission will be discussed. With both thermodynamic analysis as well as experiments, we will show that the so-called “thermal NO_x” does not contribute to the FCC regenerator NO_x emission. On the basis of the understanding of the nitrogen chemistry we have obtained, we have successfully developed different catalytic NO_x control technologies for the FCC regenerator. Direct NO_x reduction additives and a new generation of CO combustion promoters which significantly reduced NO_x emissions will be discussed. Both laboratory and commercial trial data on some of the NO_x control additives as well as the mechanism for the NO_x control additives will also be presented. Finally, the future directions for NO_x control will be discussed.

Continued from Page 100

Emission of NO_x (i.e., NO, NO₂, and N₂O) from the fluid catalytic cracking regenerator is increasingly controlled by various state and local regulations. The FCC regenerator poses a very challenging environment for controlling NO_x. Other than NO, the high-temperature flue gas contains O₂, CO, CO₂, SO₂, SO₃, H₂O, and possibly other nitrogen oxygen species. Any NO_x control technology has to be designed in a way that it neither interferes with the catalytic cracking reaction in the riser nor substantially increases the emissions of other pollutants, e.g., CO or SO₂. NO_x levels in the FCC regenerator flue gas are typically in the range of 100-500 ppm. NO is the primary component of NO_x from the FCC regenerator. NO₂ is formed only after being released to the air, while N₂O exists typically at very low levels. The current paper will mostly focus on the emission and control of NO. In addition to the level of feed nitrogen, it is also known that operating conditions and hardware design of the regenerator can significantly affect NO_x emission. For example, higher excess oxygen in the flue gas is known to correlate with higher NO_x emission, which has led to the notion that NO_x is formed from the oxidation of molecular nitrogen from the air, or the so-called thermal NO_x. Until very recently, a few systematic studies existed on the formation and control of nitrogen oxide in the FCC regenerator. In the present paper, we will try to present and review what we learned about the NO_x chemistry through laboratory experiments on a pilot plant FCC unit and discuss the available approaches to control NO emission from FCC regenerators. The future directions of NO_x control in FCC will also be discussed.

Nitrogen Balance around FCC Unit

In order to understand the nitrogen chemistry in the regenerator, it is important to know where and how much of the feed nitrogen ends up in each of the FCC product streams. To answer these questions, we conducted nitrogen balance experiments in the Davison Circulating Riser (DCR), which is a pilot scale adiabatic circulating riser with continuous regeneration (Young, 1993; Zhao et al., 1996). Some of the preliminary nitrogen balance results have been presented in a previous paper (Peters et al., 1995). This unit processes about 1 kg of feed/h. All the operations are continuous, and the coked catalyst is continuously regenerated as in a commercial FCC unit. For the nitrogen balance experiments, two feedstocks with nitrogen contents of 0.12-0.32 wt% were processed in the unit. The feed properties are shown in Table 1. A commercial equilibrium catalyst was used for the experiments. The catalyst properties are shown in Table 2. All the product streams were collected for yield as well as nitrogen analyzes by gas chromatography and Leco analyzer. In order to exclude the nitrogen from air from our nitrogen experiments, we used a mixture of argon with 5% oxygen to regenerate the catalyst.

Description	Feed A F92-444	Feed B F93-247
API gravity @ 15°C	25.8	21.1
sulfur, wt%	0.3	0.77
total nitrogen, wt%	0.12	0.32
basic nitrogen, wt%	0.052	0.12
Conradson carbon, wt%	0.53	0.12
simulated distillation, vol %, °C		
10	298	288
50	421	403
90	530	495
K factor	11.78	11.39

Table 1. Feed Properties

Chemical Analysis (As Received)		
Al ₂ O ₃	wt%	30.80
SiO ₂	wt%	63.40
RE ₂ O ₃	wt%	0.96
Na ₂ O	wt%	0.57
SO ₄	wt%	0.35
Ni	wt%	0.166
V	wt%	0.119
Physical Properties (Thermal, 3 h/537°C)		
surface area	m ² /g	170
ZSA	m ² /g	139
MSA	m ² /g	31
peak height		
unit cell size	nm	2.427
ABD	g/cm ³	0.81

Table 2. Equilibrium Catalyst Properties

Figure 1 shows a schematic diagram of the nitrogen balance around the FCC pilot plant. Since the oxygen/ argon mixture was used for the regeneration, the only nitrogen input for the whole system was from the feed nitrogen. The nitrogen distributes among the liquid products (gasoline, light cycle oil, bottoms, and water condensed from stripping steam), vapor products from the top of the recovery column, and nitrogen containing species in the flue gas. If we assume the coke on the regenerated catalyst is negligible for a full combustion operation, the total nitrogen in the flue gas should equal to the nitrogen in the coked catalyst.

Nitrogen Chemistry and NO_x Control in a Fluid Catalytic Cracking Regenerator

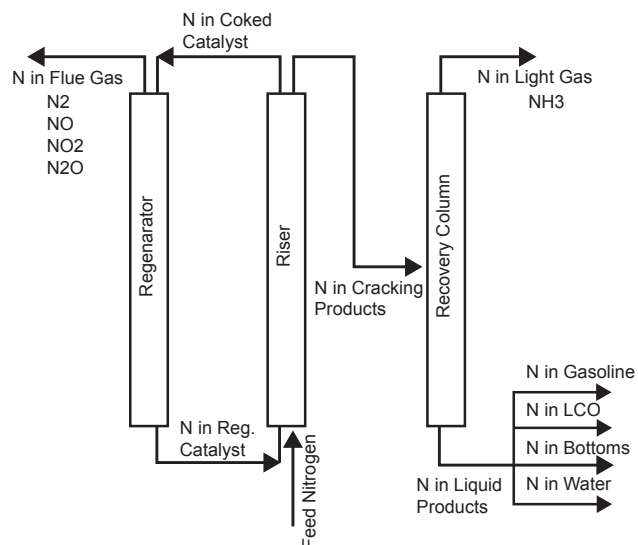


Figure 1. Nitrogen balance around Davison circulating riser.

Table 3 is the nitrogen balance from the DCR unit for both feeds. About half of the feed nitrogen appears in the liquid products. Most of the nitrogen in the liquid was concentrated in the

heavy fractions. Figure 2 shows a distribution of the nitrogen in liquid products with five different feeds (including feed A and B). Since steam was used for product stripping as well as feed atomization, water was also recovered along with the liquid products. Titration of the water showed that about 5% of the feed nitrogen is converted into ammonium and recovered in the water.

Part of the ammonia appeared in the light gases. The ammonia in the light gases was measured by bubbling the gas product through a 0.1 N HCl water solution and titrating the amount of nitrogen in the liquid. The results of this procedure from an experiment in the DCR using Feed A at a 73% conversion level showed about 3% of the feed nitrogen appeared as ammonia in the light gases.

For the low-nitrogen feed A, only about 62 ppm of NO was detected in the flue gas, while the high-nitrogen feed B produced about 221 ppm of NO. In both cases, NO only accounted for less than 3% of the feed nitrogen. For both feeds, a significant amount of molecular nitrogen in the flue gas was measured by gas chromatography, which indicates the formation of molecular nitrogen coke in the regenerator. In the two balance experiments, 32 and 38 wt% of the feed nitrogen were recovered as molecular nitrogen. The total amounts of molecular nitrogen and NO in the flue gas are equivalent to about 61 and 145 ppm of nitrogen on the coked catalyst, or 1.4 and 2.6 wt% of the nitrogen in the coke.

	Unit	Feed A		Feed B	
		products, %	N/feed N, %	products, %	N/feed N, %
conversion	wt%	73.9		59.8	
C/O		8		7.7	
H ₂ -C ₄	wt%	18.1		13.2	
NH ₃ /water			3.0 _a		3.0
liquid products	wt%	77.8	47.4	82.2	50.1
C ₅ + gasoline	wt%	51.7		40.2	
LCO	wt%	15.5		22.6	
bottoms	wt%	10.6		19.4	
NH ₃ /water			5.0 _a		5.0 _a
coke	wt%	3.7		4.3	
total mass balance		99.6		99.7	
flue gas NO	ppm	62	2.6	211	2.7
flue gas N ₂	ppm	450	38.0	1250	32.7
total N recovery			96.0		93.5

^a Estimated from different experiments.

Table 3. Nitrogen Balance around a Riser Pilot Plant

Continued on Page 103

Continued from Page 102

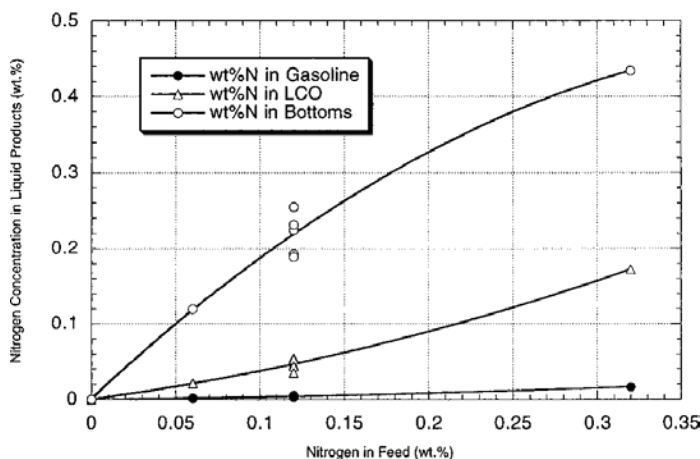


Figure 2. Nitrogen in FCC liquid products vs feed nitrogen.

The results are in good agreement with direct measurement by a CNS analyzer shown in Figure 6 (done at Leco, St. Joseph, MI). It appears that 10%-15% of the nitrogen in the coke is converted to NO in the DCR regenerator at the conditions we are using. The rest is released as molecular nitrogen. In commercial FCC regenerators, the fraction of nitrogen released as NO varies from about 3% to 25%, depending on the regenerator design and operating conditions (Miller et al., 1996). The percentage of nitrogen converted to coke in the two cases are about 40.6% for feed A and 35.4% for feed B. The ratios are comparable to the percentage of basic nitrogen in total feed nitrogen: 43% for feed A and 37.5% for feed B.

It is worth noting that the balance of nitrogen in the FCCU is different from that of sulfur. Fifty to sixty percent of the sulfur in the feed appears in the liquid products, and most of the rest, 35% to 45%, appears as H₂S. Only 2%-5% appears in the coke, and nearly all of the sulfur in the coke is oxidized to sulfur oxides (Wormsbecher et al., 1993). The case of nitrogen is very different. About half of the feed nitrogen is present in the liquid products, less than 10% of nitrogen appears as ammonia, and the rest is present in the coke. Very little of the nitrogen in the coke is oxidized to NO. Most undergoes reduction to N₂ in the regenerator. It should be noted that although a smaller fraction of sulfur than nitrogen ends up in coke, the concentration of sulfur in coke is typically similar to that of nitrogen due to the high concentration of sulfur in the feed.

NO_x Chemistry

Nitrogen Compounds in Feeds

The nitrogen content in most FCC feeds is quite low, typically between 0.005 to about 0.5 wt%. Nitrogen is found at ppm levels in light and middle distillates, but increase significantly around

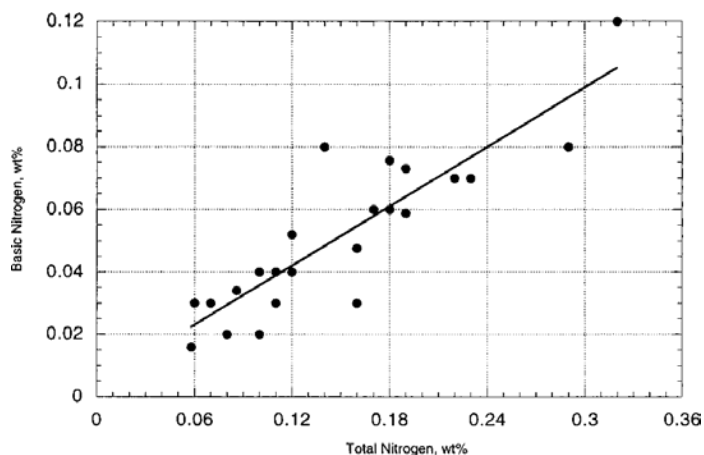


Figure 3. Basic vs total nitrogen in FCC feeds.

620 K (650°F). The nitrogen compounds are typically distinguished by their basicity. Much work has been reported to determine the basicity of each particular group of nitrogen compounds (Richter et al., 1952; McKay et al., 1975, 1976; Altgelt et al., 1994). According to their molecular structure, most of the nitrogen compounds fall into the following four groups with decreasing basicity: amines, pyridine derivatives, pyrrole derivatives, and amides. Typically, about one-third of the nitrogen is considered basic nitrogen according to titration analysis with perchloric acid (Figure 3). Most of the amine and pyridine types of nitrogen compounds are considered to be basic and are expected to be converted to coke. Literature also showed that these two types of nitrogen constitutes about one-third of the total nitrogen (Holmes, 1986). Most of the basic nitrogen is expected to be adsorbed on the acidic sites of the catalysts and be converted to coke during the cracking process, as we have shown in the nitrogen balance experiments. The percentage of nitrogen being converted to coke approximates the percentage of basic nitrogen in total nitrogen. Some of the nonbasic nitrogen may also contribute to coke. The fractions of nitrogen compounds left in the liquid products are expected to be the neutral or acidic types of nitrogen, e.g., pyrrole derivatives (Qian et al., 1995).

Nitrogen in Coke

Judging from the nature of the nitrogen compounds in the feed, a significant fraction of the nitrogen probably exists in aromatic rings. If one assumes the coke molecule contains about 15-20 aromatic rings, each molecule has to contain at least two nitrogen atoms at a nitrogen in a coke level of 5 wt% (Snape et al., 1995). One of the byproducts from the reaction between carbon and NO is C₂N₂. It has been speculated that the polymerization of C₂N₂ could in turn form a high melting point (CN)_x polymer (Chu et al., 1993). Our own XPS characterization

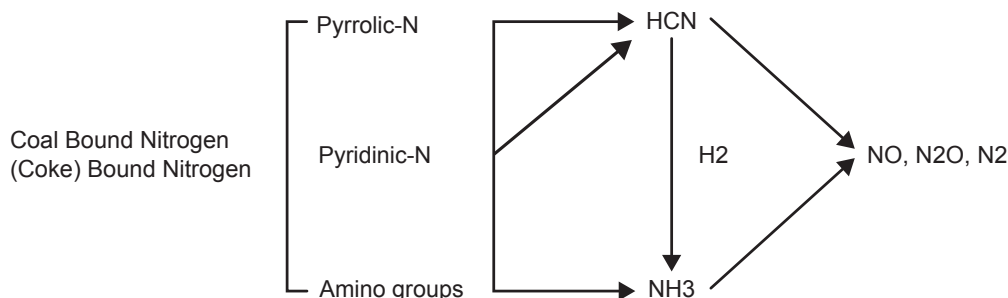


Figure 4. Schematic of the NO_x formation mechanisms (adapted from ref 16).

of the coke indicated the presence of two types of nitrogen structures in the coke. One is more strongly bonded to the catalyst surface than the other with a binding energy of 400.7 vs 398.4 eV (Qian et al., 1997).

Formation of NO_x

The exact chemistry on how the coke-bound nitrogen is being converted to NO_x/N₂ is not sufficiently understood. However, we can draw an analogy between the regeneration process (coke combustion) with fluidized bed coal combustion. There exists extensive literature on the nitrogen chemistry during coal combustion (Bassilakis et al., 1993; Wojtowicz et al., 1993). Systematic work was also reported for the formation of nitrogen compounds during the regeneration of spent hydroprocessing catalysts (Zeuthen et al., 1991; Furimsky et al., 1995, 1996). Figure 4 is a schematic showing of the transformation of coal-bound nitrogen during coal combustion (Wojtowicz et al., 1993).

Nitrogen in the coke has to go through some intermediates before being converted to NO or molecular nitrogen. For coal-bound nitrogen, HCN, and NH₃ are considered the intermediates for the formation of NO_x. Regeneration of spent hydroprocessing catalysts also follows the same mechanisms. It is expected that nitrogen in FCC coke would probably go through a similar route.

Regeneration of hydroprocessing catalysts indicated that the selectivity to HCN/NH₃/N₂ from fuel-bound nitrogen is strongly affected by the type of nitrogen in the coke, or originally in the feedstocks (Furimsky et al., 1995). Pyrrolic-N yields higher HCN than pyridinic nitrogen does. Model compounds studies for solid fuel combustion also showed that phenolic OH groups were found to increase the conversion of HCN to NH₃ (Hamalainen et al., 1994). Although there is very little evidence of amine groups in coal, the amine groups in FCC feed may be easily adsorbed on the catalyst and converted to coke. The nitrogen in amine groups are converted to ammonium intermediates before being further converted. Some of the amine groups may also be cracked and released as ammonia in the riser.

The subsequent destruction of HCN or NH₃ is more affected by the process or operating conditions. In a typical full combustion regenerator condition, most of the HCN and NH₃ should be oxidized to NO/N₂O as long as enough oxygen is available, especially with the presence of catalysts/metals. Part of the N₂O and NO can then go through reduction or decomposition to nitrogen. In the coal combustion process, there is evidence that N₂O is formed mainly from cyano species, whereas NH₃-based compounds tend to react toward NO. Laboratory experiments have shown (Tamhankar et al., 1996) that HCN is more readily oxidized than ammonia, through both are very reactive and are readily oxidized to N₂/NO_x. In partial combustion conditions, it is not difficult to imagine the presence of a significant amount of NH₃/HCN, which subsequently are converted to NO/N₂ in the downstream CO boiler. Thus, NO_x reduction in partial combustion requires different approaches from full combustion. The current paper will mostly deal with full combustion operations.

Reduction of NO_x

The nitrogen balance results described above show that nitrogen is produced in the regenerator during the burning of the nitrogen in the coke. This results suggests several possibilities. Nitrogen can be removed as either N₂ or as NO during initial combustion in the presence of coke. Another possibility is that the NO formed during combustion in the dense bed is further reduced to N₂ by reaction with either CO or carbon on an unregenerated catalyst.

Figure 5 demonstrates a laboratory simulated regeneration of a coked FCC catalyst by a temperature-programmed oxidation experiment. A coked catalyst is heated to 1010°F (550°C) in the presence of the oxygen/helium mixture and held at that temperature for 20 min. At this point the temperature is again increased. During the initial heating most of the carbon is burned to CO₂, and very little NO is formed. During the second stage most of the NO is formed and relatively little CO₂. These results show that carbon and nitrogen are burned sequentially, first carbon and then nitrogen. It appears from these experiments that the oxidation of nitrogen to NO occurs

Continued on Page 105

Continued from Page 104

at a higher temperature than the oxidation of carbon to CO₂ or to CO. These results would imply that as the amount of carbon on the regenerated catalyst decreases, the nitrogen content of the remaining coke increases. Direct measurements of nitrogen in coke have shown that this is the case (Figure 6). Nitrogen is removed last during regeneration in the DCR.

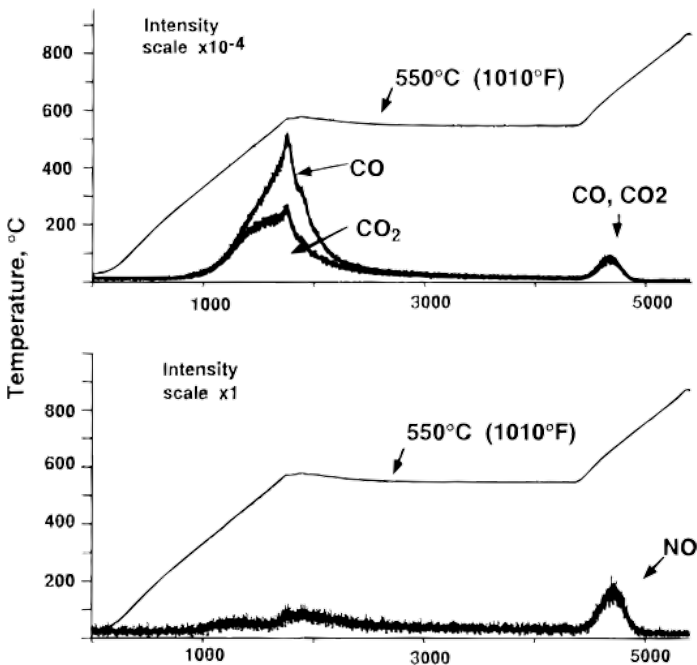


Figure 5. Regeneration of coked FCC catalyst (5 mol % oxygen in helium).

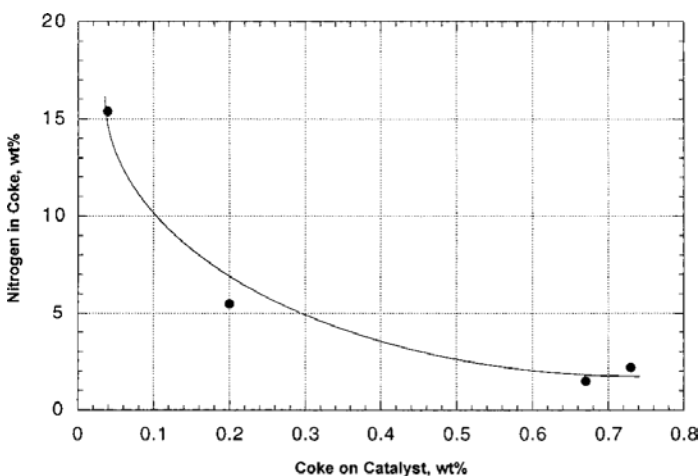


Figure 6. Nitrogen content in partially regenerated catalyst.

The reaction of NO with carbon has been reported previously as being as rapid or perhaps more rapid than the reaction of coke with oxygen (Chu et al., 1993). It is also well-known that NO can react with CO readily with the presence of various supported metal oxides or noble metals (Kobylinski et al., 1973, 1974). There is so far no conclusive evidence to differentiate the two mechanisms. The presence of carbon in the regenerator is always associated with the presence of CO. The fact that a CO combustion promoter substantially increases NO emission indicates that reduction of NO by CO is probably an important mechanism for NO conversion to N₂.

Another possible mechanism is the reaction of ammonia and NO_x competing with ammonia oxidation. As we have showed earlier, ammonia is a possible intermediate product of the NO_x formation process and it is certainly present in the regenerator. Thus, it is conceivable that this reaction occurs. At the present, we do not have evidence to prove or disprove this mechanism. Further experimental work is necessary.

Thermal Oxidation of Nitrogen

It is often alluded that some of the NO_x emission is from thermal oxidation of nitrogen from the air (Mann, 1993; Tamhankar et al., 1996). Thermodynamic calculations show that the temperature needed for having an appreciable amount of NO_x is extremely high. The result of thermodynamic calculations for this process is shown in Figure 7. Even if this reaction goes completely to equilibrium, only less than 10 ppm of NO will be produced under typical regenerator conditions of 1% excess O₂ and temperatures between 730°C (1340°F) and 780°C (1430°F). Even at 1600°F less than 30 ppm of NO is expected from this reaction. Since the concentration of NO in typical regenerators is considerably greater than the maximum equilibrium value of 30 ppm, the effect of this reaction, if it occurs, must be to convert NO back into molecular nitrogen. Consequently we feel that the oxidation of air makes no contribution to the observed NO_x in the FCCU flue gas.

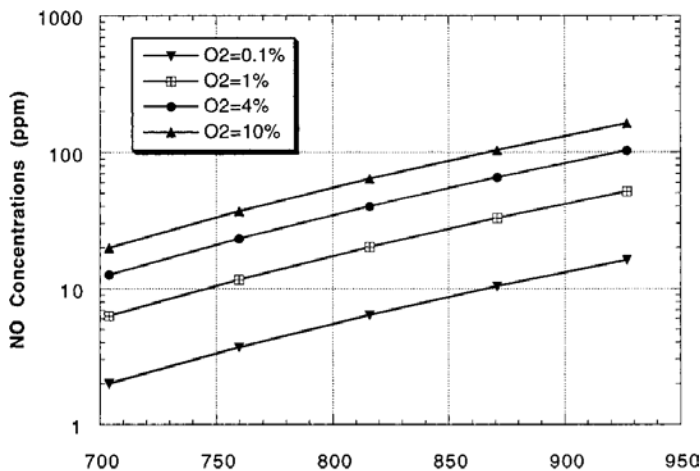


Figure 7. Equilibrium NO concentrations.

The fact that higher excess oxygen in flue gas correlated with higher NO is probably due to the decreasing CO concentrations with increasing excess oxygen, rather than the oxidation of molecular nitrogen to NO.

NO_x Emissions

From the analysis of nitrogen chemistry, we can expect the following conditions would create higher NO emissions from the FCC regenerator: high-nitrogen feed, excessive use of CO combustion promoter, and high excess oxygen.

A high-nitrogen feed produces more nitrogen-containing coke and thus emits more NO. Figure 8 shows the NO emission from a series of commercial units and the Davison circulating riser with feeds containing different levels of nitrogen. Although not all nitrogen in the feed contributes to NO emission in the same way, the general trend holds that a higher nitrogen feed typically produces more NO in the same unit.

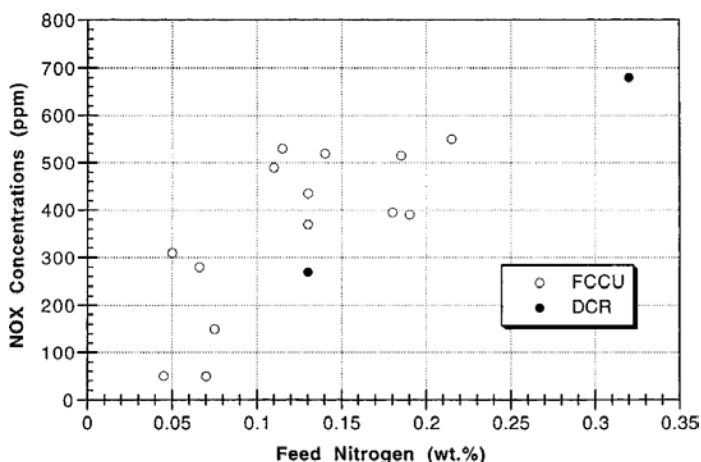


Figure 8. Correlation of NO emissions (promoted) with feed nitrogen. FCCU data from G. Bernstein, U.S. EPA Docket no. A-79-09 (1982).

Compared with partial combustion, full combustion units would have less reducing agents (e.g., CO, coke, and NH₃) in the regenerator, thus allowing more NO to be released. Another related variable is the excess oxygen level in the regenerator. Higher excess oxygen favors the oxidation of CO, coke, and other reducing agents in the regenerator and increases the level of NO in the flue gas. A set of commercial data is shown in Figure 9 to illustrate the relationship. A similar relationship is also found in the laboratory DCR pilot plant. Contrary to some reports, the correlation between excess oxygen and NO_x emission is due to the change of reducing agents such as CO or NH₃, rather than the contribution of thermal NO_x.

Excessive use of a combustion promoter would deplete CO and other reductants in both the dense and the dilute phase in the

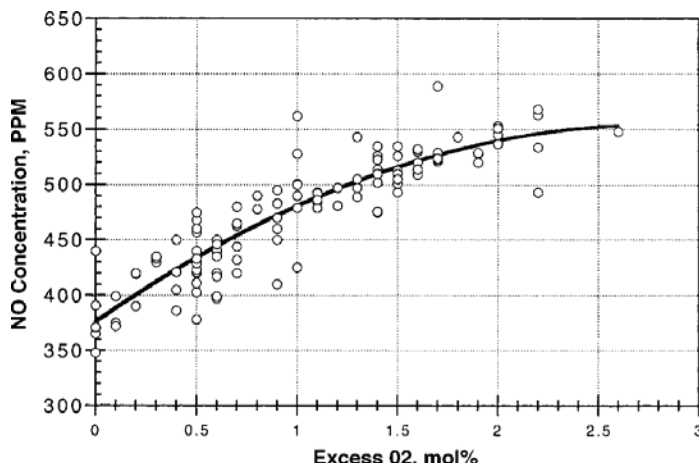


Figure 9. Excess oxygen vs NO_x emission in a commercial FCCU.

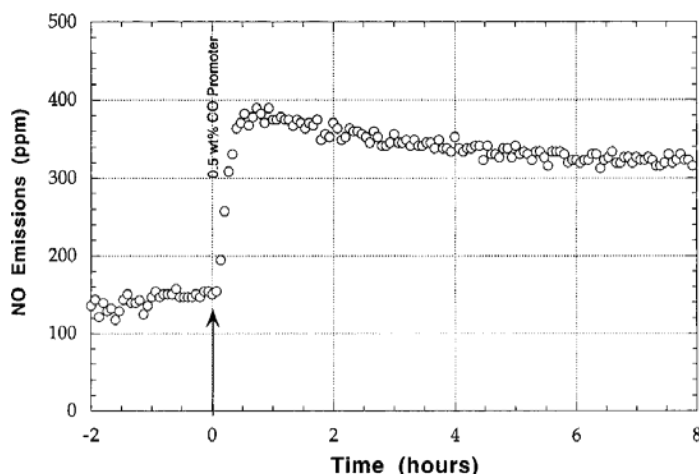


Figure 10. Effect of CO promoter on NO_x emission.

regenerator. As a result, more NO would be released. It is known from commercial observation as well as laboratory testing that a CO combustion promoter can significantly increase NO emission (Figure 10). There are speculations in the literature that a CO combustion promoter promotes the exothermic oxidation reaction so fast that it generates local hot spots. Part of the NO emission was attributed to the local high temperature. As shown in Figure 7, formation of any substantial amount of NO at thermodynamic equilibrium requires a temperature as high as 1700°F. Also, the typical NO concentration is almost always higher than the equilibrium concentration; any occurrence of this reaction would actually reduce NO, rather than produce NO. We have also conducted an experiment in the Davison circulating riser with a feed containing no nitrogen. When a combustion promoter was added to the system, no increase of NO emission

Continued on Page 107

Continued from Page 106

was observed as it did in the case of the nitrogen-containing feed. The results are shown in Figure 11.

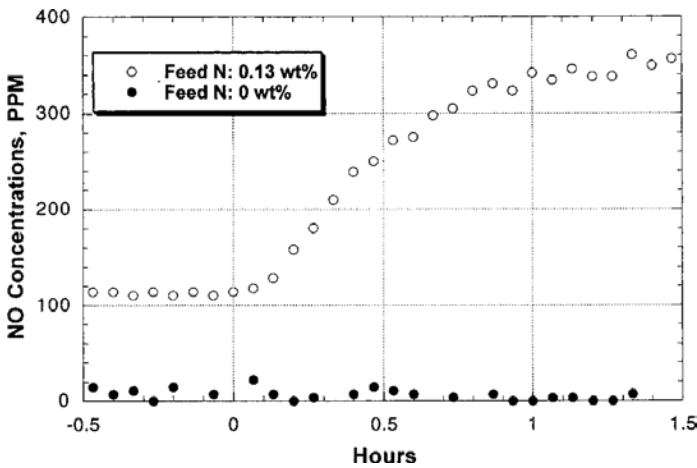


Figure 11. Effect of CO promoters on NO_x emission (EQ94-20, 0.5 wt% CP-5, 1% excess oxygen).

NO_x Control Technology

NO_x Control Additives

There are two schemes one can use to reduce NO emission: to control the formation of NO_x or to abate NO_x after its formation. Both can be accomplished by either catalytic or process approaches.

There have been numerous commercial products which claim to reduce NO_x emission when added to the FCC regenerators: commercial-based DESOX additives (Yoo et al., 1993; Cheng et al., 1997), perovskite-based NO_x additives (Dieckmann et al., 1994), and other metal oxide based additives (Chia, 1991). Reduction of NO to N₂ can also occur over a catalyst particle containing inorganic reduced components such as ceria (Figure 12). A ceria-containing material can be reduced in the riser by reacting with a hydrocarbon under cracking conditions and in the regenerator serves as a reducing agent to reduce NO to molecular nitrogen. All the additives require the presence of substantial amounts of reducing agents in the regenerator to maintain the redox process of cerium between Ce³⁺ and Ce⁴⁺. Figure 13 illustrates the NO reduction activity of some ceria-based additives with the amount of coke combusted in the regenerator. Since high delta coke is also associated with higher CO in the regenerator, the correlation could well be due to higher CO, or both CO and coke, or even higher NH₃. The NO reduction activity is apparently enhanced by the presence of more reducing agents.

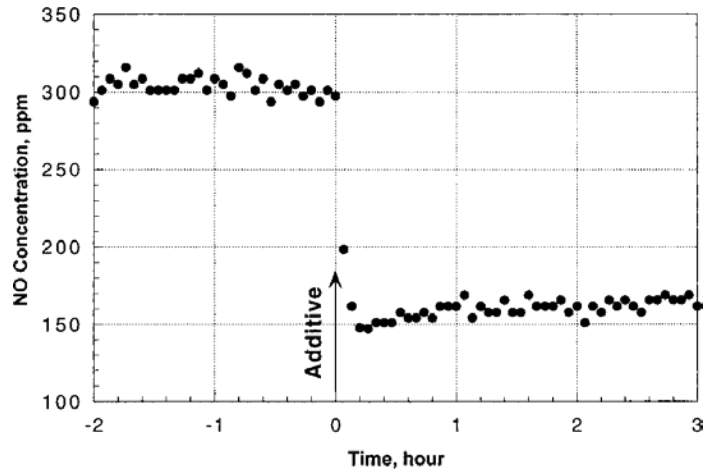


Figure 12. DCR testing of a ceria-based NO_x additive (0.5 wt% additive, 1% excess oxygen).

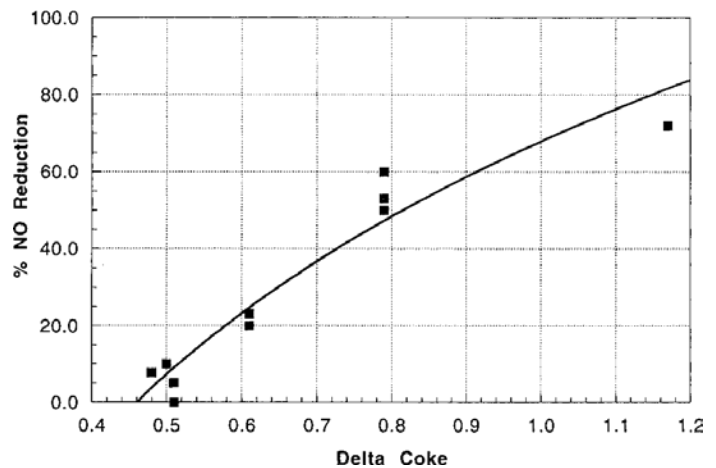


Figure 13. Effect of delta coke on the reduction of NO by Ce- based additives.

NO_x Control CO Combustion Promoter

The presence of reducing agents such as carbon monoxide can reduce NO_x emissions. Therefore, it is reasonable to expect an increase of NO emissions when CO is reduced or eliminated with the use of a combustion promoter. As we discussed earlier, the excessive use of a conventional CO combustion promoter substantially reduced the CO present in the dense phase as well as in the diluent phase of the regenerator.

A new generation of the combustion promoter has been developed at Grace Davison which selectively catalyzes the reaction between CO and NO while maintaining a good CO oxidation activity (Davey et al., 1996; Peters et al., 1996). The new generation combustion promoter does not increase NO_x emission

(Figure 14). In effect, it substantially reduces NO emissions, when compared with a conventional combustion promoter. The commercial application of the new combustion promoter has been reported elsewhere (Davey et al., 1996; Peters et al., 1996).

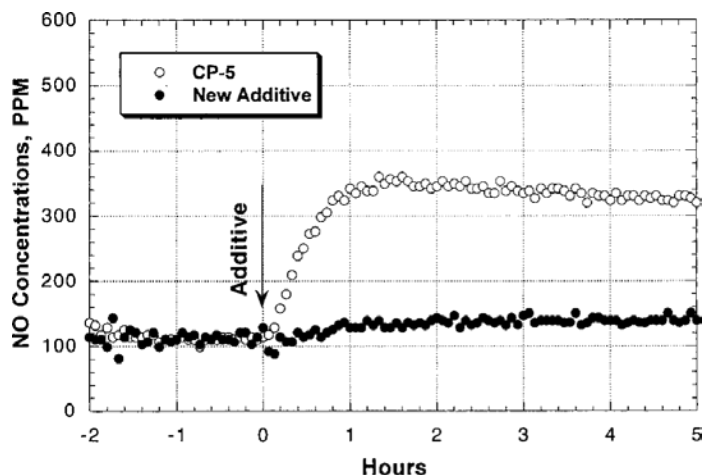


Figure 14. DCR testing of CO combustion promoters (gas oil feed, E-cat, 0.5 wt% additive, 1% excess oxygen).

Regenerator Design

NO_x reduction can be achieved by changes in the regenerator design. It has been reported that a countercurrent regenerator reduces NO_x emission due to the presence of a higher concentration of reducing agent at the top of the regenerator catalyst bed (Mann, 1993; Miller et al., 1996). Counter-current design allows a distribution of coked catalysts on the top of the regenerator catalyst bed surface. The chance of reduction of NO_x by CO or coke on catalyst is substantially improved. It is reported that the Kellogg countercurrent design reduces the percentage of nitrogen in coke being released as NO_x to about 5% from 10%-20% in other regenerator designs (Miller et al., 1996). The UOP high-efficiency regenerator typically does not require the use of combustion promoters. Therefore, the NO_x emissions in general should be lower than those of the conventional regenerator design.

Partial Combustion

All of our discussion so far has focused on full combustion operation, i.e., regeneration with the presence of excess oxygen. For partial combustion, the presence of large amounts of carbon monoxide and coke on catalysts for partial combustion can substantially reduce the emission of NO. It is expected that most of NO is reduced to nitrogen. However, the absence of enough oxygen in the dense bed could also potentially affect the oxidation of the nitrogen-containing intermediates such as NH₃ and HCN. Instead of being released as NO, some of the nitrogen might be released as NH₃ or HCN. Thermodynamic equilibrium a concentration of ammonium of over

1% was reported from a simulation of a FCC regenerator at a low-temperature partial combustion operation (McArthur et al., 1981). In commercial FCC units, a CO boiler is often used with a partial combustion regeneration to facilitate the conversion of CO in the flue gas. In such cases, the nitrogen-containing intermediate species are converted to NO_x in the CO boiler, and the NO emission from the CO boiler rather than the regenerator becomes the main issue. NO_x control for such operations requires different strategies from those for full combustion operations. Since the combustion of nitrogen comes after the combustion of coke, partial combustion may also allow the accumulation of nitrogen on the regenerated catalysts and significantly affect the catalytic-cracking performance of the catalyst, especially for high-nitrogen feeds.

Oxygen enrichment is a technology where oxygen is introduced with the regeneration air to increase the flexibility of unit operation, especially for high coke making heavy resid processing units (Tamhankar et al., 1996). For partial combustion operation, oxygen enrichment can enhance the oxidation of reduced nitrogen species such as NH₃ and HCN. However, there will be a competing effect for full combustion. Oxygen enrichment enhances the oxidation of reduced-nitrogen species, but it could reduce the presence of CO and other reductants which contribute to the reduction of NO.

Future Horizons

With the increasing regulation of NO_x emissions, it is expected that refiners will demand more NO_x control technologies. From a process point of view, some of the new hardware design technologies will help the control of NO_x emissions. However, the majority of the refineries will have to rely on operation conditions optimization or catalytic approaches. Operation changes would include processing of low-nitrogen feeds through hydrotreating, partial combustion, and prudent use of combustion promoters. The catalyst approaches would include the use of combustion promoters which do not increase NO_x, or NO_x reduction additives.

Currently, there is still a lack of knowledge of the nitrogen chemistry on the formation or destruction of NO. A better understanding of the chemistry would no doubt help the development of new technology and more intelligent use of the available technologies. With the increasing numbers of units processing resid, units operating at partial combustion mode are expected to increase. The understanding of nitrogen chemistry in the partial combustion mode is essential. There lies another challenge for NO_x control due to its difference with SO_x control. SO_x control additives adsorb SO₃ after SO₂ oxidation in the regenerator. The sulfur is released in the riser where it is reduced to H₂S. In contrast, all the NO_x control technologies rely on the reduction of NO by the reducing agents

Continued on Page 109

Continued from Page 108

available in the regenerators. Therefore, SO_x additives typically work better in a more oxidizing regenerator environment, while most of the NO_x additives work better in a more reducing regenerator environment. The simultaneous reduction of SO_x and NO_x would be a challenge for units which have both problems. It is expected many refineries will have both.

Acknowledgment

The authors thank Grace Davison for permission to publish this work. We also thank Dr. George Yaluris and Mr. John A. Rudesill for reviews of the paper and valuable discussions.

Literature Cited

- Altgelt, K. H.; Boduszynski, M. M.; *Composition and Analysis of Heavy Petroleum Fractions*; New York: Marcel Dekker, Inc., 1994.
- Bassilakis, R.; Zhao, Y.; Soloman, P. R.; Serio, M. A. Sulfur and Nitrogen Evolution in the Argonne Coals: Experiments and Modeling. *Energy Fuels* **1993**, *7*, 710-720.
- Cheng, W.-C.; Kim, G.; Peters, A. W.; Zhao, X.; Rajagopalan, K.; Ziebarth, M.; Pereira, C. Environmental Fluid Catalytic Cracking Technology. *Catal. Rev. - Sci. Eng.* **1997**, accepted.
- Chia, A. A. Reducing NO_x Emissions with Zinc Catalyst. U.S.A. Patent 5,002,654, Mobil, 1991.
- Chu, X.; Schmidt, L. D. Intrinsic Rates of NO_x-Carbon Reactions. *Ind. Eng. Chem. Res.* **1993**, *32*, 1359-1366.
- Davey, S. W.; Haley, J. T. *FCC Additive Technology Update*. Presented at the Oil & Gas Journal International Catalyst Conference & Exhibition, February 1-2, 1996, Houston, Texas, 1996.
- Dieckmann, G. H.; Labrador, E. Q. Perovskite-Spinel FCC NO_x Reduction Additive. U.S.A. Patent 5,364,517, Chevron, 1994.
- Furimsky, E.; Nielsen, M.; Jurasek, P. Formation of Nitrogen Compounds from Nitrogen-Containing Rings during Oxidative Regeneration of Spent Hydroprocessing Catalysts. *Energy Fuels*, **1995**, *9*, 439-447.
- Furimsky, E.; Siukola, A.; Turenne, A. Effect of Temperature and O₂ Concentration on N-Containing Emissions during Oxidative Regeneration of Hydroprocessing Catalysts. *Ind. Eng. Chem. Res.* **1996**, *35*, 4406-4411.
- Hamalainen, J. P.; Aho, M. J. Effect of fuel composition on the conversion of volatile solid fuel-N to N₂O and NO. *Fuel* **1994**, *74* (12), 1922-1924.
- Holmes, S. A. Nitrogen Functional Groups in Utah Tar Sand Bitumen and Produced Oils. *AOSTRA J. Res.* **1986**, *2*, 167- 175.
- Kobylinski, T. P.; Taylor, B. W. The Catalytic Chemistry of Nitric Oxide. I. The Effect of Water on the Reduction of Nitric Oxide Over Supported Chromium and Iron Oxides. *J. Catal.*, **1973**, *31*, 450-458.
- Kobylinski, T. P.; Taylor, B. W. The Catalytic Chemistry of Nitric Oxide. II. Reduction of Nitric Oxide Over Noble Metal Catalysts *J. Catal.* **1974**, *33*, 376-384.
- Mann, R. Fluid Catalytic Cracking: Some Recent Developments in Catalyst Particle Design and Unit Hardware. *Catal. Today* **1993**, *18*, 509-528.
- McArthur, D. P.; Simpson, H. D.; Baron, K. Catalytic Control of FCC SO_x Emission Looking Good. *Oil Gas J.* **1981**, *79* (2), 56- 59.
- McKay, J. F.; Cogswell, T. E.; Weber, J. H.; Latham, D. R. Analysis of Acids in High-Boiling Petroleum Distillates. *Fuel* **1975**, *54*, 50-61.
- McKay, J. F.; Weber, J. H.; Latham, D. R. Characterization of Nitrogen Bases in High-Boiling Petroleum Distillates. *Anal. Chem.* **1976**, *48*, 891-898.
- Miller, R. B.; Johnson, T. E.; Santner, C. R.; Avidan, A. A.; Beech, J. H. *Comparison Between Single and Two-Stage FCC Regenerator*. Proceedings of the 1996 Annual NPRA Meeting, San Antonio, Texas, 1996.
- Peters, A. W.; Weatherbee, G. D.; Zhao, X. Origin of NO_x in the FCCU Regenerator. *Fuel Reformulation* **1995**, *5* (3), 45-50.
- Peters, A. W.; Koranne, M.; Pereira, C.; Weatherbee, G. D.; Zhao, X.; Haley, J.; DAvey, S.; Lakhanpal, B. *Control and Origin of NO_x in the FCCU Regenerator*. ACS Annual Meeting, Orlando, FL, 1996.
- Qian, K.; Harding, R. H.; Zhao, X. *Impact of Conversion Level on Hydrocarbon Transformation in Fluid Catalytic Cracking Process Studies by Combined Chromatography and Mass Spectrometry*. Proceedings of the 43rd ASMS Conference on Mass Spectroscopy and Applied Topics, Atlanta, GA, 1995.
- Qian, K.; Tomczaka, D.; Rakiewiczza, E.; Harding, R.; Yaluris, G.; Cheng, W.-C.; Zhao, X.; Peters, A. W. A study of coke formation in fluid catalytic cracking process by combined catalytic techniques. *Energy Fuels* **1997**, *11* (3), 596-601.
- Richter, F. P.; Caesar, P. D.; Miesel, S. L.; Offenbauer, R. D. Distribution of Nitrogen in Petroleum According to Basicity. *Ind. Eng. Chem.* **1952**, *44* (11), 2601-2605.
- Snapc, C. E.; McGhee, B. J.; Andresen, J. M.; Hughes, R.; Koon, C. L.; Hutchings, G. Characterization of Coke from FCC Refinery Catalysts by Quantitative Solid State ¹³C NMR. *Appl. Catal. A: General* **1995**, *129*, 125-132.
- Tamhankar, S.; Menon, R.; Chou, T.; Ramachandran, R.; Hull, R.; Watson, R. Enrichment Can Decrease NO_x, SO_x Formation. *Oil Gas J.* **1996**, *94*, 60-68.
- Wojtowicz, M. A.; Pels, J. R.; Moulijn, J. A.; Combustion of Coal as a Source of N₂O Emission. *Fuel Process. Technol.* **1993**, *34*, 1-71.
- Wormsbecher, R. F.; Weatherbee, G. D.; Kim, G.; Dougan, T. J.; *Emerging Technology for the Reduction of Sulfur in FCC Fuels*. Proceedings of the 1993 NPRA Annual Meeting, 1993.
- Yoo, J. S.; Bhattacharyya, A. A.; Radlowski, C. A.; Karch, J. A. Mixed Spinels with Cerium-SO_x Emission Control From Fluid Catalytic Cracking (FCC) Regenerator. In *New Frontiers in Catalysis*; Gucci, J., Ed.; Elsevier: Amsterdam, 1993; pp 1391- 1403.
- Young, G. W. Realistic Assessment of FCC Catalyst Performance in the Laboratory. In *Fluid Catalytic Cracking: Science and Technology*. Magee, J. S., Mitchell, J. M. M. Eds.; Elsevier: Amsterdam, 1993; Vol. 76, pp 257-292.
- Zeuthen, P.; Blom, P.; Massoth, F. E.; Characterization of Nitrogen on Aged Hydroprocessing Catalysts by Temperature-Programmed Oxidation. *Appl. Catal.* **1991**, *78*, 265-276.
- Zhao, X.; Weatherbee, G. D.; Rajagopalan, K. R. *Simulation of Commercial FCCU Operations by a Laboratory Circulation Riser Unit*. Proceedings of The Fifth World Congress of Chemical Engineering, San Diego, CA, 1996.

Received for review February 7, 1997

Revised manuscript received May 9, 1997

Accepted May 13, 1997

IE970130P

Abstract published in Advance ACS Abstracts, September 15, 1997.

Highlights from Early Issues of *Catalagram* Magazine

A look back at interesting features in some of the early issues of Grace's *Catalagram* magazine demonstrate how much has changed...and how much has stayed the same.

***Catalagram* #1 from 1959**

The first issue – features an article on "Laboratory Equipment for Catalyst Research" that describes the facilities at the newly opened Washington Research Center (now referred to as Grace's Columbia headquarters). This issue also describes Grace's glass model of a cat cracker and gives the first industry average Ecat results. Compared to today, nickel, vanadium and activity are all incredibly low, however, in 1959 zeolite catalysts had not yet been introduced and resid was not being processed in the FCC.

***Catalagram* #7 from 1961**

Introduces the "Davison Calculator for fluid cat cracking operators" that was a paper slide chart for doing some FCC-specific calculations. Handheld electronic calculators were not available until the 1970s.

Catalagram #7 also introduced Grace's emergency after-hours phone number for catalyst orders, shipping issues and technical help – Baltimore, Saratoga 7-3912. Customers were encouraged to call collect.

***Catalagram* #14 from 1962**

Offers an article by Dr. Paul Emmett on factors influencing pore volume and ABD. Dr. Emmett is the "E" in the BET equation for determining the surface area of materials.

***Catalagram* #17 from 1963**

Includes an article on "Computers and Cat Crackers" complete with illustrations of punch cards.

***Catalagram* #20 from 1964**

Has the first report on a new zeolite containing catalyst called "XZ-15." The report was titled "20% more Gasoline with New Davison Catalyst." Davison is now Grace, and zeolites went on to revolutionize FCC.

***Catalagram* #72 from 1985**

Has an editorial by James Hattman of Grace that was written during a very challenging time for the refining industry. Mr. Hattman's statement rings true today- "Many of the problems the refiners face are also challenges and potential opportunities for an alert, aggressive, and technically oriented catalyst manufacturer. I think this describes Davison (now Grace)—we are such a company."

"We were there when the first cat cracker was built over forty years ago, and we will be there to supply the last one wherever and whenever that may be."

Hattman editorial from *Catalagram* 72

***Catalagram* #36 from 1971**

Includes the first article in a multipart series on catalytic cracking. This series later became "The Davison Chemical Guide to Catalytic Cracking" and evolved into the three volume "Grace Guide to FCC," the second edition of which was issued in 2020.

***Catalagram* #65 from 1982**

Contains a classic article on the effect of alkali and alkaline earths on zeolite. It provides data for Na, K, Ca, Mg and Ba.



Many 1970s-era *Catalagram* magazines had cartoon illustrations by John Stees, a renowned Baltimore newspaper cartoonist.

GRACE®, CATALAGRAM®, e-Catalysts.com®, FUSION®, G-Con®, MIDAS® and OlefinsUltra® are trademarks, registered in the United States and/or other countries, of W. R. Grace & Co.-Conn.

DCR™, EMISSCIAN™, Grace MILLE™, PARAGON™ and ZAVANTI™ are trademarks of W. R. Grace & Co.-Conn.

ACE™ is a trademark of Kayser Technology, Inc.

LINKEDIN & Design® is a trademark, registered in the United States and/or other countries, of LinkedIn Corporation.

ART®, ART & Design®, and ADVANCED REFINING TECHNOLOGIES® are trademarks of Advanced Refining Technologies LLC.

ART HYDROPROCESSING™ and ART HYDROPROCESSING A CHEVRON AND GRACE JOINT VENTURE & Design™ are trademarks of Advanced Refining Technologies LLC and Chevron Intellectual Property LLC.

CHEVRON & Design® is trademarks, registered in the United States and/ or other countries, of Chevron Intellectual Property LLC.

This trademark listing has been compiled using available published information as of the date of this publication and may not accurately reflect current trademark ownership or status. © Copyright 2025 W. R. Grace & Co.-Conn.

**To learn more about Grace,
please visit us at grace.com**

The information and calculation results contained herein are based upon our testing and experience and are believed to be accurate. Since operating conditions may vary and since we do not control such conditions, we must **DISCLAIM ANY WARRANTY, EXPRESS OR IMPLIED**, with regard to results to be obtained from the use of our products or with regard to application of Grace or ART Hydroprocessing's techniques, calculations, or models.

GRACE

